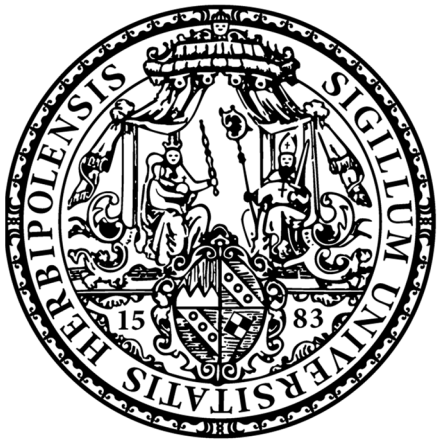

Development and preclinical evaluation of tumour-reactive T cells expressing a chemically programmable chimeric antigen receptor

Entwicklung und präklinische Evaluierung tumorreaktiver T-Zellen, die einen chemisch programmierbaren chimären Antigenrezeptor exprimieren

DOCTORAL THESIS
FOR A DOCTORAL DEGREE
AT THE GRADUATE SCHOOL OF LIFE SCIENCES,
JULIUS-MAXIMILIANS-UNIVERSITÄT WÜRZBURG,
SECTION INFECTION AND IMMUNITY

SUBMITTED BY

Lars Wallstabe

FROM

Gera

WÜRZBURG, 2018

Submitted on:

Members of the *Promotionskomitee*:

Chairperson:	Prof. Dr. Thomas Rudel
Primary Supervisor:	Dr. Michael Hudecek
Supervisor (Second):	Prof. Dr. Hermann Einsele
Supervisor (Third):	Prof. Dr. Thomas Herrmann
Supervisor (Fourth):	Prof. Dr. Christoph Rader

Date of Public Defence:

Date of Receipt of Certificates:

Table of contents

Summary

The genetic modification of T cells for the expression a chimeric antigen receptor (CAR) endows them with a new specificity for an antigen. Adoptive immunotherapy with CD19-CAR T cells has achieved high rates of sustained complete remissions in B cell malignancies. However, the downregulation or loss of the targeted antigen after mono-specific CAR T cell therapy, e.g. against CD19 or CD22, has been reported. Targeting multiple antigens on tumour cells, sequentially or simultaneously, could overcome this limitation. Additionally, targeting multiple antigens with CAR T cells could drive the translation from hematologic malignancies to prevalent solid cancers, which often express tumour-associated antigens heterogeneously. We hypothesised that expression of a universal CAR, which can be programmed with hapten-like molecules, could endow T cells with specificities for multiple antigens.

In this study we introduce a novel chemically programmable CAR (cpCAR) based on monoclonal antibody h38C2. Our data show, that cpCARs form a reversible chemical bond to molecules containing a diketone-group and therefore can be programmed to acquire multiple specificities. We programmed cpCAR T cells with hapten-like compounds against integrins $\alpha_v\beta_3$ and $\alpha_4\beta_1$ as well as the folate receptor. We observed tumour cell lysis, IFN-ɣ and IL-2 production and proliferation of programmed cpCAR T cells against tumour cells expressing the respective target antigen *in vitro*.

As a reference to cpCARs programmed against $\alpha_v\beta_3$, we further introduced novel conventional $\alpha_v\beta_3$-CARs. These CARs, based on humanised variants of monoclonal antibody LM609 (hLM609), directly bind to integrin $\alpha_v\beta_3$ via their scFv. The four $\alpha_v\beta_3$-CAR constructs comprised either an scFv with higher affinity (hLM609v7) or lower affinity (hLM609v11) against $\alpha_v\beta_3$ integrin and either a long (IgG4 hinge, C_H2, C_H3) or short (IgG4 hinge) extracellular spacer. We selected the hLM609v7-CAR with short spacer, which showed potent anti-tumour reactivity both *in vitro* and in a murine xenograft model, for comparison with the cpCAR programmed against $\alpha_v\beta_3$. Our data show specific lysis of $\alpha_v\beta_3$-positive tumour cells, cytokine production and proliferation of both hLM609-CAR T cells and cpCAR T cells *in vitro*. However, conventional hLM609-CAR T cells mediated stronger anti-tumour effects compared to cpCAR T cells in the same amount of time. In line with the *in vitro* data, complete destruction of tumour lesions in a murine melanoma xenograft model was only observed for mice treated with conventional $\alpha_v\beta_3$-CAR T cells.

Collectively, we introduce a cpCAR, which can be programmed against multiple tumour antigens, and hLM609-CARs specific for the integrin $\alpha_v\beta_3$. The cpCAR technology bears the potential to counteract current limitations, e.g. antigen loss, of current monospecific CAR T cell therapy. Targeting $\alpha_v\beta_3$ integrin with CAR T cells could have clinical applications in the treatment of solid malignancies, because $\alpha_v\beta_3$ is not only expressed on a variety of solid malignancies, but also on tumour-associated vasculature and fibroblast.

Zusammenfassung

T-Zellen können durch genetische Modifizierung zur Expression eines chimären Antigen-Rezeptors (CAR) neue Antigenspezifität erhalten. Durch adoptive Immuntherapie mit CD19-CAR T-Zellen können hohe Raten von anhaltenden vollständigen Remissionen bei Patienten mit malignen B-Zell-Erkrankungen erzielt werden. In klinischen Studien mit mono-spezifischen CAR T-Zellen wurden allerdings der Verlust oder eine verringerte Expression der Ziel-Antigene, z.B. CD19 oder CD22, auf Tumor-Zellen beobachtet. Außerdem sind bei soliden Krebserkrankungen tumor-assoziierte Antigene häufig unterschiedlich stark auf Krebszellen exprimiert. Wir haben die Hypothese aufgestellt, dass CARs, die mit einem hapten-ähnlichen Molekül programmiert werden können, es ermöglichen, mehrere Antigene mit einer T-Zelle anzugreifen.

In dieser Arbeit stellen wir einen neuartigen chemisch programmierbaren CAR (cpCAR) auf Basis des monoklonalen Antikörpers h38C2 vor. Unsere Daten zeigen, dass cpCARs eine reversible chemische Bindung zu Molekülen mit einer Diketongruppe bilden und daher so programmiert werden können, dass sie mehrere Spezifitäten aufweisen. Wir haben cpCAR T-Zellen mit hapten-ähnlichen Molekülen gegen die Integrine $\alpha_v\beta_3$ und $\alpha_4\beta_1$ sowie den Folat-Rezeptor programmiert. *In vitro* beobachteten wir sowohl die spezifische Lyse von Tumorzellen als auch T-Zell-Proliferation und Sekretion von IFN-ɣ und IL-2 durch programmierte cpCAR T-Zellen als Reaktion auf Antigen positive Tumorzellen.

Als Referenz zu cpCARs, die gegen $\alpha_v\beta_3$ programmiert wurden, haben wir in dieser Arbeit zudem neue konventionelle $\alpha_v\beta_3$-CARs vorgestellt. Diese basieren auf humanisierten Varianten des monoklonalen Antikörpers LM609 (hLM609) und binden mittels ihres scFv direkt an Integrin $\alpha_v\beta_3$. Die vier $\alpha_v\beta_3$-CAR-Konstrukte enthielten entweder ein scFv mit höherer Affinität (hLM609v7) oder niedrigerer Affinität (hLM609v11) gegenüber $\alpha_v\beta_3$ und entweder einem langen (IgG4-Hinge, C_H2, C_H3) oder einem kurzen (IgG4-Hinge) extrazellulären „Spacer“. Für den Vergleich von konventionellem CAR und cpCAR wählten wir den hLM609v7-CAR mit kurzem „Spacer“. T-Zellen, die diesen CAR exprimierten, vermittelten eine starke Anti-Tumor Reaktion sowohl *in vitro* als auch in einem Maus-Xenograft Modell. Unsere *in vitro* Daten zeigen spezifische Lyse von $\alpha_v\beta_3$-positiven Tumorzellen, Sekretion von Zytokinen und Proliferation sowohl durch hLM609-CAR T-Zellen als auch durch

cpCAR T-Zellen. Konventionelle hLM609-CAR T-Zellen vermittelten jedoch in gleicher Zeit eine stärkere Anti-Tumorwirkung als cpCAR T-Zellen.

Zusammengefasst präsentieren wir in dieser Arbeit einen cpCAR, der gegen mehrere Tumorantigene programmiert werden kann, und hLM609-CARs, die spezifisch für das Integrin $\alpha_v\beta_3$ sind. Die cpCAR-Technologie birgt das Potenzial, aktuellen Limitationen der mono-spezifischen CAR-T-Zelltherapie, z.B. dem Antigenverlust, entgegenzuwirken. Zudem könnte das Integrin $\alpha_v\beta_3$ klinische Anwendung bei der Behandlung von soliden Tumoren finden, da es nicht nur auf einer Reihe von Tumor-Entitäten, sondern auch auf Tumor-assoziiertem Gewebe zu finden ist.

1 Introduction

1.1 Adoptive immunotherapy with tumour reactive T cells

Cancer is one of the leading causes of disease-related deaths worldwide (Torre *et al.*, 2015). As our understanding of cancer biology evolves, the landscape of treatment modalities expands from conventional therapy with chemotherapeutics, radiation or surgical removal of tumour lesions to immunotherapy. The main immunologic treatments include monoclonal antibody (mAB) therapy, immune-check-point inhibitor therapy, cancer vaccines and adoptive T cell therapy (ATCT) (Yang, 2015).

In ATCT, either autologous or allogeneic T cells are obtained from a patient or a human leukocyte antigen (HLA) compatible donor, respectively. The T cells are expanded *in vitro* and then reinfused into the patient where they are supposed to destroy malignant cells (Figure 1) (Perica *et al.*, 2015). During *ex vivo* culture the T cells can be gene-modified to specifically recognise tumour cells. Native T cells recognise antigens that are presented in major histocompatibility complex (MHC) molecules on other cells with their T cell receptors (TCR). This induces a primary activating signal. To completely activate T cells, a second signal is required, induced through activating costimulatory receptors binding their respective ligands (Fesnak, June and Levine, 2016)

The first clinical evidence that adoptively transferred T cells can have anti-tumour effects was provided by allogeneic hematopoietic stem cell transplantation (HSCT) for the treatment of hematologic malignancies. In this approach, donor cells, and in particular T cells, can mediate a graft-versus-leukaemia effect and reduce the tumour burden (Kolb *et al.*, 1995). However, in this setting, the T cells primarily react against allogeneic antigens that are not exclusively presented on malignant cells but also on healthy cells of the host. Therefore, side effects, i.e. acute and chronic graft-vs-host disease, can occur that limit the applicability of HSCT (Welniak, Blazar and Murphy, 2007).

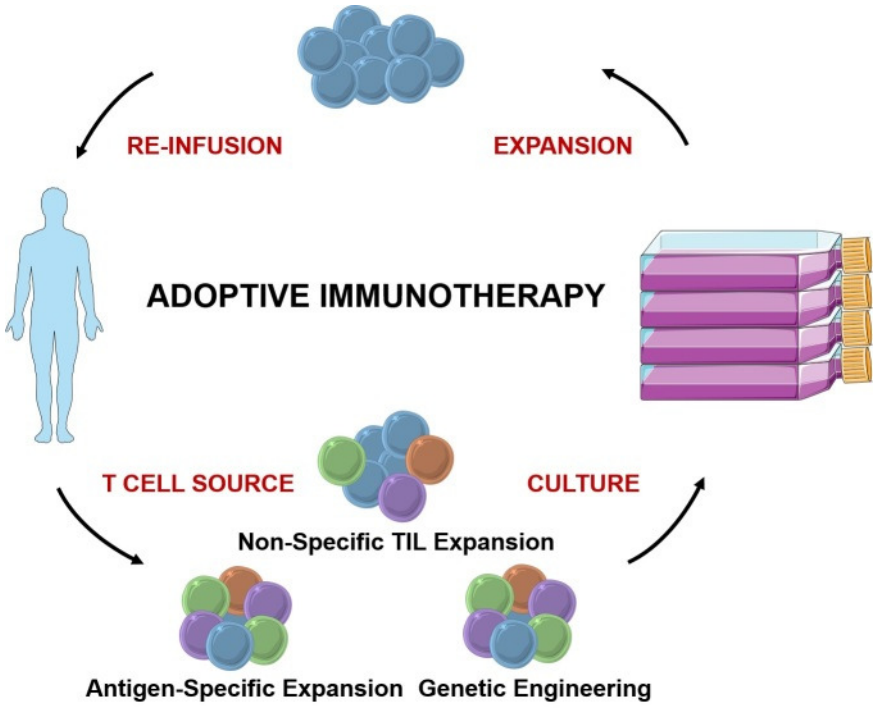

Figure 1: Adoptive T cell therapy (Perica *et al.*, 2015)**.**
In ATCT, autologous or allogeneic T cells with anti-tumour properties are infused into a patient. During *in vitro* culture, T cells with specificity for tumour-associated antigens can be enriched with antigen-specific expansion or T cells can be endowed with tumour specificity by genetic engineering.

In 1988, Rosenberg and colleagues isolated tumour infiltrating lymphocytes (TILs) from melanoma patients, expanded them *in vitro* and re-infused the resulting cell product into the patients (Rosenberg *et al.*, 1988). As the majority of re-infused cells were CD3-positive, this is the first reported clinical trial with *in vitro* expanded adoptively transferred T cells. The treatment procedure was later refined to achieve higher response rates, e.g. by adding lymphodepleting regimens prior to cell re-infusion (Gattinoni *et al.*, 2005). However, TILs with anti-tumour reactivity cannot be manufactured for every patient, particularly for patients with a hematologic malignancy or solid tumour entities other than melanoma (Perica *et al.*, 2015). The adoptive transfer of T cells that have been selectively expanded for reactivity towards tumour-associated antigens, e.g. by co-incubation with dendritic cells pulsed with a tumour-associated antigen, could facilitate the manufacturing of tumour-reactive T cell grafts and open up new treatment modalities. After infusion of such T cells, a regression of tumour burden was observed in a fraction of melanoma patients in phase I clinical trials. However, some patients did not respond to the treatment and complete tumour regression was rare (Yee *et al.*, 2002; Mackensen *et al.*, 2006). The limited response

could have been caused by a lack of specificity of the transferred T cells or a too small number of tumour reactive T cells. Genetic engineering of T cells could solve such limitations.

Mainly, two different approaches are used to introduce new specificities for tumour-associated antigens into T cells: clonal expression of antigen-specific TCRs or artificial chimeric antigen receptors (CARs). The target antigens of TCR-engineered T cells are small peptides that are presented in context of MHC-molecules. Intracellular and extracellular proteins are processed by the proteasome and afterwards loaded to MHC molecules and transferred to the cell surface (Fesnak, June and Levine, 2016). The processing of endogenous and exogenous proteins allows for a great variety of potential targets. On the other hand, the dependence on MHC-TCR interactions is also a major limitation of this approach because MHC-molecules are often lost or down-regulated on tumour cells (Algarra, Cabrera and Garrido, 2000). To address these challenges, T cells can be modified to express a CAR, which directly binds to target antigens. This enables CAR T cells to specifically target antigens on the cell surface independently of the MHC (Sadelain, 2015). This novel technology is in the centre of this study.

1.2 Chimeric Antigen Receptors

1.2.1 Design and mode of action of chimeric antigen receptors

CARs are artificial molecules that consist of an antigen-binding domain, a spacer domain, a transmembrane domain, and a signalling domain (Figure 2) (Sadelain, Rivière and Riddell, 2017). A single chain variable fragment (scFv) usually mediates the specific interaction with an antigen. However, protein ligands have also been described as targeting units (Fu *et al.*, 2013). The length of the spacer domain is thought to determine the distance between cell membrane of the T cell and antigen binding domain as well as the flexibility of the CAR. The composition of the spacer can greatly affect CAR T cell function (Hudecek *et al.*, 2013, 2015). The amino acid sequence is typically derived from the hinge region of CD8α (cluster of differentiation) or the hinge domain and constant fragments of immunoglobulins (Moritz *et al.*, 1994; Guest *et al.*, 2005). The transmembrane region of the costimulatory receptor CD28 or CD8α are often used as the transmembrane region of the CAR (Sadelain, 2015). The first generation of CAR T cells only used the intracellular domain of the TCR chain CD3ζ as signal moiety (Irving and Weiss, 1991; Eshhar *et al.*, 1993). The additional

integration of an intracellular domain of a costimulatory receptor significantly enhanced cytokine production, proliferation and persistence of CAR T cells in preclinical models (Finney *et al.*, 1998; Finney, Akbar and Lawson, 2004; Kowolik *et al.*, 2006). These second generation CAR T cells mostly contained the intracellular domains of CD28 or CD137 (4-1BB). Current clinical studies investigate if CAR T cell activation can be further increased by additional costimulatory domains (Fesnak, June and Levine, 2016).

When a CAR binds to its respective ligand, the intracellular CD3ζ provides a TCR-like signal while the intracellular costimulatory domain provides a costimulatory signal. This leads to complete activation of the T cell signalling cascade (Finney, Akbar and Lawson, 2004). The cascade culminates in the activation of transcription factors, e.g. nuclear factor of activated T cells (NFAT) or nuclear factor-κB (NF-κB), that regulate the expression of inflammatory proteins, such as the cytokines IL-2 or IFN-ɣ (Frigault *et al.*, 2015; Gomes-Silva *et al.*, 2017).

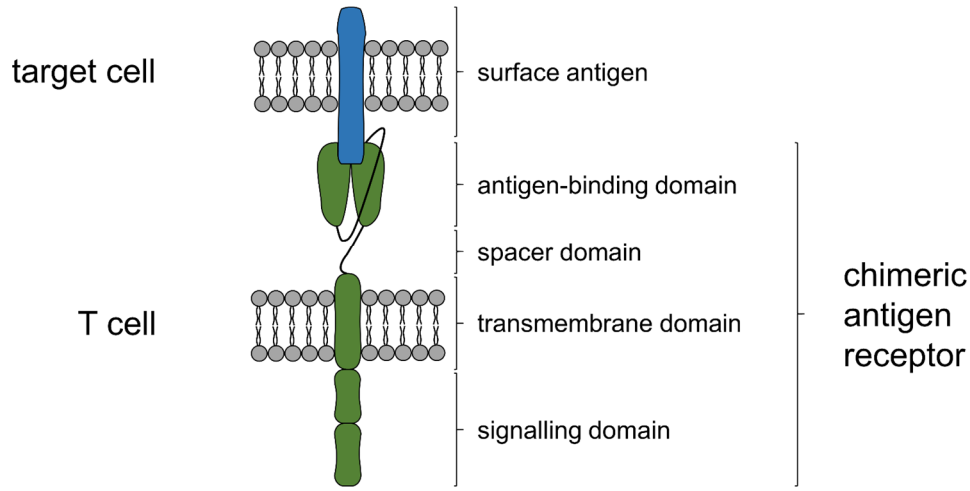

Figure 2: Structure of a chimeric antigen receptor.
CARs consist of an antigen-binding domain, a spacer domain, a transmembrane domain and a signalling domain.

1.2.2 The success of CD19-CAR T cells

The B-lymphocyte antigen CD19 is the most extensively studied target for CAR T cell therapy. CD19 has a favourable expression pattern, as it is exclusively expressed on healthy and malignant B cells, which limits on-target off-tumour effects to B cell aplasia (Scheuermann and Racila, 1995). In clinical trials with CD19-CAR T cells, more than 80 % of patients with B cell acute lymphoblastic leukaemia (B-ALL) (Brentjens *et al.*, 2013; Maude *et al.*, 2014; Turtle *et al.*, 2016) and between 50 – 80 % of patients with refractory lymphoma responded to the treatment (Kochenderfer *et al.*, 2015; Schuster *et al.*, 2017). Recently, the efficacy of CD19-CAR T cells led to the approval of the first commercially available CAR products by the U.S. Food and Drug Administration and the European Commission (Wohlfarth, Worel and Hopfinger, 2018). In a phase II clinical trial, CD19-CAR T cells were detectable in patients' blood for up to 20 months after T cell administration, demonstrating the potential of CAR T cell therapy to provide long-term protection against tumour remission (Maude *et al.*, 2018). However, CD19 can be downregulated or mutated by malignant cells and relapse with CD19-negative tumour cells limits the durability of responses (Yang *et al.*, 2005; Sotillo *et al.*, 2015).

Aside from CD19, other antigens on B cell malignancies have been targeted with CAR T cells. A clinical trial with CAR T cells targeting CD20 reported complete remission in 2 of 3 patients (Till *et al.*, 2012). When B-ALL patients were treated with CD22-CAR T cells, depending on the T cell dosage, up to 73 % presented with a complete remission (Fry *et al.*, 2018). Interestingly, the majority of patients included in this trial had previously been treated with CD19-CAR T cells and 5 of 5 patients either negative for CD19 or with a very low expression responded to the CD22-CAR T cell therapy. However, Fry *et al.* report that some patients relapsed with CD22-negative or CD22-dim tumour. These data illustrate that the success of CAR T cell therapy against a single antigen is limited due to antigen loss on the tumour cells. In the present study, we therefore introduce CAR T cells that are able to detect multiple antigens on tumour cells.

1.2.3 Improving CAR T cell therapy by targeting multiple antigens

A pragmatic way to generate a CAR T cell product with reactivity towards multiple antigens is to express different receptors that have different specificities. It has been shown that such an approach, targeting both CD19 and CD123, can improve the anti-tumour response in a murine xenograft model simulating CD19 loss (Ruella *et al.*, 2016). The positive effect was even greater when the mice were treated with CAR T cells that expressed both CARs at the same time instead of a mixture of CAR T cells that each expressed one CAR. Additionally, CARs have been developed that possess two different scFvs that are linked together as antigen-binding domain. These receptors have been termed tandem or bispecific CARs. The first described tandem CAR encompassed scFvs against CD19 and Her2, a purely experimental combination of tumour-associated antigens (Grada *et al.*, 2013). This proof-of-principle tandem CAR displayed anti-tumour activity against tumour cells expressing both or either one of the antigens *in vitro* and in a murine xenograft model. Therefore, tandem CARs that detect the more clinical relevant combinations of antigens CD19 and CD20 or Her2 and IL13Rα2 have been developed (Hegde *et al.*, 2016; Zah *et al.*, 2016). Further, CARs have been designed that do not have a specificity towards a tumour-associated antigen but bind hapten-like molecules. A hapten is a small chemical that can bind to an antibody, but only elicits an immune response when attached to a carrier-molecule, e.g. a protein. Thereby, these molecules, for example a fluorescein isothiocyanate (FITC)-labelled mAB, equip the CAR with a specificity (Tamada *et al.*, 2012). This approach can be used to target multiple antigens with a single CAR construct, because different hapten-molecules with different targets can be bound to the CAR. Since such CAR T cells are only activated in the presence of a hapten-molecule that is administered separately, they are presumed to be safer compared to conventional CARs.

A major focus of CAR T cell research is to transfer the excellent efficacy of CAR T cells against CD19 towards prevalent solid malignancies. Targeting several antigens simultaneously could support this effort, as solid cancer cells often display a heterogeneous expression of tumour-associated targets. One example for such an antigen is the epidermal growth factor receptor variant III (EGFRvIII), which can be expressed at different levels on glioblastoma cells of the same patient (Furnari *et al.*, 2015). Thus, therapy directed against a single antigen could lead to selection and outgrowth of antigen negative tumour cells (Fesnak, June and Levine, 2016).

Identifying novel target antigens on solid tumour entities is another major focus of CAR T cell research in order to generate effective CAR T cells for the therapy of solid cancers. Potential targets are often overexpressed on malignant cells but are also present on healthy tissues. The affinity of the targeting structure can be tuned to enable CAR T cells to preferentially target cells expressing high levels of the respective antigen (Chmielewski *et al.*, 2004; Caruso *et al.*, 2015). Recently, we and others introduced integrin $\alpha_v\beta_3$ as a novel target for CAR T cell therapy of solid tumours.

1.3 Integrin $\alpha_v\beta_3$ - a target on tumour cells

Integrins are heterodimeric cell surface receptors expressed by all nucleated cells. They are involved in adhesion and signalling processes between cells and their microenvironment. The non-covalent association of one α- and one β-subunit assembles the integrin dimer (Hynes, 2002). Upon binding of their respective ligands, integrins recruit large signalling complexes to their cytoplasmic domain and transmit a signal from the outside into the cell. They are also able to transmit signals from the inside to the outside of the cell as they can modulate the binding affinity to their ligands by conformational changes (Campbell and Humphries, 2011). Integrins are being pursued as targets in cancer therapy due to their influence on tumour cell migration, invasion, proliferation and survival (Desgrosellier and Cheresh, 2010).

Integrin $\alpha_v\beta_3$, also known as vitronectin receptor, is one of the best-studied integrins in cancer research. It primarily interacts with ligand proteins containing an arginyl-glycyl-aspartic acid (RGD)-motif and can increase tumour cell survival (Felding-Habermann and Cheresh, 1993; Petitclerc *et al.*, 1999). Several mechanisms have been identified that link the expression of integrin $\alpha_v\beta_3$ on tumour cells to increased metastatic spread (Liapis, Flath and Kitazawa, 1996; Sloan *et al.*, 2006). First, the activated form of integrin $\alpha_v\beta_3$ enables the tumour cells to bind to platelets, protecting them from shear stress and enhancing their adhesion to blood vessels (Felding-Habermann *et al.*, 2001; Gay and Felding-Habermann, 2011). Second, recruitment and activation of the tyrosine kinase c-Src by the cytoplasmic tail of the β_3 subunit of integrin $\alpha_v\beta_3$ promotes anchorage-independent cell survival (Desgrosellier *et al.*, 2009). Third, integrin $\alpha_v\beta_3$ promotes the epithelial-mesenchymal transition of tumour cells by direct interaction with the TGF-β receptor II and binding of TGF-β. Exposure to TGF-β also leads to increased integrin $\alpha_v\beta_3$ expression (Ludbrook *et al.*, 2003; Galliher and Schiemann, 2006).

Expression of integrin $\alpha_v\beta_3$ has been demonstrated to occur in several tumour entities such as melanoma and glioblastoma as well as breast, pancreatic and prostate cancer (Albelda *et al.*, 1990; Hosotani *et al.*, 2002; Sloan *et al.*, 2006; McCabe *et al.*, 2007; Schnell *et al.*, 2008). In melanoma, transition from benign radial growth to malignant vertical growth correlates with a *de novo* expression of integrin $\alpha_v\beta_3$ (Hsu *et al.*, 1998). In addition to tumour cells themselves, integrin $\alpha_v\beta_3$ is also expressed on cells that are essential components of the tumour environment including cancer-associated fibroblasts (CAFs), tumour-associated macrophages and angiogenic endothelial cells (Brooks *et al.*, 1994; Zhou *et al.*, 2015; Attieh *et al.*, 2017).

In cancer therapy, integrin $\alpha_v\beta_3$ has been targeted with different therapeutic agents in preclinical and clinical trials, including small molecules and mABs. The small molecule Cilengitide (EMD 121974), an RGD-mimetic that binds to integrin $\alpha_v\beta_3$, induced apoptosis in endothelial cells and some tumour cells in a murine xenograft model of glioblastoma (Yamada *et al.*, 2006). Cilengitide proceeded into clinical testing but failed to meet primary endpoints in a phase III clinical trial (Demircioglu and Hodivala-Dilke, 2016). Another drug, the anti-$\alpha_v\beta_3$ mAB LM609, was able to inhibit angiogenesis in preclinical models (Figure 3) (Brooks *et al.*, 1995). The potential of an integrin $\alpha_v\beta_3$ targeted cancer therapy with humanised LM609 mABs has been evaluated in phase I and phase II clinical trials (Raab-Westphal, Marshall and Goodman, 2017). The treatment was well tolerated but only showed a limited therapeutic effect. Rader *et al.* described a method to target integrin $\alpha_v\beta_3$ with a novel class of mABs termed chemically programmable antibodies (cpABs) (Rader, Sinha, *et al.*, 2003). Small molecules can be chemically conjugated to cpABs equipping them with the specificity for a desired target.

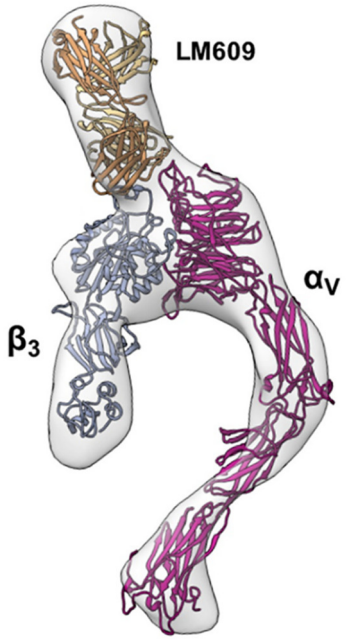

Figure 3: Structure of integrin $\alpha_v\beta_3$ with mAB LM609 attached (modified from Borst *et al.*, 2017).
Orthogonal view of integrin $\alpha_v\beta_3$ in its extended state with mAB LM609 attached, displayed as a pseudo-atomic model fitted with a random conical tilt 3D reconstruction.

1.4 h38C2 - the prototype of chemically programmable antibodies

A cpAB is an invariable antibody component that serves as carrying moiety, which can be covalently bound to a variable synthetic component that serves as a targeting moiety (Rader, 2014). Thus, cpABs differ in the mode of antigen recognition from that of conventional mABs. The specificity of mABs is defined by their complementarity-determining regions (CDRs), which are located in the variable heavy chain (V_H) and variable light chain (V_L) domains (Figure 4 A). In contrast, a hapten-like, synthetic component that is covalently and site-specifically bound to a cpAB mediates recognition of antigens by cpABs (Figure 4 B). Therefore, the cpAB needs to contain a unique reactivity centre, which can be formed by reactive lysine residues, cysteine residues or selenocysteine residues (Rader, Sinha, *et al.*, 2003; Xiao *et al.*, 2009; Cui *et al.*, 2012). The synthetic component comprises, in a single molecule, a reactive group that facilitates the covalent association with the cpAB, a pharmacophore that specifically binds to an extracellular antigen, and a spacer molecule separating pharmacophore and reactive group (Rader, 2014). Typically, a peptide, a peptidomimetic or another small molecule is used as pharmacophore. Because cpABs form a conjugate of mABs and small molecules, they possess properties characteristic for both substance classes (Table 1). The antibody part confers a long circulating half-

life and effector functions through the Fc (fragment crystallisable) domain, such as complement dependent cytotoxicity and antibody dependent cellular cytotoxicity (Buss *et al.*, 2012). The small hapten-molecules add their unlimited structural diversity, their comparatively simple production and their ability to recognise small and highly conserved pockets to cpABs.

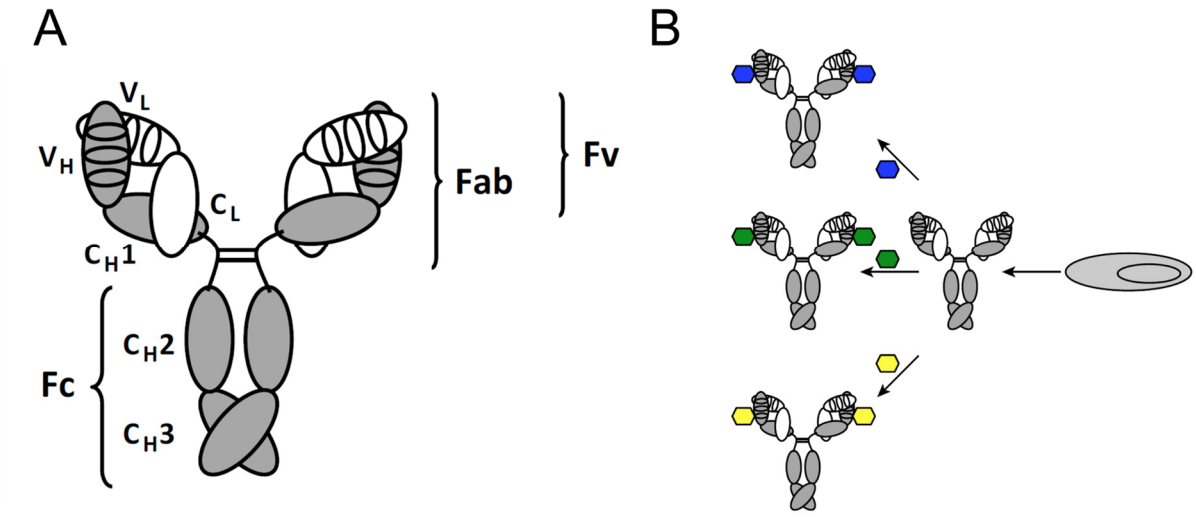

Figure 4: Design of mABs and basic concept of cpABs (modified from Rader, 2014). **(A)** Schematic depiction of an IgG1 molecule that contains two heavy and two light chains. The variable fragment (Fv) consists of the variable heavy chain (V_H) and variable light chain (V_L) domains, each containing three complementarity-determining regions (CDRs) (ovals). The V_H and V_L are followed by the constant heavy one (C_H1) and constant light (C_L) domains and form the antigen-binding fragment (Fab). A flexible hinge region (bent lines) connects the C_H1 and the fragment crystallisable (Fc), which consists of the constant heavy two (C_H2) and constant heavy three (C_H3) domains. Interchain disulfide bridges are formed between the C_H1 and C_L domains (not shown) and between the hinge domains (straight lines). **(B)** A cpAB can covalently and site-specifically bind a hapten-like molecule (hexagon). Therefore, a single cpAB construct can be equipped with multiple specificities by adding hapten-molecules with specificities for different antigens.

Table 1: Properties of small molecules, mABs and cpABs (modified from Rader, 2014)

	small molecules	mABs	cpABs
chemical diversity	unlimited	limited	unlimited
molecular weight	< 1 kDa	150 kDa	50-150 kDa
target binding sites	1	2	1-2
target binding specificity	medium to high	high	high
target binding affinity	µM to nM	nM	nM
target location	intracellular and extracellular	extracellular	extracellular
circulatory half-life	min to h	weeks	days to weeks
effector functions	no	yes	yes
route of administration	topical, enteral and parenteral	parenteral	parenteral
manufacturing costs	low	high	medium

The concept of cpABs was first described in 2003 by Rader *et al.* (Rader, Sinha, *et al.*, 2003). Rader and colleagues programmed the aldolase mAB 38C2 with a synthetic peptidomimetic that contained an RGD targeting moiety. Administration of both compounds resulted in reduced tumour growth in preclinical models, both *in vitro* and *in vivo*. The mAB 38C2 is a catalytic antibody with aldolase activity and was originally generated in mice by reactive immunisation with a 1,3-diketone hapten (Wagner, Lerner and Barbas, 1995; Barbas *et al.*, 1997; Karlstrom *et al.*, 2000) and humanised (h38C2) in subsequent work (Rader, Turner, *et al.*, 2003). The reactive centre, a lysine residue at the bottom of a hydrophobic cleft, is located in the FR3 domain of the V_H chain (Rader, Turner, *et al.*, 2003). Several amino acids (aa) in the V_H and V_L region contribute to the formation of an 11 Å deep hydrophobic pocket. The ε-amino group of the reactive lysine forms an enaminone by reversible covalent binding of an 1,3-diketone (DK) molecule that is stabilized by imine-enamine tautomerism (Rader, 2014) (Figure 5). 38C2 can also form irreversible covalent connections with molecules containing a vinyl ketone (Guo *et al.*, 2006) or a β-lactam functional group (Gavrilyuk *et al.*, 2009).

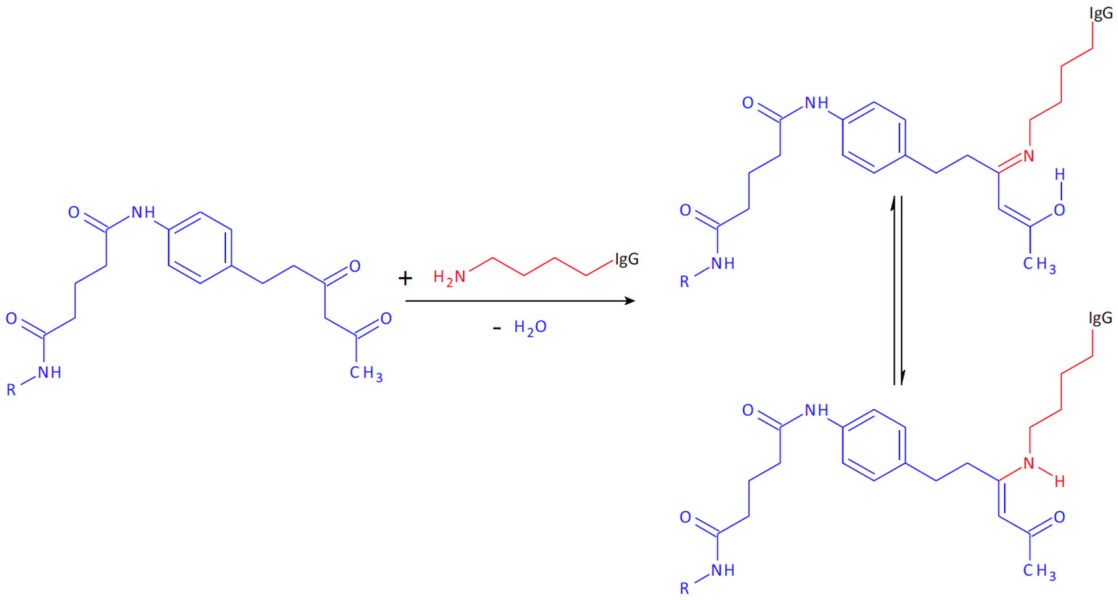

Figure 5: Conjugation of 1,3-diketone molecules to h38C2 (modified from Rader, 2014). The mAb h38C2 can be covalently and site-specifically conjugated to hapten-like molecules. The variable fragment contains a hydrophobic pocket with a reactive lysine (red) at its bottom. The lysine ε-amino group can be covalently conjugated to molecules derivatised with an electrophilic 1,3-diketone group (blue). Imine–enamine tautomerism stabilises the adduct.

The chemical reactivity of 38C2 can be used to conjugate synthetic hapten-compounds to its reactive lysine residue, equipping the cpAB with a specificity against a target antigen. Several antigens have been targeted with specifically programmed cpAB 38C2, either in the conventional immunoglobulin (IgG) format or as a bispecific antibody. This includes i) integrins $\alpha_v\beta_3$, $\alpha_v\beta_5$, $\alpha_v\beta_6$ and $\alpha_5\beta_1$ that can be targeted with peptidomimetics (Rader, Sinha, *et al.*, 2003; Guo *et al.*, 2006; Popkov *et al.*, 2006; Goswami *et al.*, 2011), ii) folate receptor alpha (FOLR1) with its natural small molecule ligand (Walseng *et al.*, 2016) or iii) receptors with peptide ligands such as the luteinizing hormone releasing hormone (LHRH) receptor, endothelin receptor A and κ opioid receptor (Doppalapudi *et al.*, 2007; Gavrilyuk *et al.*, 2009; Roberts *et al.*, 2012). Interestingly, the hapten-molecule can be designed to contain more than one targeting moiety. A cpAB programmed with such a compound can detect multiple antigens simultaneously, as was shown for 38C2 that detected both LHRH receptor and $\alpha_v\beta_3$ after programming with a bispecific cRGD/LHRH-compound (Gavrilyuk *et al.*, 2009). When the cpAB h38C2 was programmed with another bispecific hapten-molecule, which neutralises angiopeoietin-2 and vascular endothelial growth factor (VEGF), it reduced tumour growth in murine xenograft models. This conjugate proceeded to clinical testing (Doppalapudi *et al.*, 2010).

In total, four h38C2 conjugates, also referred to as CovX-Bodies, have been validated in phase I and II clinical trials. CVX-045 (mimics thrombospondin-1), CVX-060 (neutralises angiopoietin-2), CVX-241 (neutralises both angiopeoietin-2 and VEGF) were used for cancer immunotherapy while CVX-096 (mimics GLP1) was used for the treatment of type II diabetes mellitus (Rader, 2014). Monotherapy with CovX-Bodies was generally well tolerated but the clinical development has been discontinued because Pfizer, the company that acquired the CovX-Body platform in 2008, decided to prioritise other drugs.

1.5 Hypothesis and specific aims

Adoptive immunotherapy with T cells modified to express a CAR against CD19 has achieved high response rates in the treatment of B cell malignancies. However, antigen loss after treatment with monospecific CAR T cells can limit the durability of the response. Additionally, the often heterogeneous expression of tumour-associated antigens on solid tumours provides a rationale for simultaneous targeting of multiple antigens in order to extend the use of CAR T cells to solid malignancies. Accordingly, the objective of this study was to generate a single CAR construct that could be directed to recognise multiple antigens on tumour cells simultaneously or sequentially.

We hypothesised that, by modifying T cells to express a CAR that can be chemically programmed with hapten-molecules, the T cells could be directed against multiple antigens. Such a chemically programmable CAR (cpCAR) could thereby challenge the paradigm that one T cell has only one specific antigen.

In this study we pursued three specific aims to test this hypothesis.

I) To express a chemically programmable CAR, which could be programmed with hapten-molecules, in primary human T cells and to investigate the kinetics of hapten binding and release.

II) To determine the function of cpCAR T cells programmed with cRGD-hapten-molecules against integrin $\alpha_v\beta_3$ on tumour cells and to compare it with a conventional CAR that binds to integrin $\alpha_v\beta_3$ through an scFv.

III) To demonstrate that T cells expressing the cpCAR can be programmed to recognise multiple distinct antigens on tumour cells.

We selected the established cpAB h38C2 as basis for the design of the cpCAR. It has previously been shown that h38C2 can be programmed *in vitro* and *in vivo* with 1,3-diketone based hapten-molecules (Rader, Sinha, *et al.*, 2003). Integrin $\alpha_v\beta_3$ was chosen as the primary target antigen to evaluate cpCARs because it has previously been used to program h38C2 against tumour cells. We developed an experimental strategy to accomplish the specific aims of the study. First, we sought to establish integrin $\alpha_v\beta_3$ as a suitable target for CAR T cells. For this, we affirmed the expression

of integrin $\alpha_v\beta_3$ on hematologic and solid tumour cell lines. Cell lines offer a robust test system to investigate novel technologies. We then tested a panel of conventional scFv based $\alpha_v\beta_3$-CAR constructs to demonstrate that $\alpha_v\beta_3$ can be effectively targeted with CAR T cells. Further, this would provide a conventional $\alpha_v\beta_3$-CAR, we could later use to compare the anti-tumour efficacy of cpCAR T cells and conventional CAR T cells.

Thereafter, we designed a cpCAR based on the cpAB h38C2. The reactive centre of h38C2, which contains the reactive lysine that can form a covalent bond to 1,3-diketone molecules, is located in the V_H and V_L domains. To form the programmable domain of the cpCAR, both domains were merged as an scFv. We investigated if the cpCAR retained the function to be programmed with hapten-molecules.

Subsequently, we investigated if cpCAR T cells programmed to detect $\alpha_v\beta_3$ could mediate anti-tumour effects and compared their efficacy to conventional $\alpha_v\beta_3$-CAR T cells. The complexity of the utilised test systems was increased gradually, from *in vitro* studies with an immortal cpCAR reporter cell line to complex murine xenograft models with primary human cpCAR T cells.

To demonstrate the ability of the cpCAR to detect different antigens, we used synthetic hapten-molecules targeting integrin $\alpha_4\beta_1$ and FOLR1.

Demonstrating that cpCAR T cells can be programmed with hapten-molecules and mediate specific anti-tumour effects, preferably against multiple antigens, would suggest utility of cpCAR T cells in adoptive T cell therapy.

2 Materials

2.1 Human subjects

Peripheral blood was obtained from healthy donors after written informed consent to participate in research protocols approved by the Institutional Review Board of the University of Würzburg. Hematopoietic stem cells were obtained from healthy donors after written informed consent to participate in research protocols approved by the Institutional Review Board of the University of Frankfurt and were kindly provided by Dr. Halvard Bönig (University of Frankfurt/ Blutspendedienst DRK, Frankfurt, Germany)

2.2 Mouse Experiments

All mouse experiments were approved by the Institutional Animal Care and Use Committee of the University of Würzburg. Six- to 8-week old female NOD.Cg-*Prkdc*^{scid} *Il2rg*^{tm1Wjl}/SzJ (NSG) mice were obtained from Charles River (Sulzfeld, Germany).

2.3 Cell lines

Table 2: Cell lines

Name (RRID)	Supplier	Description
A-375 (RRID:CVCL_0132)	ATCC (Manassas, VA, USA)	malignant melanoma, transduced to express ffluc_GFP
A-549 (RRID:CVCL_0023)	Leibniz Institute DSMZ-German Collection of Microorganisms and Cell Cultures (Braunschweig, Germany)	lung adenocarcinoma, transduced to express ffluc_GFP
BW OKT3	Dr. P. Steinberger	BW5147 transduced with membrane-bound OKT3 scFv
BW5147 (RRID:CVCL_3896)	Dr. P. Steinberger	mouse lymphoma
JeKo-1 (RRID:CVCL_1865)	DSMZ	mantle cell lymphoma, transduced to express ffluc_GFP
Jurkat E6.1 (RRID:CVCL_0367)	DSMZ	childhood T acute lymphoblastic leukemia
K562 (RRID:CVCL_0004)	DSMZ	chronic myelogenous leukemia, transduced to express ffluc_GFP

Name (RRID)	Supplier	Description
K562_β_3	in-house production	K562 transduced to express integrin subunit β_3 and ffluc_GFP
Lenti-X 293T (RRID:CVCL_4401)	Takara Bio Europe SAS, Saint-Germain-en-Laye, France	subclone of the transformed human embryonic kidney cell line HEK 293
M14 (RRID:CVCL_1395)	Dr. B. Schilling	amelanotic melanoma
Malme-3M (RRID:CVCL_1438)	Dr. B. Schilling	melanoma
MDA-MB-231 (RRID:CVCL_0062)	DSMZ	breast adenocarcinoma, transduced to express ffluc_GFP
reporter cells	Dr. P. Steinberger	Jurkat E6.1 transduced with NF-κB and NFAT inducible reporter genes
THP-1 (RRID:CVCL_0006)	DSMZ	childhood acute monocytic leukemia
TM-LCL	Dr. S. Riddell	lymphoblastoid EBV-transformed B cell line
UACC-257 (RRID:CVCL_1779)	Dr. B. Schilling	melanoma
UACC-62 (RRID:CVCL_1780)	Dr. B. Schilling	melanoma

2.4 Media

Table 3: T cell medium

Ingredient	Volume (f.c.)
RPMI 1640 medium with 25 mM HEPES and L-Glutamine	500 ml
Human Serum (heat inactivated at 56 °C for 30 min)	50 ml (9 v/v %)
Penicillin/Streptomycin (10,000 U/ml)	5 ml (90 U/ml)
GlutaMAX Supplement (100 x)	5 ml (0.9 x)
2-Mercaptoethanol (50 mM)	0.5 ml (45 µM)

All ingredients were mixed and sterilised with 0.22 µm PES-membrane filter

Table 4: RPMI based tumour cell medium (cRPMI)

Ingredient	Volume (f.c.)
RPMI 1640 medium with 25 mM HEPES and L-Glutamine	500 ml
Fetal Calf Serum (heat inactivated)	50 ml (9 v/v %)
Penicillin/Streptomycin (10,000 U/ml)	5 ml (90 U/ml)
GlutaMAX Supplement (100 x)	5 ml (0.9 x)

All ingredients were mixed and sterilised with 0.22 µm PES-membrane filter

Table 5: DMEM based tumour cell line medium (cDMEM)

Ingredient	Volume (f.c.)
DMEM medium with 4,5 g/l glucose and 25 mM HEPES	500 ml
Fetal Calf Serum (heat inactivated)	50 ml (9 v/v %)
Penicillin/Streptomycin (10,000 U/ml)	5 ml (90 U/ml)
GlutaMAX Supplement (100x)	5 ml (0.9 x)

All ingredients were mixed and sterilised with 0.22 µm PES-membrane filter

Table 6: IMDM based tumour cell medium (cIMDM)

Ingredient	Volume (f.c.)
IMDM medium with 25 mM HEPES and L-Glutamine	500 ml
Fetal Calf Serum (heat inactivated)	50 ml (9 v/v %)
Penicillin/Streptomycin (10,000 U/ml)	5 ml (90 U/ml)
GlutaMAX Supplement (100x)	5 ml (0.9 x)

All ingredients were mixed and sterilised with 0.22 µm PES-membrane filter

Table 7: Freezing medium

Ingredient	Volume (f.c.)
Fetal Calf Serum (heat inactivated)	45 ml (90 v/v %)
DMSO	5 ml (10 v/v %)

2.5 Buffers

Table 8: MACS Buffer

Ingredient	Volume (f.c.)
DPBS	500 ml
Fetal Calf Serum (heat inactivated)	2.5 ml (0.5 v/v %)
EDTA (0.5 M)	2 ml (2 mM)

Table 9: FACS Buffer

Ingredient	Volume (f.c.)
DPBS	500 ml
Fetal Calf Serum (heat inactivated)	2.5 ml (0.5 v/v %)
EDTA (0.5 M)	2 ml (2 mM)
Sodium azide (1.5 M)	0.5 ml (1.5 mM)

Table 10: PBS/EDTA Buffer

Ingredient	Volume (f.c.)
DPBS	500 ml
EDTA (0.5 M)	2 ml (2 mM)

Table 11: TAE Buffer

Ingredient	Volume (f.c.)
TRIS-acetate-EDTA (TAE) 50x concentrate	20 ml (1x)

Mixed with 980 ml dH_2O

Table 12: Sucrose Buffer

Ingredient	Volume (f.c.)
Sucrose	20 w/v %

Dissolved in dH_2O and sterilised with filter (0.22 µm PES-membrane)

Table 13: TBS-5 Buffer

Ingredient	Volume (f.c.)
TRIS - HCl pH 7.8 (1 M)	50 mM
NaCl (5 M)	130 mM
KCl (1 M)	10 mM
$MgCl_2$ (1 M)	5 mM

Dissolved in cell culture grade H_2O and sterilised with filter (0.22 µm PES-membrane)

2.6 Plasmids

Table 14: Plasmids

Number	Name of transgene	Description
pLW0003	hLM609v7 short	epHIV7 plasmid, EF-1 promoter, GM-CSF signal peptide, hLM609v7 scFv, IgG4 hinge, CD28 transmembrane, CD28 intracellular domain, CD3ζ intracellular domain, T2A sequence, EGFRt transduction marker
pLW0004	hLM609v7 long	epHIV7 plasmid, EF-1 promoter, GM-CSF signal peptide, hLM609v7 scFv, IgG4 hinge-C_H2-C_H3, CD28 transmembrane, CD28 intracellular domain, CD3ζ intracellular domain, T2A sequence, EGFRt transduction marker
pLW0005	hLM609v11 short	epHIV7 plasmid, EF-1 promoter, GM-CSF signal peptide, hLM609v11 scFv, IgG4 hinge, CD28 transmembrane, CD28 intracellular domain, CD3ζ intracellular domain, T2A sequence, EGFRt transduction marker
pLW0006	hLM609v11 long	epHIV7 plasmid, EF-1 promoter, GM-CSF signal peptide, hLM609v11 scFv, IgG4 hinge-C_H2-C_H3, CD28 transmembrane, CD28 intracellular domain, CD3ζ intracellular domain, T2A sequence, EGFRt transduction marker

Number	Name of transgene	Description
pLW0011	β_3	epHIV7 plasmid, EF-1 promoter, integrin β_3, T2A sequence, EGFRt transduction marker
pLW1004	cpCAR	epHIV7 plasmid, EF-1 promoter, GM-CSF signal peptide, h38C2 scFv, IgG4 hinge, CD28 transmembrane, CD28 intracellular domain, CD3ζ intracellular domain, T2A sequence, EGFRt transduction marker
pJ01668	ffluc_GFP	epHIV7 plasmid, firefly luciferase, T2A sequence, GFP
pMH0171	EGFRt	epHIV7 plasmid, EF-1 promoter, GM-CSF signal peptide, EGFRt transduction marker
pCHGP-2	-	Packaging plasmid 1 for lentivirus production
pCMV-Rev2	-	Packaging plasmid 2 for lentivirus production
pCMV-G	-	Envelope plasmid for lentivirus production

2.7 Antibodies and reagents for flow cytometry

Table 15: Antibodies for flow cytometry

Antigen	Clone	Conjugate	Isotype	Supplier
CD3	HIT3a	FITC	mouse IgG2a, κ	BioLegend
CD4	M-T466	VioBlue	mouse IgG1, κ	Miltenyi
CD8	BW135/80	FITC	mouse IgG2a, κ	Miltenyi
CD8	BW135/80	VioBlue	mouse IgG2a, κ	Miltenyi
CD14	M5E2	APC/Cy7	Mouse IgG2a, κ	BioLegend
CD19	LT19	VioBlue	mouse IgG1, κ	Miltenyi
CD28	CD28.2	Pacific Blue	mouse IgG1, κ	BioLegend
CD29 (integrin β_1)	TS2/16	Alexa Fluor 647	mouse IgG1, κ	BioLegend
CD34	561	Brilliant Violet 421	mouse IgG2a, κ	BioLegend
CD45	HI30	APC	mouse IgG1, κ	BioLegend
CD45	HI30	APC/Cy7	mouse IgG1, κ	BioLegend
CD45RA	HI100	APC	mouse IgG2b, κ	BioLegend

Antigen	Clone	Conjugate	Isotype	Supplier
CD45RO	UCHL1	FITC	mouse IgG2a, κ	Miltenyi
CD49d (integrin α_4)	9F10	PE	mouse IgG1, κ	BioLegend
CD51 (integrin α_v)	NKI-N9	PE	mouse IgG2a, κ	BioLegend
CD51/CD61 (integrin $\alpha_v\beta_3$)	23C6	Alexa Fluor 647	mouse IgG1, κ	BioLegend
CD61 (integrin β_3)	VI-PL2	APC	mouse IgG1, κ	BioLegend
CD62L	DREG-56	PE	mouse IgG1, κ	BioLegend
CD80	2D10	APC	mouse IgG1, κ	BioLegend
CD270 (HVEM)	122	PE	mouse IgG1, κ	BioLegend
CD272 (BTLA)	MIH26	PE	mouse IgG2a, κ	BioLegend
CD279 (PD-1)	PD1.3.1.3	PE	mouse IgG2b, κ	Miltenyi
EGFR	C225 (Cetuximab)	-	human IgG1, κ	Bristol-Myers Squibb
EGFR	C225 (Cetuximab)	Biotin	human IgG1, κ	in-house
EGFR	C225 (Cetuximab)	Alexa Fluor 647	human IgG1, κ	in-house

Table 16: Isotype controls for flow cytometry

Isotype	Clone	Conjugate	Supplier
mouse IgG1, κ	MOPC-21	Alexa Fluor 647	BioLegend
mouse IgG1, κ	MOPC-21	APC	BioLegend
mouse IgG1, κ	MOPC-21	PE	BioLegend
mouse IgG2a, κ	MOPC-173	PE	BioLegend

Table 17: Reagents for flow cytometry

Reagent	Conjugate	Supplier
123count eBeads™	-	Thermo Fisher Scientific
7-AAD	-	BD Biosciences
Human TruStain FcX™	-	BioLegend
Streptavidin	PE	BioLegend

2.8 Reagents for cpCAR programming

Table 18: Reagents for cpCAR programming

Designation	Supplier	Chemical name
biotin-DK	Dr. C. Rader	1,3-diketone-biotin
CN-31	Dr. C. Rader	LLP2A-biotin-diketone
DH-11	Dr. C. Rader	cRGD-$[PEG]_2$-diketone
DH-12	Dr. C. Rader	cRGD-$[PEG]_4$-diketone
DH-13	Dr. C. Rader	cRGD-$[PEG]_6$-diketone
DH-14	Dr. C. Rader	cRGD-$[PEG]_8$-diketone
folate-DK	Dr. C. Rader	folate-biotin-diketone

The chemical structure of each compound is depicted as a figure in the results section.

2.9 Chemicals, reagents and solutions

Table 19: Chemicals, reagents and solutions

Name	Company, Location
2-Mercaptoethanol (50 mM)	Thermo Fisher Scientific, Darmstadt
Ampicillin Sodium Salt	AppliChem, Darmstadt
Anti-biotin MicroBeads	Miltenyi, Bergisch Gladbach
Anti-CD62L MicroBeads	Miltenyi, Bergisch Gladbach
Biocoll Separation Solution, isotone	Merck, Darmstadt
Carbenicillin Ready Made Solution (100 mg/ml)	Sigma-Aldrich, Steinheim
CD3 pure - functional grade, human (clone OKT3)	Miltenyi, Bergisch Gladbach
Dimethyl sulfoxide (DMSO)	AppliChem, Darmstadt
D-Luciferin firefly, Potassium Salt	Biosynth, Staad, Switzerland
DMEM (Dulbecco's Modified Eagle Medium) with 4,5 g/l glucose and 25 mM HEPES	Thermo Fisher Scientific, Darmstadt
DPBS (Dulbecco's Phosphate-Buffered Saline) without calcium and magnesium	Thermo Fisher Scientific, Darmstadt
Dynabeads® Human T-Activator CD3/CD28	Thermo Fisher Scientific, Darmstadt
Ethanol absolute	AppliChem, Darmstadt
Ethylenediaminetetraacetic acid (EDTA) (0.5 M)	Thermo Fisher Scientific, Darmstadt
Fetal Calf serum (heat inactivated)	Thermo Fisher Scientific, Darmstadt
GlutaMAX Supplement (100x)	Thermo Fisher Scientific, Darmstadt
Glutamine 200 mM	Life Technologies, Darmstadt
HEPES 1M	Life Technologies, Darmstadt
Human serum	DRK-Blutspendedienst

Name	Company, Location
IMDM (Iscove's Modified Dulbecco's Medium) with 25 mM HEPES and L-Glutamine	Thermo Fisher Scientific, Darmstadt
Ionomycin calcium salt	Sigma-Aldrich, Steinheim
Isopropyl alcohol	Sigma-Aldrich, Steinheim
LB Agar Plates with 100 µg/ml Carbenicillin 100 mm	TEKnova (distributed by Thermo Fisher Scientific, Darmstadt)
Methanol	Sigma-Aldrich, Steinheim
PBS-Tween tablets	Millipore, Billerica
Penicillin/Streptomycin (10,000 U/ml)	Thermo Fisher Scientific, Darmstadt
Phorbol 12-myristate 13-acetate (PMA)	Sigma-Aldrich, Steinheim
Polybrene (10 mg/ml)	Merck, Darmstadt
Recombinant human IL-2 (PROLEUKIN® S)	Novartis, Basel, Switzerland
Rimadyl	Zoetis Deutschland, Berlin
RPMI 1640 Medium, GlutaMAX™ Supplement, HEPES	Thermo Fisher Scientific, Darmstadt
Sodium azide (NaN_3) pure	AppliChem, Darmstadt
Sucrose analytical grade	Serva, Heidelberg
TRIS-acetate-EDTA (TAE) 50x	Sigma-Aldrich, Steinheim
Trypan Blue Solution, 0.4%	Thermo Fisher Scientific, Darmstadt
Trypsin EDTA (0.05%), phenol red	Thermo Fisher Scientific, Darmstadt
UltraPure™ Agarose	Thermo Fisher Scientific, Darmstadt
Water cell culture grade	AppliChem, Darmstadt
Water molecular biology grade	AppliChem, Darmstadt

2.10 Commercially available kits

Table 20: Commercially available kits

Name	Company, Location
Alexa Fluor™ 647 Protein Labeling Kit	Thermo Fisher Scientific, Darmstadt
$CD4^+$ T Cell Isolation kit, human	Miltenyi, Bergisch Gladbach
$CD8^+$ Memory T Cell Isolation kit, human	Miltenyi, Bergisch Gladbach
$CD8^+$ T Cell Isolation kit, human	Miltenyi, Bergisch Gladbach
CellTrace™ CFSE Cell Proliferation Kit, for flow cytometry	Thermo Fisher Scientific, Darmstadt
Cytokine Human Magnetic 10-Plex Panel	Thermo Fisher Scientific, Darmstadt
ELISA MAX™ Deluxe Set, human IFNγ	BioLegend, San Diego
ELISA MAX™ Deluxe Set, human IL-2	BioLegend, San Diego

Name	Company, Location
EZ-Link™ Sulfo NHS-SS Biotinylation Kit	Thermo Fisher Scientific, Darmstadt
MAGPIX ® Calibration Kit	Luminex Corporation, Austin
MAGPIX ® Performance verification Kit	Luminex Corporation, Austin
Nucleobind ® Xtra Maxi EF	MACHEREY-NAGEL, Düren

2.11 Consumables

Table 21: Consumables

Name	Company, Location
Cell culture flasks 25 and 75 cm^2 surface area	Corning, Kaiserslautern
Centrifuge tubes Thinwall 38.5 ml	Beckman Coulter, Krefeld
Conical glass flask 500 ml	DWK Life Sciences, Wertheim am Main
Dish Nunclon™ Delta 10 cm	Thermo Fisher Scientific, Darmstadt
Falcon® tube conical bottom 175 ml	Corning, Kaiserslautern
Filter tips 2.5, 10, 20, 200 and 1000 µl	Sarstedt, Nümbrecht
Flow cytometry tubes 5 ml	Sarstedt, Nümbrecht
Half-area plate 96-Well	Corning, Kaiserslautern
Leucosep tubes 50 ml	Greiner Bio-One, Frickenhausen
MACS cell separation LS Columns	Miltenyi, Bergisch Gladbach
PARAFILM® M	Sigma-Aldrich, Steinheim
PCR Single Cap Soft Strips 0.2 ml	Biozym, Hessisch Oldendorf
Plate flat bottom 96-Well	Corning, Kaiserslautern
Plates U bottom 24-, 48- and 96-Well	Corning, Kaiserslautern
SafeSeal micro tubes 1.5 and 2 ml	Sarstedt, Nümbrecht
Serological pipettes 2, 5, 10, 25 and 50 ml	Greiner Bio-One, Frickenhausen
Sterile Syringe Filter 0.45 µm	Sarstedt, Nümbrecht
Sterile filtration vacuum tube 50 ml 0.45 µm	Merck, Darmstadt
Sterile syringe 20 ml	B. Braun, Melsungen
Suspension TC-plate 12-Well	Sarstedt, Nümbrecht
Tubes conical bottom 15 and 50 ml	Greiner Bio-One, Frickenhausen
Tube with ventilation cap 13 ml	Sarstedt, Nümbrecht
Vacuum Filter PES 0.22 µm	Sarstedt, Nümbrecht
White flat bottom plate 96-Well	Corning, Kaiserslautern

2.12 Equipment

Table 22: Equipment

Name	Company, Location
Biological safety cabinet Herasafe™ KS	Thermo Fisher Scientific, Darmstadt
Cell Sorter FACSAria™ III	BD Biosciences, Heidelberg
Centrifuge Heraeus™ Megafuge™ 40R	Thermo Fisher Scientific, Darmstadt
CO_2 Incubators Heracell™ 150i and 240i	Thermo Fisher Scientific, Darmstadt
DynaMag™-15 magnet	Thermo Fisher Scientific, Darmstadt
Electrophoresis chamber system	Febikon, Wermelskirchen
Flow cytometer FACSCanto™ II	BD Biosciences, Heidelberg
Gel imaging system ChemiDoc™ MP	Bio-Rad, München
Heating block neoBlock 1	neoLab, Heidelberg
Ice maker	Scotsman, Vernon Hills, IL, USA
Irradiator Faxitron CP-160	Faxitron Bioptics, Tucson, AZ, USA
Microcentrifuge Fresco 17	Thermo Fisher Scientific, Darmstadt
Microscope Primo Vert	ZEISS, Jena
Mr. Frosty™ Freezing Container	Thermo Fisher Scientific, Darmstadt
Multiplate reader Infinite 200 PRO	TECAN, Männedorf, Switzerland
Orbital Compact Digital Microplate shaker	Thermo Fisher Scientific, Darmstadt
PCR Mastercycler ep Gradient S	Eppendorf, Hamburg
Pipette controller accu-jet® pro	Brand, Wertheim am Main
Pipettes Eppendorf Research plus 2.5, 10, 20, 200 and 1000 µl	Eppendorf, Hamburg
Plate washer HydroSpeed™	TECAN, Männedorf, Switzerland
Power supply E802	Consort, Turnhout, Belgium
Refrigerator -4 and -20 °C	Liebherr, Bulle, Switzerland
Rocking shaker DRS-12	neoLab, Heidelberg
Shaker incubator	INFORS HT, Basel, Switzerland
Ultracentrifuge Sorvall WX80	Thermo Fisher Scientific, Darmstadt
Ultra-low temperature freezer -80 °C FORMA 900	Thermo Fisher Scientific, Darmstadt
UV transilluminator	neoLab, Heidelberg
Water bath	Memmert, Schwabach

2.13 Software

Table 23: Software

Software	Application	Company
FACS Diva 6.1.3	Flow cytometry	BD Biosciences, Heidelberg
GraphPad Prism 6.07	Statistical analysis	La Jolla, CA, USA
FlowJo X 10.0.7	Flow cytometry analysis	Tree Star Inc. Ashland, OR, USA
iControl 1.12	Luminescence and protein analysis	TECAN, Männedorf, Switzerland

3 Methods

3.1 Culture of cell lines and primary human T cells

The adherent cell lines Lenti-X 293T and A-375 were cultured in cDMEM medium and A-549, M14, Malme-3M, MDA-MB-231, UACC-257 and UACC-62 were cultured in cRPMI medium in 25 cm^2 or 75 cm^2 cell culture flasks. The suspension cell lines BW5147, BW OKT3, JeKo-1, Jurkat E6.1, K562, K562_β_3, THP-1 and TM-LCL cells were cultured in cRPMI medium and reporter cells were cultured in cIMDM medium in 25 cm^2 or 75 cm^2 cell culture flasks.

Primary human T cells were cultured in T cell medium supplemented with 50 U/ml recombinant human IL-2 depending on cell density in 6-, 12-, 24-, 48- or 96-well plates or in 25 cm^2 cell culture flasks. After 2 - 3 days, a half-medium change was conducted, whereby half of the medium was replaced with fresh T cell medium supplemented with 50 U/ml recombinant human IL-2.

3.2 Generation of CAR-modified T cell and tumour cell lines

3.2.1 Construction of lentiviral expression plasmids

For generation of lentiviral expression vectors containing CAR transgenes, codon optimised scFvs based on the mABs h38C2, hLM609v7 and hLM609v11 were synthesized (GeneArt, Thermo Fisher Scientific, Regensburg) (Rader, Cheresh and Barbas, 1998; Rader, Turner, *et al.*, 2003). The synthesized fragments contained a $(G_4S)_3$ linker for joining the V_H and V_L chains. The fragments were cloned into previously described epHIV7-based vectors containing CD19-CARs, using the restriction enzymes NheI and RsrII (GeneArt), thereby replacing the CD19-scFv (Hudecek *et al.*, 2015). The finale CAR-transgenes contained the respective scFvs either fused to a long (IgG4 hinge-C_H2-C_H3, 229 aa) or short (IgG4 hinge only, 12 aa) extracellular spacer domain, adjoined by a CD28 transmembrane domain, and the cytoplasmic signalling domains of CD28 and CD3ζ. *In cis*, a truncated epidermal growth factor receptor (EGFRt) was expressed using a T2A element (Wang *et al.*, 2011).

A lentiviral expression vector containing integrin subunit β_3 was generated by synthesising (GeneArt) the codon optimised cDNA sequence derived from the Universal Protein Resource Knowledgebase (UniProtKB) (identifier: P05106-1). The fragment was cloned into the epHIV7 expression vector with the restriction enzymes

NheI and BspEI (GeneArt) replacing the CAR transgene. EGFRt was expressed *in cis* using a T2A element.

3.2.2 Amplification of plasmids by *Escherichia coli*

One Shot™ TOP10 Chemically Competent *E. coli* were transformed with DNA plasmids according to the manufacturer's instructions (heat shock at 42 °C for 30 s). After the heat shock 250 µl SOC medium were added to the bacteria. Following incubation at 37 °C for 1 h, 40 µl of the *E. coli* solution were pated on LB agar plates with 100 µg/mL carbenicillin and cultured over night at 37 °C. A bacterial colony was picked to inoculate 5 ml LB medium supplemented with 50 µg/ml carbenicillin which was incubated at 37 °C. Six h later, 1 ml of the bacterial culture were added to 170 ml LB medium supplemented with 100 µg/ml ampicillin and cultured over night at 37 °C. The NucleoBond® Xtra Maxi EF Kit (Macherey-Nagel) was used according to the manufacturer's instructions to isolate plasmid DNA from *E. coli* cells. Plasmid DNA was eluted in cell culture grade water.

3.2.3 Lentiviral vector production

The Lenti-X 293T cell line was used to produce lentiviral vectors. Six million Lenti-X 293T cells were seeded in cDMEM medium per 100 mm dish and incubated for 6 h at 37 °C. Transfection was performed with the CalPhos Mammalian Transfection Kit (Takara) according to manufacturer's instruction. 15 µg of the epHIV7 lentiviral expression plasmids were mixed with 10 µg of pCHGP-2, 1 µg of pCMV-Rev2 and 2 µg of pCMV-G helper plasmids in 2 M $CaCl_2$. An equal volume of 2x HEPES-buffered saline was added. After 20 min incubation at room temperature, the solution was added drop-wise to the Lenti-X 293T dishes. The plates were incubated over night at 37 °C, then the cells were washed with PBS and cultured in fresh cDMEM medium for two days. For harvesting the virus particles, the cell culture supernatant was centrifuged at 2160 x g for 15 min at 8 C, filtered through a sterile 0.45 µm vacuum filter, transferred to a Thinwall centrifuge tube and underlaid with Sucrose Buffer. Virus particles were pelleted by centrifugation at 138 510 x g for 2 h and then dissolved in TBS-5 Buffer. Aliquots of 20 µl were frozen on dry ice and stored at -80 °C.

3.2.4 Determination of the lentivirus titre

Jurkat cells were used to determine the quantity of transforming units (TU) in the lentivirus preparations. In a 48-well plate, 2.5 x10^5 cells were seeded per well in 250 µl cRPMI medium supplemented with 5 µg/ml polybrene. Different volumes (0.1 µl, 0.5 µl, 1 µl, 2.5 µl, 5 µl and 10 µl) of the lentivirus preparation were added. After 4 h incubation at 37 °C, the total volume was adjusted to 1000 µl with cRPMI. Subsequently, after 48 h incubation at 37 °C, the expression of the transduction marker EGFRt was assessed by flow cytometry, because EGFRt was co-expressed via a T2A sequence with the transgenes. The lentivirus titre as TU/µl was calculated from the flow cytometry data with the following equation:

$$\text{titre [TU/µl]} = \frac{\text{cell count at time of transduction x EGFRt+ ratio}}{\text{volume of virus added [µl]}}$$

3.2.5 Isolation of human peripheral blood mononuclear cells

Density gradient centrifugation with Biocoll separation solution was used to isolate peripheral blood mononuclear cells (PBMCs) from blood of healthy donors. 50 ml Leucosep tubes were equilibrated with room temperature Biocoll separation solution by centrifugation. Meanwhile, room temperature DPBS was added to donor blood samples up to a final volume of 35 ml. The mixture was transferred to an equilibrated Leucosep tube and centrifuged at 310 x g for 15 min at 22 °C, with acceleration level 9 and break level 2. After centrifugation, the white phase on top of the porous barrier, which contained the PBMCs, was carefully extracted and washed twice with 4 °C PBS/EDTA Buffer by centrifugation (220 x g for 10 min at 4 °C). Dependent on downstream application, PBMCs were resuspended in MACS Buffer or T cell medium.

3.2.6 Isolation of primary human T cells from PBMCs

All primary T cell subsets were isolated from PBMCs by magnetic cell separation using the MACS MicroBead technology (Miltenyi) according to the manufacturer's instructions. Untouched $CD4^+$ bulk T cells, $CD8^+$ bulk T cells and $CD8^+$ memory T cells ($CD45RA^-$, $CD45RO^+$) were collected by negative selection using the respective kits (Miltenyi). $CD8^+$ central memory T cells were obtained from previously isolated $CD8^+$ memory T cells by positive selection for CD62L (Miltenyi). The cell separation was performed with LS columns (Miltenyi). Isolated T cells were resuspended in T cell medium supplemented with 50 U/ml recombinant human IL-2.

3.2.7 Transduction of primary T cells and cell lines with lentiviral vectors

0.5 - 1.0x10^6 $CD4^+$ bulk, $CD8^+$ bulk or $CD8^+$ central memory T cells were seeded per well in a 48-well plate in 1 ml T cell medium supplemented with 50 U/ml IL-2 at the day of cell isolation. T cells were activated with anti-CD3/CD28 Dynabeads (Thermo Fisher Scientific) at a bead to cell ratio of 1:1. The following day, 650 µl of the medium were removed and polybrene was added to a final concentration of 5 µg/ml. Lentiviral vectors were added at a multiplicity of infection (MOI) of 5. T cells were spinoculated by centrifugation at 800 x g for 45 min at 32 °C, followed by incubation for 4 h at 37 °C. Then the volume was filled up to 1 ml with pre-warmed T cell medium supplemented with 50 U/ml IL-2 and T cells were incubated at 37 °C. Every second day, a half-medium change was conducted with T cell medium supplemented with 50 U/ml IL-2. The density of the T cells was observed daily by microscopy and, if necessary, the T cells were transferred into larger vessels. Six days after transduction, anti-CD3/CD28 Dynabeads were removed (Thermo Fisher Scientific). Subsequently, transgene expression on primary T cells was analysed by flow cytometry.

Suspension tumour cell lines were transduced by adding 0.25x10^6 cells in 250 µl culture medium supplemented with 5 µg/ml polybrene to one well of a 48-well plate. Lentiviral vectors were added at an MOI of 3 or 5 to the cells. After 4 h incubation at 37 °C, the volume was filled up to 1 ml with pre-warmed medium. Transduced cells where incubated at 37 °C until analysis of transgene or transduction marker expression by flow cytometry.

For transduction of adherent tumour cell lines, 1x10^6 and 2x10^6 tumour cells were seeded in the appropriate medium in a 24-well plate and incubated at 37 °C. The following day, cell confluence was assessed by microscope and wells with a confluence between 70 % - 90 % were selected for transduction. The medium was replaced with 400 µl fresh medium supplemented with 5 µg/ml polybrene. Lentiviral vectors were added at an MOI of 3 or 5. After 4 h incubation at 37 °C, the volume was filled up to 2 ml with pre-warmed medium. Transduced cells were incubated at 37 °C until analysis of transgene or transduction marker expression was assessed by flow cytometry.

3.2.8 Enrichment of transgene-positive T cells and tumour cells

T cells and tumour cells were enriched for transgene-expressing cells by positive selection using the transduction marker EGFRt and the MACS MicroBead technology (Miltenyi). EGFRt-positive cells were labelled with the in-house biotinylated (Thermo Fisher Scientific) mAB cetuximab (Bristol-Myers Squibb, New York, USA). Then, Anti-Biotin MicroBeads (Miltenyi) were used according to the manufacturer's instructions and separation was performed with LS columns (Miltenyi). Enriched cells were suspended in their appropriate medium and cultured (tumour cells) or expanded (T cells).

3.2.9 Antigen-independent expansion of T cells

T cells were expanded using irradiated feeder cells and anti-CD3 mAB (OKT3, Miltenyi) as described previously (Riddell and Greenberg, 1990). In brief, $5x10^4$ T cells, $5x10^6$ irradiated TM-LCL (80 Gy) and $30x10^6$ irradiated PBMCs (30 Gy) were mixed in T cell medium and OKT3 was added to a final concentration of 30 ng/ml. After overnight incubation at 37 °C, recombinant IL-2 was added to a final concentration of 50 U/ml. On day 4, a complete medium change was conducted with T cell medium supplemented with 50 U/ml recombinant IL-2. Subsequently, half-medium changes were performed every second day and the phenotype of T cells was analysed by flow cytometry between day 8 and day 14.

3.3 Functional analysis of CAR-modified T cell and tumour cell lines *in vitro*

3.3.1 Quantification of tumour cell lysis

The lysis of ffluc_GFP-transduced target cells was determined in a bioluminescence-based assay described elsewhere (Brown *et al.*, 2005) In brief, $5x10^3$ target cells and $CD8^+$ T cells at the indicated effector:target cell ratios were mixed in 200 µl cRPMI supplemented with 0.15 mg/ml D-Luciferin substrate. When experiments with cpCAR T cells were performed, hapten-compounds were added to the samples. Three technical replicates were applied to a 96-well plate. After 4 h of incubation at 37 °C, the luminescence signal was measured with an Infinite 200 PRO plate reader (Tecan, Männedorf, Switzerland). Specific lysis conferred by CAR T cells was calculated using the following formula, values from wells with tumour cells and untransduced T cells were used as a reference.

$$\text{specific Lysis (\%)} = \frac{\text{Mean (target cells + reference T cells) - Single value (target cells + modified T cells)}}{\text{Mean (target cells + reference T cells)} \times 100}$$

3.3.2 Quantification of $CD34^+$ hematopoietic stem cell survival by flow cytometry

The lysis of $CD34^+$ hematopoietic stem cells (HSCs) was assessed in a flow cytometry-based assay. $5x10^3$ HSCs and T cells were co-cultured at the indicated effector:target cell ratios for 4 h and 24 h. After incubation, samples were stained with mABs against CD34 and CD3 to discriminate T cells and HSCs, and 7-AAD to discriminate live and dead cells. 123count eBeads (ThermoFisher) were used according to the manufacturer's instructions to determine the number of live HSCs.

3.3.3 Quantification of cytokine release by ELISA and multiplex

$1x10^5$ T cells were mixed with target cells (effector:target cell ratio = 5:1) in 200 µl cRPMI medium. When experiments with cpCAR T cells were performed, hapten-compounds were added. After 22 h incubation at 37 °C, the cell culture supernatants were harvested and frozen at -20 °C. ELISAs (BioLegend) were performed to quantify the IFN-ɣ and IL-2 concentration. Absorption was measured with an Infinite 200 PRO plate reader. Cytokine concentrations were calculated based on a standard curve with 5-parameter logistic curve fitting.

Cytokine concentrations in mouse serum samples were assessed by a multiplex cytokine immunoassay (Luminex). 10 cytokines were measured simultaneously by using the Cytokine Human Magnetic 10-Plex Panel (Thermo Fisher Scientific) and a MAGPIX-Luminex reader (Luminex Corporation) according to the manufacturer's instructions.

3.3.4 Quantification of T cell proliferation

For analysis of proliferation, T cells were first labelled with 0.1 µM carboxyfluorescein succinimidyl ester (CFSE, ThermoFisher). Then $5x10^4$ CFSE-labelled T cells were mixed with irradiated tumour cells (effector:target cell ratio = 5:1) in 200 µl T cell medium and incubated at 37° C. When experiments with cpCAR T cells were performed, hapten-compounds were added prior to incubation. After 72 h, T cells were labelled with mABs against CD4 and CD8. The samples were measured by flow cytometry and the division of T cells was assessed by CFSE dilution. The proliferation index was calculated using the standard formula.

3.3.5 Quantification of NFAT and NF-κB activation with reporter cells

Reporter cells ($5x10^4$) and target cells ($1.5x10^4$) were mixed in 100 µl cIMDM medium, applied as duplicates to a 96-well plate. When experiments with cpCAR T cells were performed, hapten-compounds were added. After incubation at 37 °C for 24 h, the samples were stained with APC-conjugated anti-CD45 mAB to distinguish between target cells and reporter cells. Reporter gene activation was assessed by flow cytometry as CFP and GFP signal. The CFP and GFP signals mediated by reporter cells after co-culture with target cells were normalised to the signals of the same reporter cell line upon stimulation with BW OKT3 cells, while the signal generated against BW5147 cells was deducted as blank value.

3.3.6 Programming of cpCAR T cells and reporter cells with biotin-DK

$2x10^5$ T cells or reporter cells in 100 µl of their culture medium or DPBS with 0.5 % FCS were transferred to a 5 ml FACS tube. The biotin-DK compound was added and the tube was sealed with PARAFILM M (Sigma-Aldrich) and incubated at the indicated temperature for the indicated time. After incubation, the cells were washed twice with FACS Buffer and stained with streptavidin-phycoerythrin (SA-PE). Programming was assessed as PE signal by flow cytometry.

3.4 *In vivo* xenograft experiments

Murine xenograft models were conducted in female NSG mice (Charles River) that were at least 8 weeks old at the day of tumour injection. Generally, $1x10^6$ A-375/ffluc_GFP cells were injected into the tail vein on day 0. On day 7, engraftment of the tumour cells was verified by bioluminescence imaging. Mice were randomly assigned to treatment cohorts and treated with $2.5x10^6$ $CD8^+$ and $2.5x10^6$ $CD4^+$ T cells, either unmodified or modified to express a CAR, by tail vein injection or remained untreated. Bioluminescence imaging was performed weekly and at indicated time points using an IVIS Lumina (PerkinElmer) after mice received 0.3 mg/g body weight D-Luciferin i.p. (Biosynth). Data analysis was performed using Living Image Software (PerkinElmer). The experimental endpoint was reached, when mice presented with either >20% weight loss or when bioluminescence exceeded $3x10^7$ p/s/cm²/sr.
Human T cells in bone marrow, peripheral blood and spleen were analysed by flow cytometry and cytokine concentrations in mouse serum were assessed using a MAGPIX-Luminex reader (Luminex Corporation).

3.4.1 Xenograft with hLM609-CAR T cells

On day 7 after tumour inoculation, groups of n = 6 mice received either unmodified T cells, T cells modified to express hLM609v7 short or hLM609v11 short CARs or remained untreated (n = 2). Blood samples of mice were obtained on day one after T cell transfer for analysis of cytokine levels in serum and on day 3 and day 7 after T cell transfer for flow cytometry analysis.

3.4.2 Xenograft with cpCAR T cells programmed *in vivo* by cRGD-DK injections

Mice were injected with $1x10^6$ A-375/ffluc_GFP$^+$ tumour cells i.v. as well as $1x10^6$ A-375/ffluc_GFP$^+$ tumour cells i.p. and because of the higher amount of T cells located in the abdomen, the threshold for radiance was adjusted to $1x10^{10}$ p/s/cm²/sr for this experiment. Groups of n = 4 mice either received untransduced, hLM609v7 short CAR or cpCAR T cells. One group of animals treated with untransduced T cells and two groups treated with cpCAR T cells received injections of 20.5 µg DH-12 either i.v. or i.p. on days 7, 9, 11, 14, 16 and 18. Blood samples of mice were obtained on day 7 after T cell transfer for flow cytometry analysis.

At day 22, mice from the groups that received untransduced T cells + DH-12 i.p., cpCAR T cells, cpCAR T cells + DH-12 i.p., cpCAR T cells + DH-12 i.v. were randomly reassigned to new groups of n = 2 mice. Mice were treated with an additional dose of $5x10^6$ T cells i.p., either untransduced, or modified to express hLM609v7/short CAR or cpCAR. Mice of the cpCAR groups received injections of DH-12 (c_I = 205 µg/ml, c_{II} = 62.5 µg/ml, c_{III} = 20.5 µg/ml, c_{IV} = 6.25 µg/ml, c_V = 2.05 µg/ml, c_{VI} = 0.625 µg/ml) i.p. on day 22 and day 24. Blood samples of mice were obtained on day 28 after the initial T cell transfer for flow cytometry analysis.

3.4.3 Xenograft with cpCAR T cells programmed *in vivo* with cRGD-DK compound released by osmotic pumps

On day 7 after tumour inoculation, groups of n = 3 mice received either unmodified T cells or T cells modified to express hLM609v7/short CAR or cpCAR. Four groups of n = 2 mice received cpCAR T cells and were also implanted with an osmotic pump (Alzet, Model 1007d). Pumps were loaded with 250 ng, 25 ng, 2.5 ng or 0.25 ng DH-14 compound solved in Ampuwa water for injection (Fresenius). Pumps were implanted s.c. in the neck area of each mouse. After surgery, mice were treated with Rimadyl (Zoetis Deutschland) to reduce pain. The pumps were removed 8 days after they were implanted.

3.4.4 Xenograft with cpCAR T cells programmed *in vitro* with cRGD-DK

On day 7 after tumour inoculation, groups of n = 5 mice either received unmodified T cells or T cells modified to express the hLM609v7 short CAR, the cpCAR or the cpCAR pre-programmed with DH-14. For *in vitro* pre-programming, 1 µM DH-14 was added to $CD4^+$ and $CD8^+$ T cells in T cell medium and incubated for 1 h at 37 °C. Cells were washed twice with DPBS supplemented with 0.5 % FCS and stored on ice until injection into mice. Blood samples of mice were obtained on day 7 after the initial T cell transfer for flow cytometry analysis

3.5 Statistical analysis

Statistical analyses were performed with GraphPad Prism 6.07 software. For *in vitro* cytokine release and proliferation assays, the statistical significance of n = 3 experiments with T cells from n = 3 healthy donors was evaluated by two-way ANOVA with Tukey's multiple comparison test. For reporter assays, the statistical significance of n = 3 experiments was evaluated by two-way ANOVA with Sidak's multiple comparison test. For programming of cpCAR reporter cells with biotin-DK, the statistical significance of n = 4 experiments was evaluated with Mann-Whitney test. *In vivo* cytokine secretion was evaluated by Kruskal-Wallis test with Dunn's multiple comparison test, and survival was evaluated by Mantel-Cox test with Bonferroni corrected threshold. Results with $p<0.05$ were considered significant.

4 Results

4.1 An integrin $\alpha_v\beta_3$-targeting CAR with an scFv derived from mAB LM609

4.1.1 Expression of $\alpha_v\beta_3$ on solid and hematologic tumour cell lines and healthy haematopoietic cell subsets

First, we analysed expression of the integrin $\alpha_v\beta_3$ complex on a panel of tumour cell lines by flow cytometry. We stained the cells with mAB 23C2, which detects integrin heterodimers, in order to select cell lines with different expression levels for subsequent experiments (Figure 6).

We detected high integrin $\alpha_v\beta_3$ surface expression on melanoma cell lines A-375, UACC-62, UACC-257, Malme-3M and M14 as well as on the triple-negative breast cancer cell line MDA-MB-231. All of these cell lines had fold MFI (xMFI = $MFI_{mAB}/MFI_{isotype}$) ratios of >7. Intermediate expression was observed for the T cell acute lymphoblastic leukaemia (ALL) cell line Jurkat (xMFI = 3.6). Chronic myelogenous leukaemia (CML) cell line K562, mantle cell lymphoma (MCL) cell line JeKo-1, lung adenocarcinoma cell line A-549 and acute monocytic leukemia cell line THP-1 showed a minor shift of MFI after staining with the anti-$\alpha_v\beta_3$ mAB as compared to the isotype control (xMFI = 1.8 - 2.0). To discriminate if this minor shift was due to low level expression of the $\alpha_v\beta_3$ integrin complex or unspecific interaction of the staining mAB, we further analysed the expression of α_v and β_3 subunits on these tumour cells (Figure 7 A+B). We detected high levels of the integrin subunit α_v on the cell surface of K562 and A-549, but none on JeKo-1 cells. A-549 and THP-1 cells did not express the subunit β_3. A subset of K562 cells expressed low levels of the integrin subunit β_3. Transduction of K562 with the integrin subunit β_3 (K562_β_3) led to high $\alpha_v\beta_3$ expression (xMFI = 13.3).

To complete the expression analysis, we investigated integrin $\alpha_v\beta_3$ levels on the surface of healthy hematologic cells. We did not detect $\alpha_v\beta_3$ integrin on T-lymphocytes, monocytes or B-lymphocytes (Figure 8). In addition, mobilised CD34-positive hematopoietic stem cells expressed neither the $\alpha_v\beta_3$ integrin complex nor either of the two subunits (Figure 9).

Together, these data confirmed the prior notion, that integrin $\alpha_v\beta_3$ is expressed on tumour cells of multiple cancer entities. We selected A-549 as negative control, K562 as low-expressing and UACC-62, UACC-257, K562_β_3, MDA-MB-231 and A-375 as high-expressing target cell lines for our subsequent experiments.

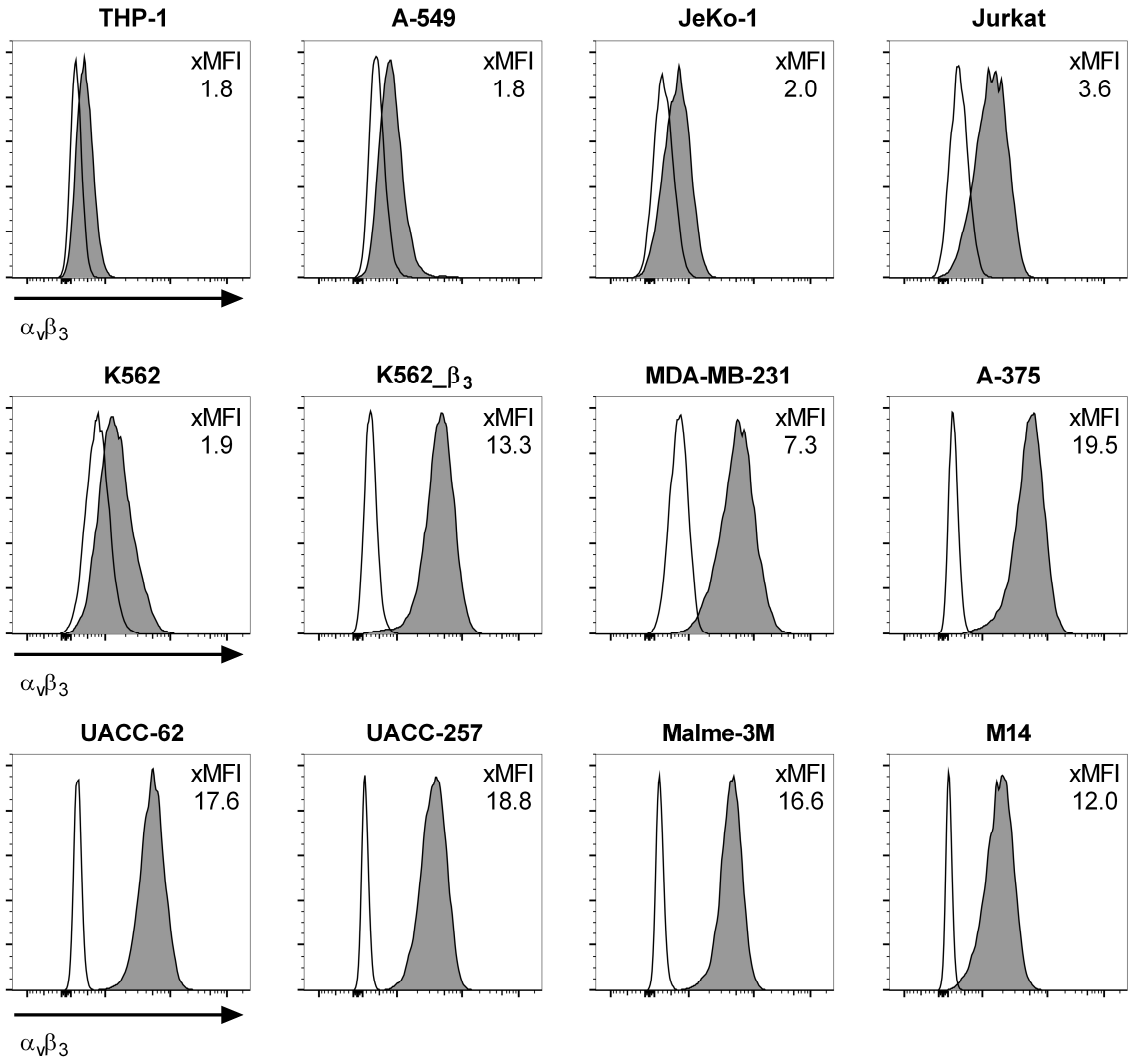

Figure 6: Expression of integrin $\alpha_v\beta_3$ on solid and hematologic tumour cell lines.
Flow cytometric analysis of $\alpha_v\beta_3$-heterodimer expression on tumour cell lines. The ratio between the geometric mean fluorescent intensity of anti-$\alpha_v\beta_3$ mAB (dark grey) and their corresponding isotype controls (clear) is provided as fold MFI (xMFI).

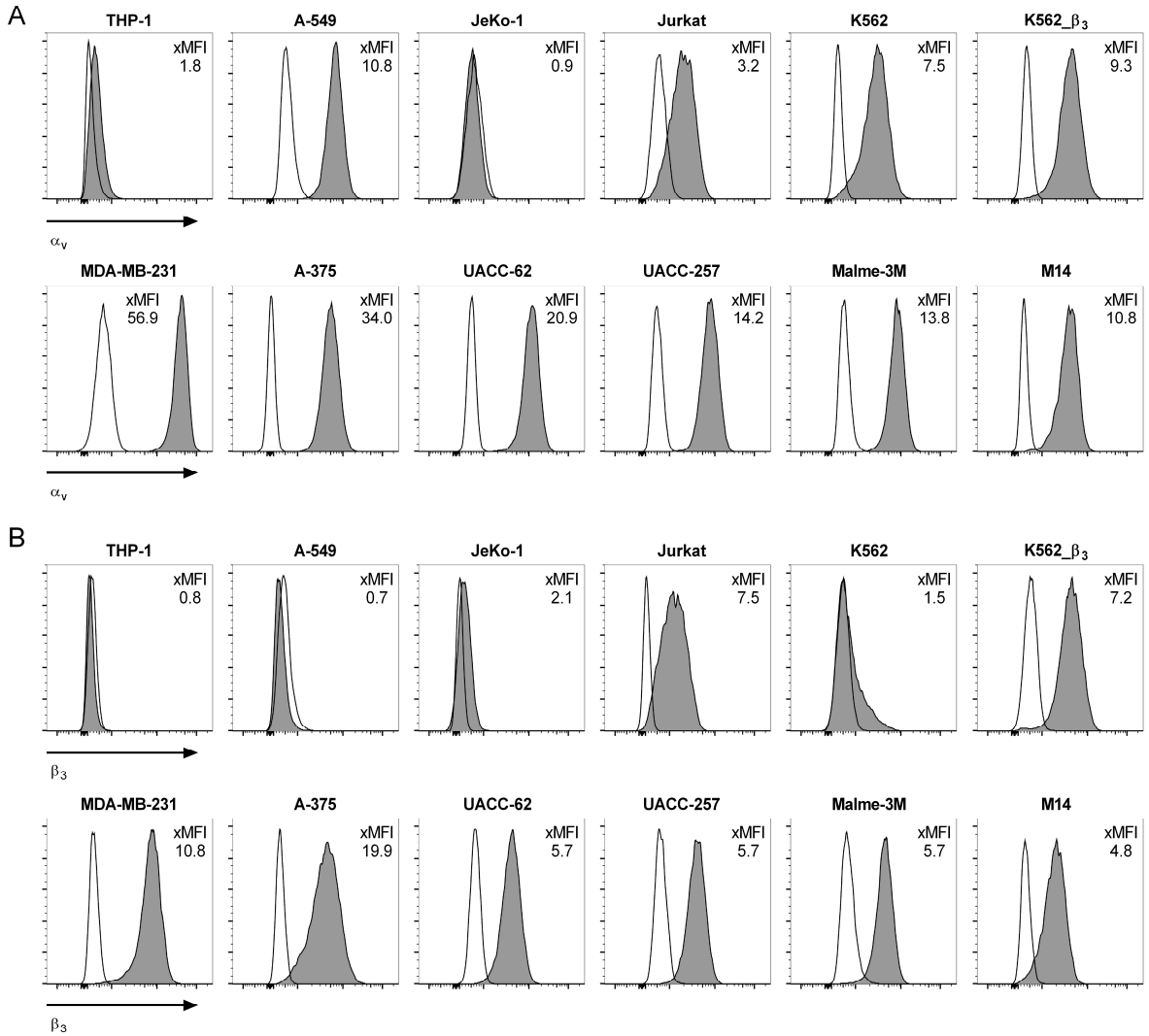

Figure 7: Integrin $\alpha_v\beta_3$ subunit expression on solid and hematologic tumour cell lines. **(A)** Flow cytometric analysis of α_v and **(B)** β_3 integrin-subunit expression on tumour cell lines. The ratio between the geometric mean fluorescent intensity of anti-α_v or anti-β_3 mABs (dark grey) and their corresponding isotype controls (clear) is provided as fold MFI (xMFI).

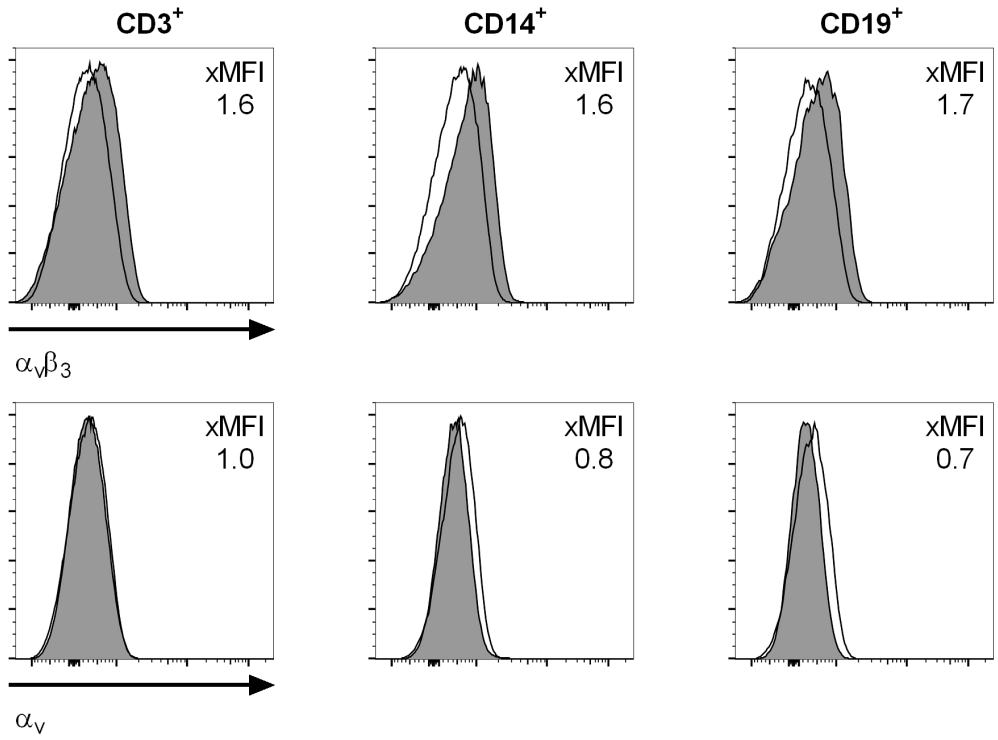

Figure 8: Integrin $\alpha_v\beta_3$ expression on PBMC subsets.
Flow cytometric analysis of $\alpha_v\beta_3$-heterodimer expression and α_v integrin-subunit expression on $CD3^+$, $CD14^+$ and $CD19^+$ cell subsets of PBMC from a healthy donor. The ratio between the geometric mean fluorescent intensity of anti-$\alpha_v\beta_3$ or anti-α_v mABs (dark grey) and their corresponding isotype controls (clear) is provided as fold MFI (xMFI).

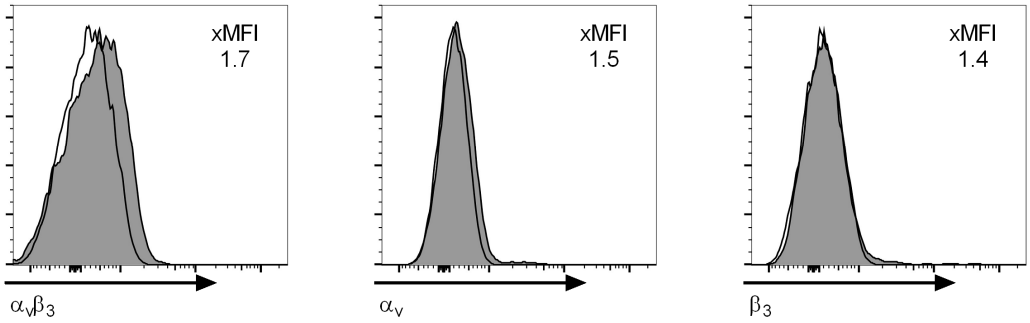

Figure 9: Integrin $\alpha_v\beta_3$ expression on HSCs.
Flow cytometric analysis of $\alpha_v\beta_3$-heterodimer expression and α_v and β_3 integrin-subunit expression on $CD34^+$ HSCs. The ratio between the geometric mean fluorescent intensity of anti-$\alpha_v\beta_3$, anti-α_v or anti-β_3 mABs (dark grey) and their corresponding isotype controls (clear) is provided as fold MFI (xMFI).

4.1.2 Design of an hLM609-CAR panel and expression on human T cells

We designed a panel of four $\alpha_v\beta_3$-CARs, each equipped with an intracellular signalling domain comprised of the cytoplasmic domains of CD28 and CD3ζ (Figure 10 A). We used two superhumanised variants of the integrin $\alpha_v\beta_3$-specific mAB LM609 with high (hLM609v7; K_d = 3 nM) or low (hLM609v11; K_d = 160 nM) monovalent affinity as targeting domains. “Superhumanised” refers to the phage display method termed V gene shuffling, which was used to humanise LM609 and only retained the third complementarity-determining region of the parental mouse heavy and light chains while replacing everything else with fully human sequences (Rader, Cheresh and Barbas, 1998). Each targeting domain was fused to either a long (IgG4 hinge, C_H2 and C_H3) or a short (IgG4 hinge) spacer domain, based on our prior work (Hudecek *et al.*, 2013). A truncated epidermal growth factor receptor (EGFRt) was co-expressed with each CAR as a selection and transduction marker (Wang *et al.*, 2011). $CD8^+$ and $CD4^+$ cells stably expressed all constructs after lentiviral gene transfer (Figure 10 B). We confirmed absence of integrin $\alpha_v\beta_3$ on $CD8^+$ and $CD4^+$ hLM609v7 short CAR T cells as well as on unmodified control T cells after expansion (Figure 10 C).

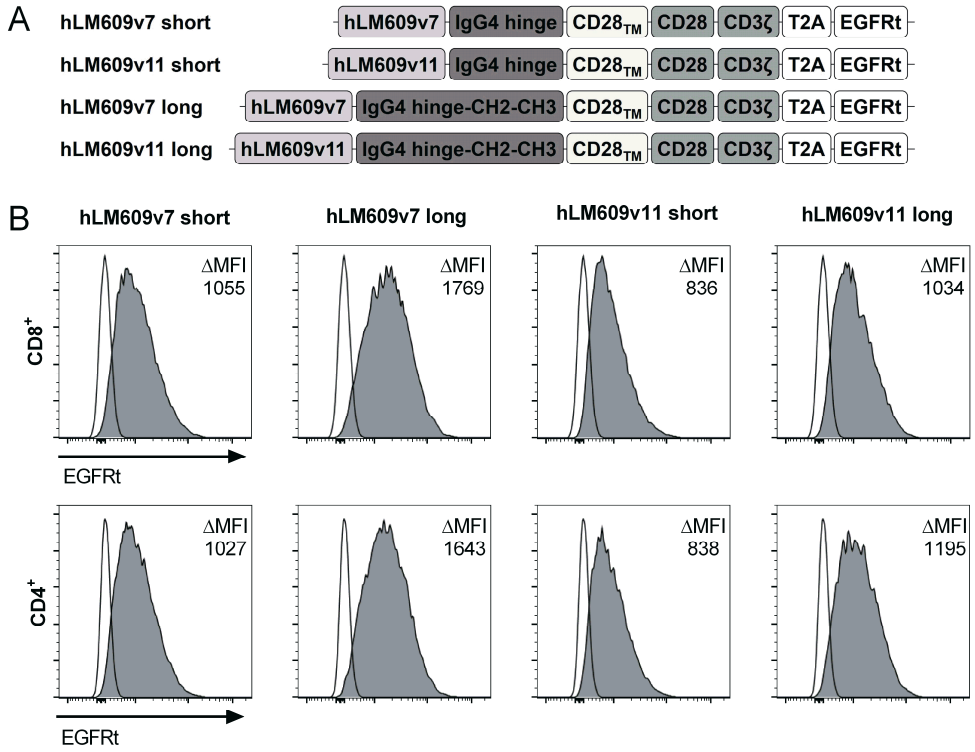

Figure 10: Design of $\alpha_v\beta_3$-CARs.
(A) Schematic depiction of the $\alpha_v\beta_3$-CAR constructs. **(B)** Flow cytometric analysis of EGFRt expression on $CD8^+$ and $CD4^+$ T cells transduced with $\alpha_v\beta_3$-CARs to assess CAR expression after expansion. The ΔMFI depicts the difference in geometric mean fluorescent intensity between CAR-transduced (dark grey) and untransduced (clear) samples.

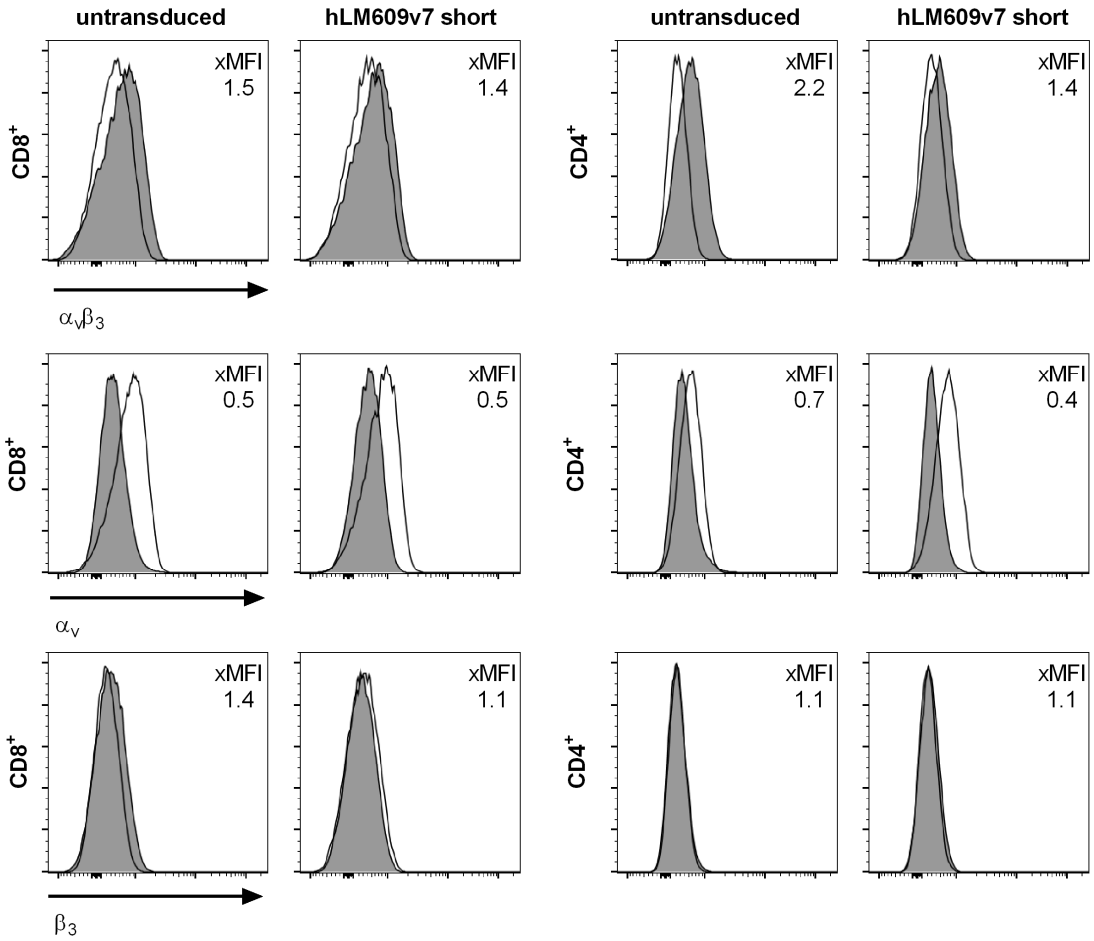

Figure 11: Expression of integrin $\alpha_v\beta_3$ on unmodified and hLM609v7-CAR T cells. Expression of the $\alpha_v\beta_3$-heterodimer and corresponding subunits on untransduced and $\alpha_v\beta_3$-CAR modified human T cells after expansion.

4.1.3 *In vitro* anti-tumour activity of hLM609-CAR T cells

We analysed $\alpha_v\beta_3$-CAR T cell-mediated tumour cell lysis, as well as cytokine production and proliferation to identify the CAR construct with the strongest anti-tumour function *in vitro*. The lytic capability of $\alpha_v\beta_3$-CAR T cells was assessed in a luminescence-based cytotoxicity assay. All four $\alpha_v\beta_3$-CAR T cells specifically lysed $\alpha_v\beta_3^+$ target cells with similar efficacy (Figure 12 A). K562_β_3 cells were more susceptible to being lysed by $\alpha_v\beta_3$-CAR T cells than the melanoma cell lines and MDA-MB-231, especially at low effector-to-target ratios. We detected low level lysis of K562 cells, probably due to the low expression of integrin $\alpha_v\beta_3$, as shown in the expression analysis (Figure 6). The vitality of $\alpha_v\beta_3^-$ A-549 cells was not affected by $\alpha_v\beta_3$-CAR T cells.

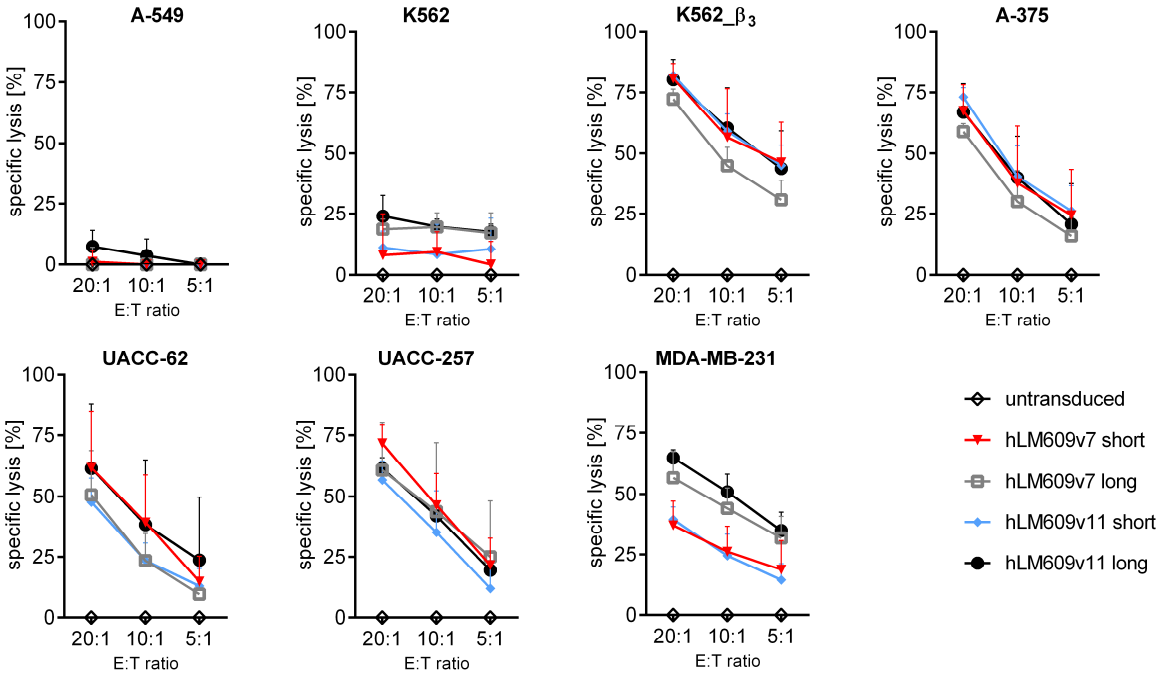

Figure 12: $\alpha_v\beta_3$-CAR T cells mitigate lysis of $\alpha_v\beta_3$-positive tumour cell lines *in vitro*. Specific lysis of ffluc_GFP$^+$ tumour cell lines by $\alpha_v\beta_3$-CAR modified CD8$^+$ T cells after 4 h of culture. Presented is the mean of n = 3 experiments, error bars depict the standard deviation (SD).

Next, we analysed the antigen-specific cytokine production by CAR T cells by quantifying the levels of IFN-ɣ and IL-2 in culture medium supernatants after co-culture with tumour cells (Figure 13 B+C). All four $\alpha_v\beta_3$-CAR T cells secreted high levels of IFN-ɣ after stimulation with K562_β_3 or A-375 target cells. The hLM609v7 short variant induced the strongest IFN-ɣ production, most prominently when CD4$^+$ CAR T cells were tested against A-375. IL-2 was produced by T cells equipped with hLM609v7 short or hLM609v11 short and, to a lower extent, by T cells equipped with hLM609v11 long. As for IFN-ɣ, hLM609v7 short induced the highest production of IL-2 within the tested panel. In general, we detected higher cytokine concentrations in the supernatants of CD4$^+$ as compared to CD8$^+$ CAR T cells.

In order to evaluate the extent of T cell activation induced by the different CAR constructs in more detail, we assessed T cell proliferation via a CFSE dilution assay (Figure 14 D+E). We generally detected stronger proliferation of CD4$^+$ than CD8$^+$ CAR T cells in response to tumour cells with high $\alpha_v\beta_3$ expression. CD4$^+$ hLM609v7 short and hLM609v11 short and long CAR T cells proliferated in response to K562_β_3 and A-375 cells. Neither $\alpha_v\beta_3$-CAR T cell line showed specific proliferation in response to K562. The two $\alpha_v\beta_3$-CARs with the short extracellular spacer induced stronger

proliferation of T cells than the two CARs with the long spacer domain. Surprisingly, T cells equipped with the hLM609v7 long variant proliferated in basal medium without further stimulation, possibly due to tonic signalling of this particular CAR.

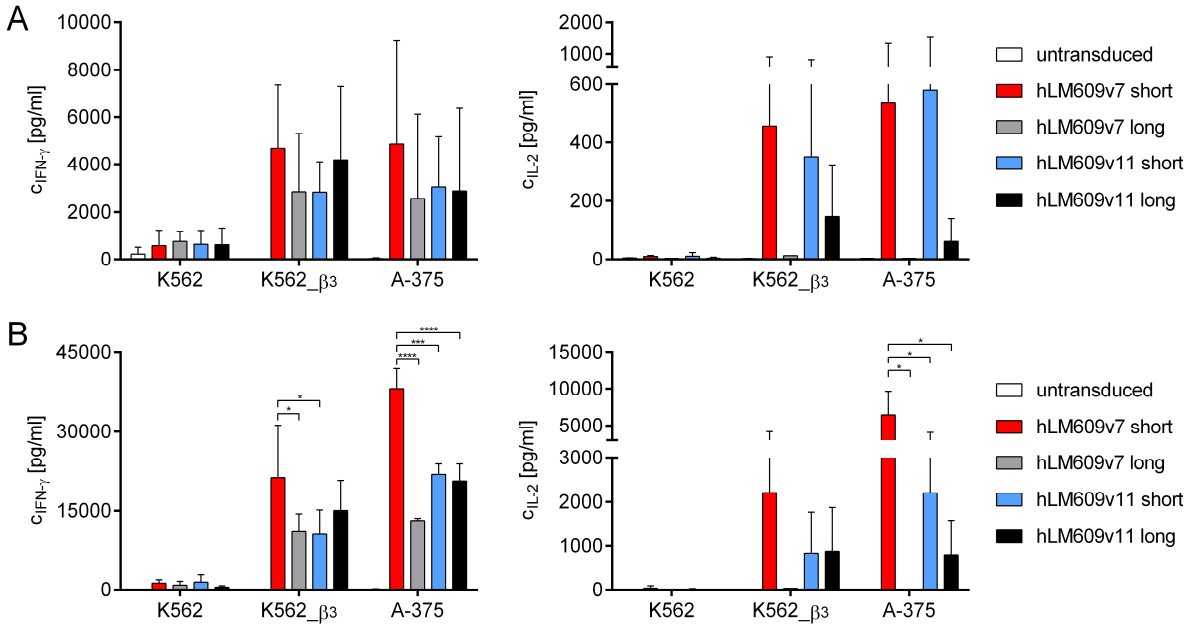

Figure 13: $\alpha_v\beta_3$-CAR T cells with a short spacer mediate stronger cytokine production *in vitro*.

(A) Concentration of IFN-ɣ and IL-2 in supernatants after 22 h culture of CAR modified or untransduced $CD8^+$ or **(B)** $CD4^+$ T cells and tumour cell lines. Presented is the mean of n = 3 experiments, error bars depict SD; only significant differences between the CAR constructs are indicated (* p<0.05, *** p<0.001, **** p<0.0001)

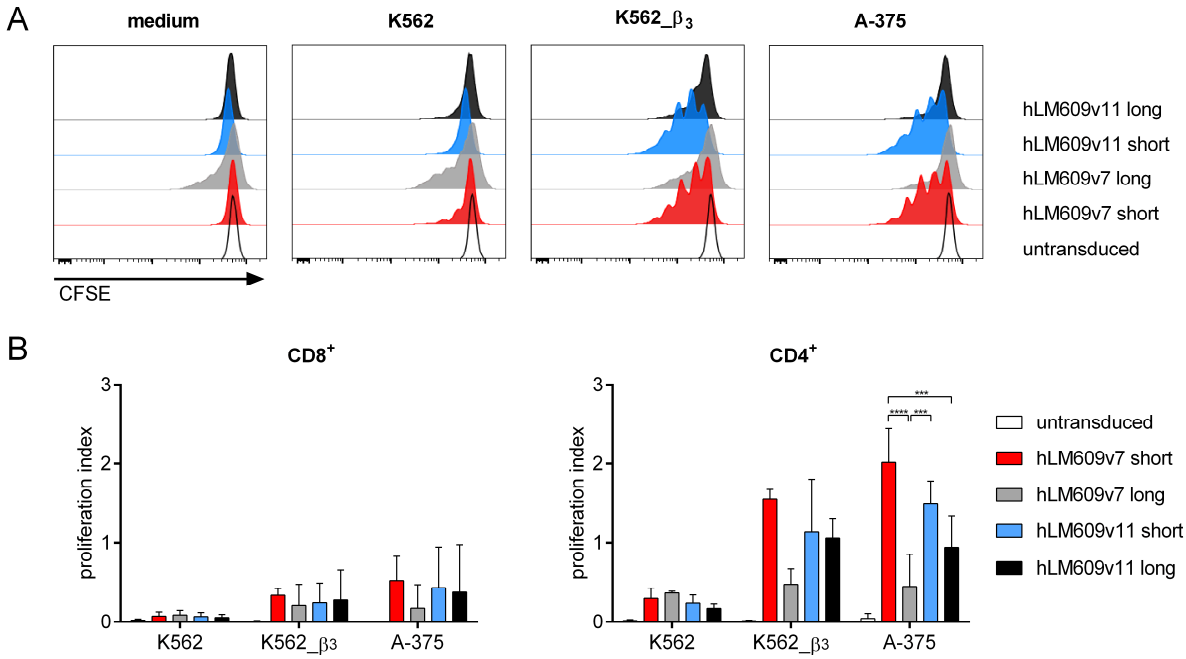

Figure 14: $\alpha_v\beta_3$-CAR T cells with a short spacer mediate stronger T cell proliferation *in vitro*.
(A) Proliferation of CFSE-labelled CD4$^+$ T cells after 72 h culture with irradiated tumour cells. The histograms show data from one representative out of n = 3 experiments. **(B)** Proliferation index of CD8$^+$ and CD4$^+$ T cells of n = 3 experiments, error bars depict SD; only significant differences between the CAR constructs are indicated (*** p<0.001, **** p<0.0001).

We further analysed, whether $\alpha_v\beta_3$-CAR T cells would lyse CD34$^+$ HSCs. In line with the absence of $\alpha_v\beta_3$ on HSCs, which we detected by flow cytometry, the vitality of HSCs was not reduced in the presence of $\alpha_v\beta_3$-CAR T cells compared to untransduced T cells (Figure 15).

In summary, all four $\alpha_v\beta_3$-CAR constructs induced specific lysis of $\alpha_v\beta_3^+$ target cells. We detected stronger proliferation and higher cytokine levels for $\alpha_v\beta_3$-CAR T cells equipped with a short spacer, which is in line with prior work that demonstrated the influence of spacer length on CAR-induced T cell activation (Hudecek *et al.*, 2013). Due to their superior function *in vitro*, we selected the $\alpha_v\beta_3$-CARs with short spacer to be tested *in vivo*.

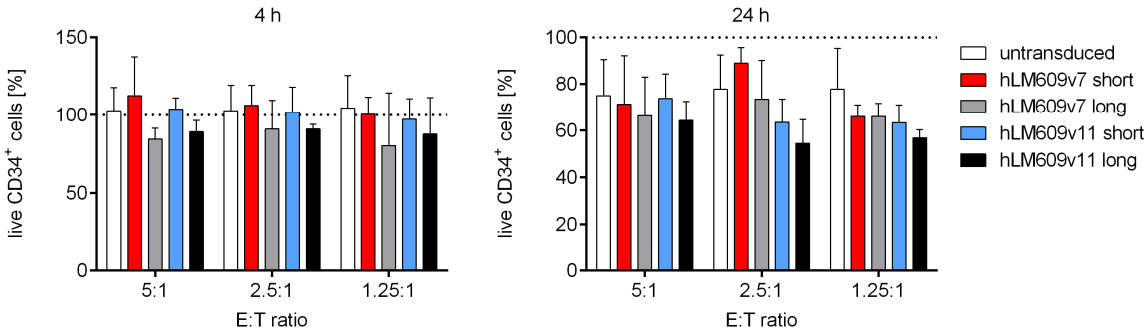

Figure 15: Vitality of HSCs is not affected by $\alpha_v\beta_3$-CAR T cells.
Percentage of live (7-AAD$^-$) HSCs (CD34$^+$) after 4 h and 24 h co-incubation with CD8$^+$ $\alpha_v\beta_3$-CAR T cells or untransduced T cells. Presented is the mean of n = 3 experiments with T cells obtained from 3 different donors and HSCs from one donor, error bars depict SD.

4.1.4 A murine xenograft model with A-375 melanoma cells

We sought to assess the anti-tumour effect of $\alpha_v\beta_3$-CAR T cells against solid tumours in a mouse xenograft model and selected the aggressively growing A-375 melanoma cell line as target. We established a mouse model that simulates the metastatic spread of melanoma cells to the lungs. We injected n = 2 NSG mice with 0.5 or 1x10^6 A-375/ffluc_GFP$^+$ tumour cells and monitored the localization of melanoma cells using bioluminescence imaging (Figure 16 A). Two days after tumour cell injection, all mice presented with tumour cells, which were primarily located in the lungs. We also detected tumour cells in the lower back region of mice treated with 1x10^6 A-375 cells. We followed the tumour progression and observed a similar growth kinetic in both groups (Figure 16 B). After 6 and 37 days, we dissected one mouse per group and verified the tumour engraftment visually. After 37 days, mice of both groups had several tumour lesions, e.g. in the liver. We defined an average bioluminescence intensity of >3x10^7 p/s/cm²/sr per mouse as experimental endpoint for subsequent experiments.

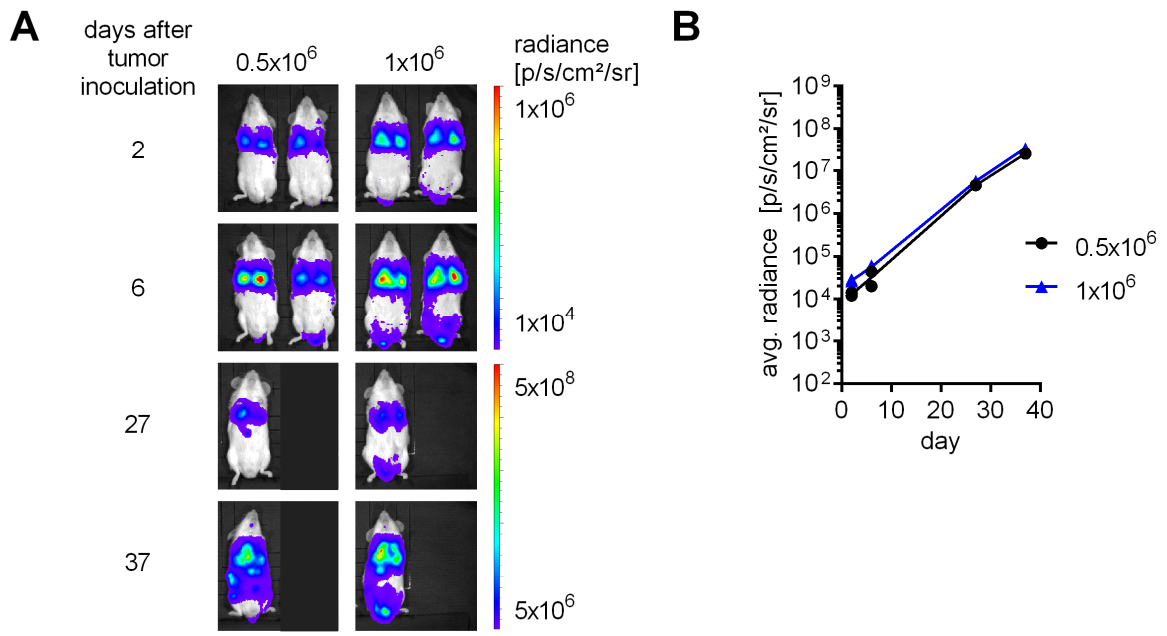

Figure 16: A-375/ffluc_GFP⁺ tumour cells engraft in NSG mice.
Groups of n = 2 mice were injected i.v. with either 0.5x10⁶ or 1x10⁶ A-375/ffluc_GFP⁺ tumour cells. **(A)** Bioluminescence images depicting signal intensity and localisation generated by A-375/ffluc_GFP⁺ tumour cells after luciferin injection. **(B)** Progression of bioluminescence signal obtained from regions of interests encompassing the entire body of each mouse.

4.1.5 *In vivo* anti-tumour activity of LM609 CAR T cells

To assess if $\alpha_v\beta_3$-CAR T cells could eradicate tumour cells in a metastatic melanoma model, we injected NSG mice with 1x10⁶ A-375 cells i.v. on day 0 and treated them with a single dose of 5x10⁶ T cells after 7 days of tumour engraftment. The mice either received the high-affinity hLM609v7 short CAR T cells, the low-affinity hLM609v11 short CAR T cells, untransduced T cells or remained untreated. On day 3 and day 7 after adoptive T cell transfer, we analysed peripheral blood samples and confirmed T cell engraftment in all treatment-groups (Figure 17 A). Between day 3 and day 7, the percentage of $\alpha_v\beta_3$-CAR T cells increased, in particular in the group of mice that had received the low-affinity hLM609v11 short $\alpha_v\beta_3$-CAR. In serum samples, we measured elevated concentrations of IFN-ɣ and GM-CSF in both groups of mice that received $\alpha_v\beta_3$-CAR T cells, but not in control groups (Figure 17 B). Interestingly, the cytokine concentrations were higher in mice that had been treated with the low-affinity hLM609v11 short CAR T cells compared to the high-affinity hLM609v7 short $\alpha_v\beta_3$-CAR. Treatment with $\alpha_v\beta_3$-CAR T cells conferred a potent anti-tumour effect. On day 3 after T cell transfer (i.e. day 10 after tumour inoculation), we already detected diminished

bioluminescence in all mice that had received CAR T cells. By contrast, the bioluminescence increased in all mice in the control groups that had either received untransduced T cells or no treatment (Figure 17 C). At day 28, the bioluminescence had reached background levels in 4 out of 6 mice in the hLM609v7 short group, and 5 out of 6 mice in the hLM609v11 short group, indicating that all tumour lesions had been eradicated (Figure 17 C+D). Out of the 12 mice treated with $\alpha_v\beta_3$-CAR T cells, 3 did not show a decline of bioluminescence to background level and had a recurrent tumour near the site of one of the primary tumours. Three of the 6 mice in the hLM609v7 short treatment group were unavailable to follow-up for reasons unrelated to tumour progression. Kaplan-Meier analysis showed that, by day 44, all mice in the control groups had to be sacrificed due to tumour progression (Figure 17 E). In contrast, all of the mice that completed follow-up were alive in the hLM609v7 short (3 out of 3), and in the hLM609v11 long group (6 out of 6). Bone marrow analysis at the end of the experiment confirmed that CAR T cells and untransduced T cells had persisted for the entire duration of the experiment (Figure 17 F). The $CD4^+$:$CD8^+$ ratio was strongly shifted towards $CD4^+$.

Taken together, these data show that $\alpha_v\beta_3$-CAR T cells confer potent anti-tumour efficacy *in vivo*. Several observations, including stronger CAR T cell expansion and cytokine secretion, and a higher rate of complete responses indicate that $\alpha_v\beta_3$-CAR T cells with the low-affinity binding domain hLM609v11 conferred stronger antitumor reactivity than $\alpha_v\beta_3$-CAR T cells with the high-affinity hLM609v7 binding domain. These observations are contrary to the results of the *in vitro* experiments, where high affinity correlated with stronger effector functions.

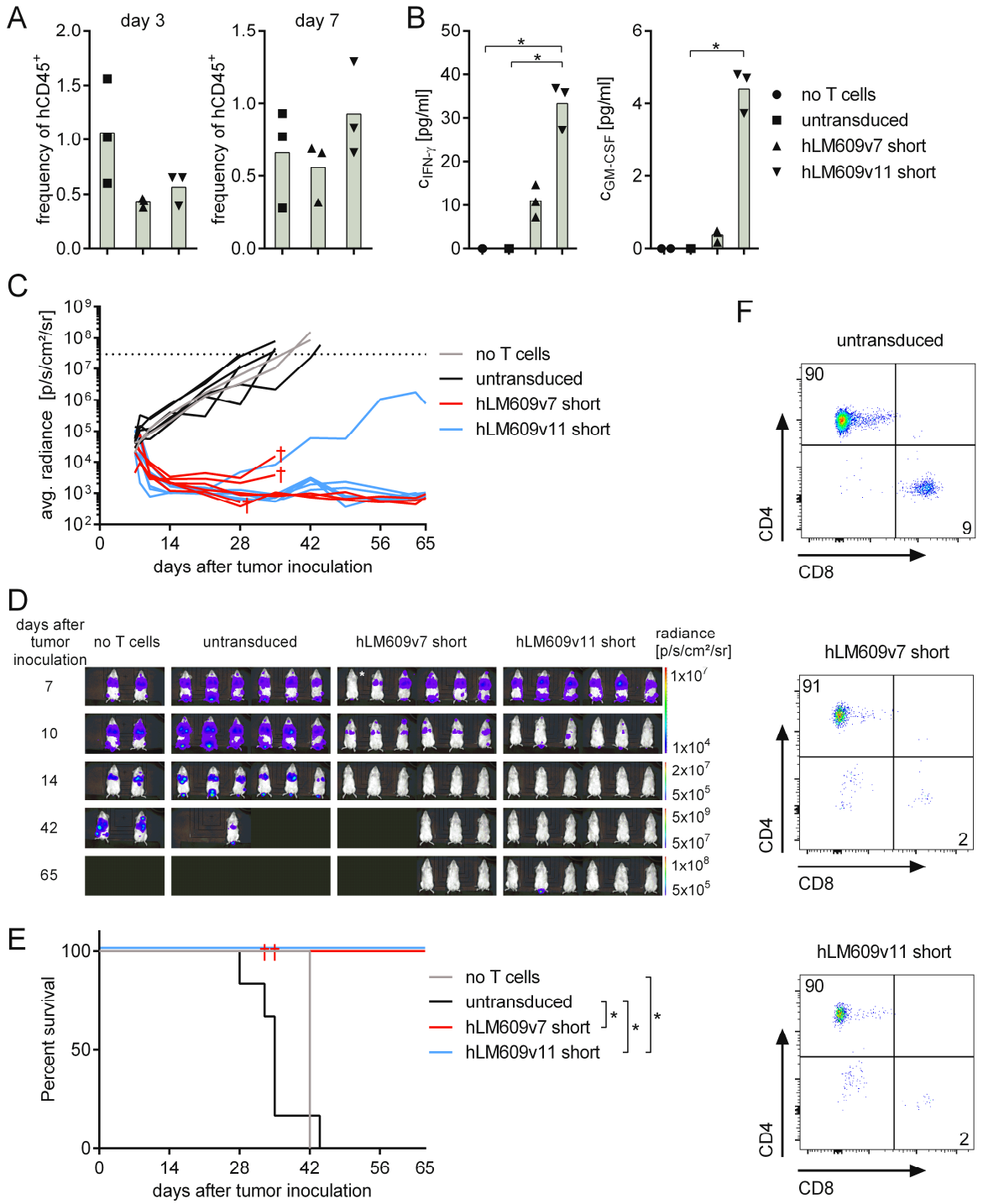

Figure 17: $\alpha_v\beta_3$-CAR T cells eliminate metastatic melanoma in a murine xenograft model.

Mice were injected with 1x10^6 A-375/ffluc_GFP$^+$ tumour cells i.v. and treated with a single dose of 5x10^6 T cells i.v. 7 days later. Groups of n = 6 mice either received untransduced T cells, hLM609v7 short or hLM609v11 short $\alpha_v\beta_3$-CAR T cells, and one group of n = 2 mice remained untreated. **(A)** Percentage of hCD45$^+$ (gated on live 7-AAD$^-$ cells) in peripheral blood of mice on day 3 and day 7 after T cell transfer. **(B)** Serum concentration of IFN-ɣ and GM-CSF on day 1 after T cell transfer. **(C)** Progression/regression of bioluminescence signal obtained from regions of interests encompassing the entire body of each mouse. The experiment endpoint was reached at a predefined signal threshold (dotted line). † indicates that mice were lost to

follow-up. **(D)** Bioluminescence images depicting signal intensity and localisation of A-375/ffluc_GFP$^+$ tumour cells in groups of mice that remained untreated or were treated with untransduced T cells, hLM609v7 short or hLM609v11 short $\alpha_v\beta_3$-CAR T cells. * Tumour engraftment in this mouse was confirmed using a more sensitive biolumiscence setting. **(E)** Kaplan-Meier analysis of survival in groups of mice until the end of the predefined observation period on day 65 after tumour engraftment (* p<0.05). **(F)** Flow cytometric analysis to detect human T cells (gated on live 7-AAD$^-$ and hCD45$^+$ cells) in the bone marrow of mice at the experimental endpoint.

4.1.6 Interim summary and conclusion

We demonstrated expression of integrin $\alpha_v\beta_3$ on tumour cell lines derived from multiple cancer entities. We designed $\alpha_v\beta_3$-CAR T cells, based on the superhumanised mAB hLM609, with long and short extracellular spacer domains as well as a high-affinity or a low-affinity scFv. By *in vitro* testing, we demonstrated enhanced cytokine production and proliferation of $\alpha_v\beta_3$-CAR T cells equipped with the short spacer and high-affinity scFv. We further assessed the anti-tumour function of $\alpha_v\beta_3$-CAR T cells with short spacer domains in an *in vivo* xenograft model of metastatic melanoma and observed complete eradication of tumour lesions in a majority of the $\alpha_v\beta_3$-CAR T cell treated mice. Our data demonstrate that $\alpha_v\beta_3$ integrin can be used as a target for CAR T cell therapy. This provided a rationale for subsequently targeting integrin $\alpha_v\beta_3$ with cpCAR T cells.

4.2 A novel chemically programmable CAR to target integrin $\alpha_v\beta_3$ with a targeting domain derived from hapten mAB h38C2

4.2.1 Design of a cpCAR and expression of cpCAR in reporter cells

The humanised aldolase-antibody h38C2 can be chemically programmed to target different antigens on tumour cells (Rader, Sinha, *et al.*, 2003; Gavrilyuk *et al.*, 2009). To assess whether the ability to specifically bind to a hapten-compound is preserved in a CAR format (Figure 18 A), we developed a 2nd generation CAR with an scFv derived from h38C2 (Figure 18 B). The receptor comprised an IgG4-hinge domain as extracellular spacer, the transmembrane domain of CD28, and intracellular signalling domains derived from CD28 and CD3ζ. Linked by a T2A ribosomal skip sequence, EGFRt was used as a transduction and selection marker. The construct was encoded in a lentiviral expression vector.

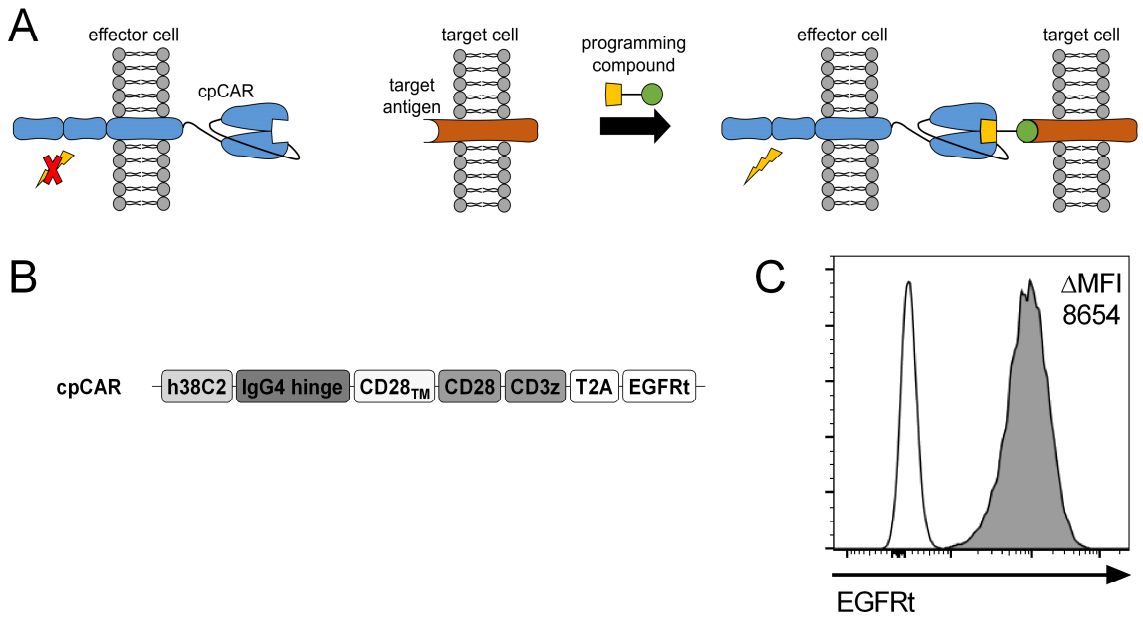

Figure 18: Design and expression of the cpCAR.
(A) Schematic representation of cpCAR programming. **(B)** Schematic representation of the cpCAR construct. **(C)** Flow cytometric analysis of EGFRt expression on reporter cells transduced to express the cpCAR to assess CAR expression after expansion. The ΔMFI depicts the difference in geometric mean fluorescence intensity between CAR-transduced (dark grey) and untransduced (clear) samples.

We wanted to compare the anti-tumour activity mediated by a conventional receptor binding directly to integrin $\alpha_v\beta_3$ (hLM609) and a programmable receptor binding indirectly to integrin $\alpha_v\beta_3$ through a hapten-compound (cpCAR). To facilitate this comparison, the cpCAR had the same design as the hLM609 CARs with a short spacer. As cell culture conditions and activation state of primary T cells influence the expression of CARs, we transduced reporter cells to express the cpCAR (Figure 18 C). Being an immortal T cell line, reporter cells offer stable CAR expression that allowed us to determine the properties of the programmable receptor with fewer variations than with primary T cells. In addition, the reporter cells contain two reporter gene cassettes with either a GFP or a CFP transgene, whose expression is controlled by NFAT or NF-κB response elements (Jutz *et al.*, 2016, 2017). Thus, GFP and CFP were used to gather information about the activation state of the T cell signalling cascade.

4.2.2 Programming of cpCAR reporter cells with a biotin-DK compound

In order to determine if a cpCAR can be used to target different antigens on tumour cells, we first needed to investigate if a hapten-compound could be specifically bound to the cpCAR. Therefore, we examined whether a cpCAR can be programmed with DK compounds and defined the conditions that would permit this interaction.

cpCAR reporter cells were incubated with biotinylated DK-compound (biotin-DK). After staining with fluorophore conjugated streptavidin, programmed cells could be identified via flow cytometry (Figure 19 A+B). Initially, cells were programmed for 2 hours at room temperature in PBS buffer, as indicated in studies of the aldolase antibody (Rader, Sinha, *et al.*, 2003). Biotin-DK in concentrations between 1 nM and 5000 nM were tested (Figure 19 C+D). Within a range of 5 nM to 1000 nM specific programming of cpCAR reporter cells was observed. The programming was dose-dependent, with an increased MFI at higher biotin-DK concentrations. At 5000 nM, an unspecific interaction between untransduced reporter cells and the compound occurred, characterised by an increased MFI in relation to untreated cells. No programming was detected for concentrations below 5 nM.

For subsequent analysis regarding the impact of temperature, time and buffer composition, we programmed reporter cells with 1000 nM of the biotin-DK compound, because this was the highest concentration that resulted in specific programming. At 37 °C, the fastest interaction between the biotin-DK and the receptor was observed (Figure 20 A). With increasing incubation time, the MFI also increased following a

sigmoidal course, whereby the maximum signal intensity was reached within one hour. The detected signal intensity was higher if the cells were incubated in cell culture medium instead of PBS. The kinetics of programming changed dramatically at lower temperatures. At room temperature, the MFI increased linearly over the entire experiment duration of 4 hours. Also, cpCAR reporter cells incubated with the biotin-DK compound in PBS were able to bind more of the compound after 4 hours than cpCAR reporter cells incubated at 37 °C. The MFI of cpCAR reporter cells incubated with the compound at 4 °C was 2-3 times higher than the MFI of unprogrammed cells, but did not increase with prolonged incubation time. When we analysed biotin-DK release from programmed cpCAR reporter cells, we also observed a strong influence of temperature. The MFI of cpCAR reporters after 4 hours of incubation at 22 °C and 4 °C remained at 82 % and 90 % of the initial value obtained immediately after programming with biotin-DK. On the other hand, when programmed cpCAR reporter cells were incubated in medium at 37 °C, the MFI decreased to 40 % of the initial value after 4 hours. This suggests that the programming was less stable at 37 °C than at 4 °C and 22 °C.

Collectively, these results show that the cpCAR can be specifically programmed with molecules containing a DK-group. Temperature and buffer composition had a strong influence on the programming kinetics. We observed the fastest conjugation of biotin-DK to the cpCAR at 37 °C in cell culture medium. As described for the cpAB h38C2, when it was programmed with molecules containing a DK-group, our data suggest that the connection between cpCAR and biotin-DK is reversible (Rader, 2014).

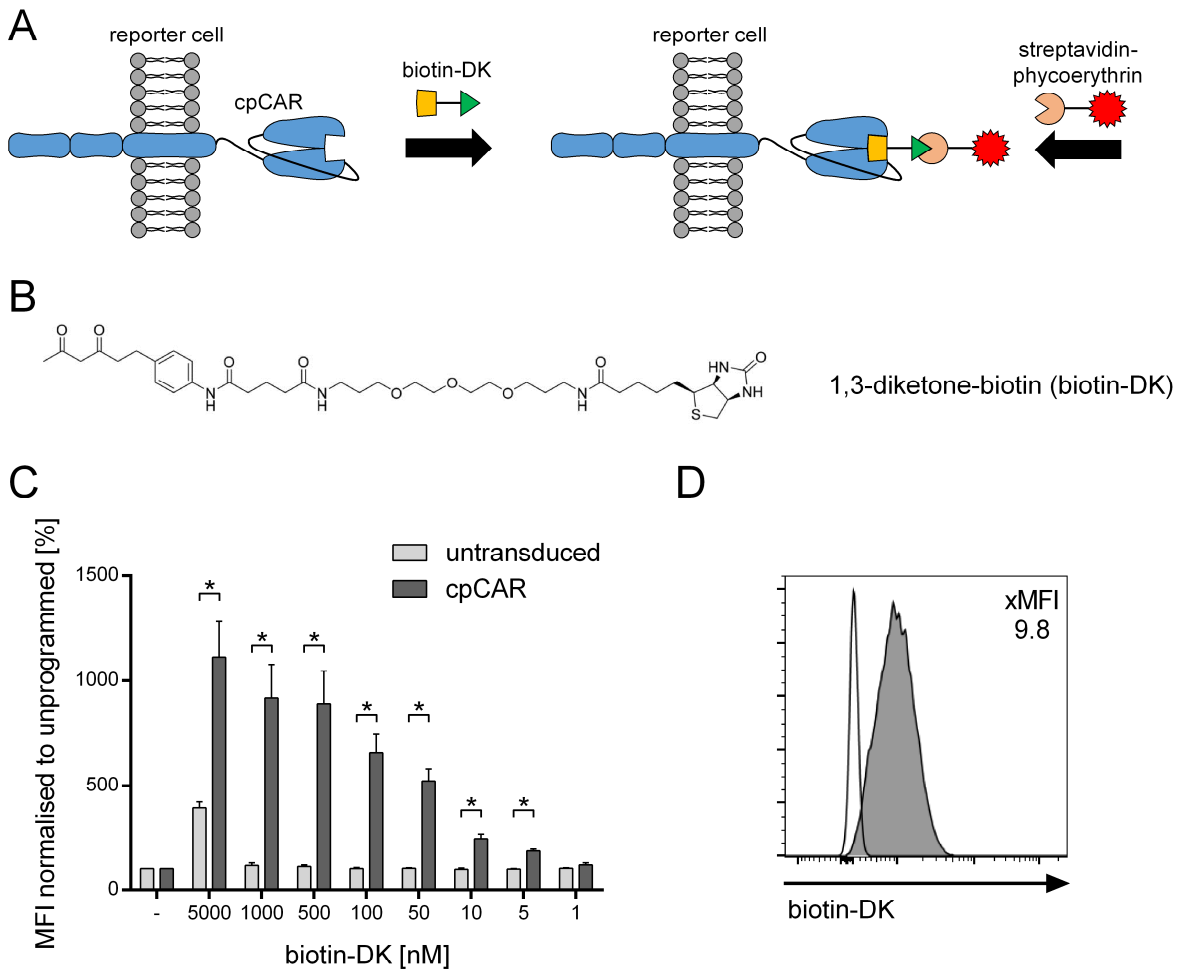

Figure 19: cpCAR reporter cells can be programmed with molecules containing a diketone group.

(A) Schematic of cpCAR programming with biotin-DK. **(B)** Structural formula of biotin-DK. **(C)** cpCAR or untransduced reporter cells incubated for 1 h at room temperature with biotin-DK in concentrations between 1 nM and 5000 nM and stained with streptavidin-phycoerythrin (SA-PE). Depicted is the ratio between the geometric mean fluorescent intensity of programmed and unprogrammed reporter cells of n = 4 experiments as fold MFI (xMFI). Error bars represent the SD. **(D)** cpCAR reporter cells incubated with 1000 nM biotin-DK. The ratio between the geometric mean fluorescent intensity of programmed (dark grey) and unprogrammed cells (clear) is provided as xMFI.

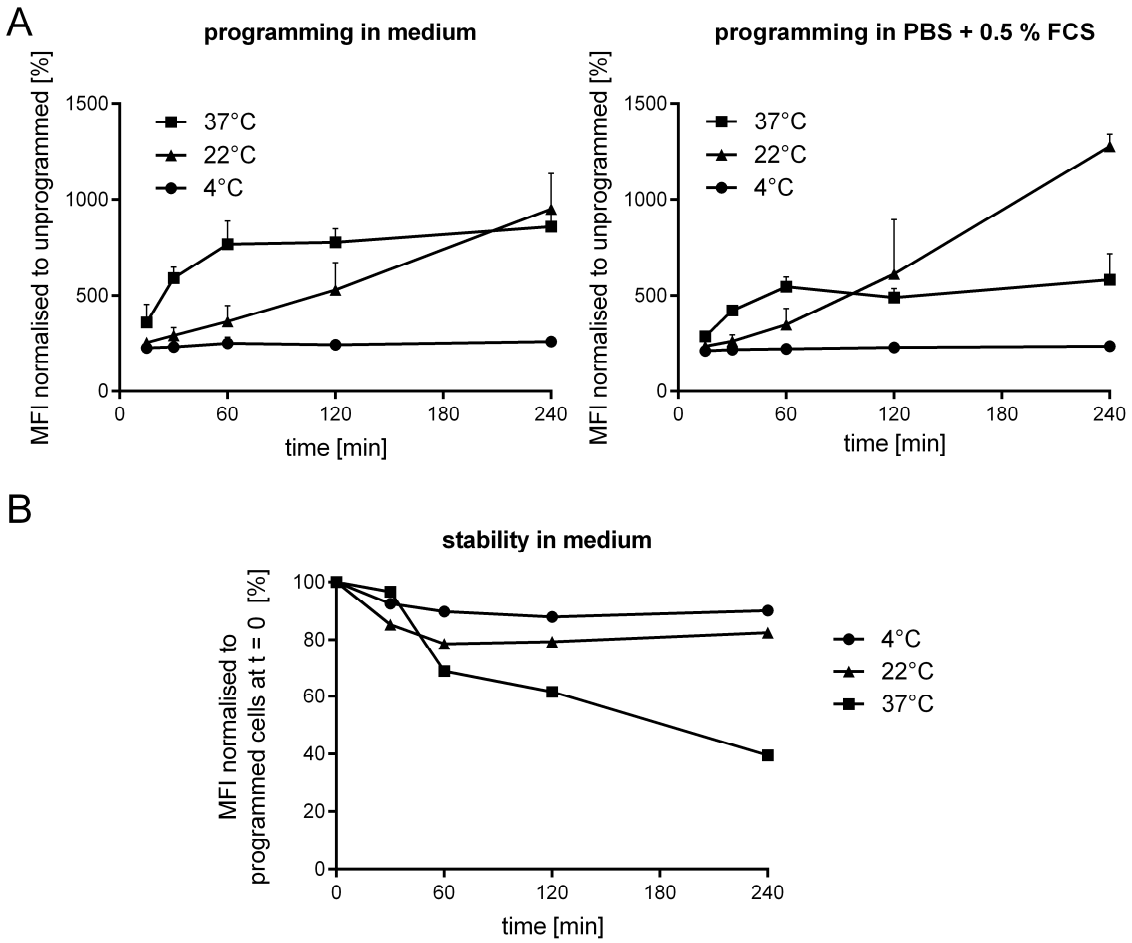

Figure 20: The binding and release kinetics of diketone compounds to cpCAR reporter cells is temperature dependent.

(A) cpCAR reporter cells were incubated with 1000 nM biotin-DK for 15 min to 240 min either at 4°C, 22°C or 37°C. Depicted is the ratio between the geometric mean fluorescent intensity of programmed and unprogrammed reporter cells of n = 4 experiments as xMFI. Error bars represent the SD. **(B)** cpCAR reporter cells were incubated with 1000 nM biotin-DK for 120 min at 22°C. The cells were then incubated for 30 min to 240 min at 4 °C, 22 °C or 37 °C in medium. Depicted is the ratio between the geometric mean fluorescent intensity of programmed reporter cells that were analysed after incubation in medium and programmed reporter cells that were analysed instantly (t = 0 min) of n = 1 experiment as xMFI.

4.2.3 Programming of primary human cpCAR T cells with a biotin-DK compound

We wanted to determine next, if primary cpCAR T cells could also be programmed with a biotin-DK compound. We transduced $CD4^+$ and $CD8^+$ T cells to express the cpCAR. The expression of the transduction marker EGFRt was assessed by flow cytometry (Figure 21 A). We detected greater ΔMFIs between untransduced and cpCAR T cells, when cells were incubated overnight in medium containing IL-2 compared to medium without IL-2. This effect was probably caused by the elongation factor 1 (EF1) promoter, which controls the transgene expression, which would be in line with observations from others (Eyquem *et al.*, 2017). To determine if the activation state would also influence the ability of cpCAR T cells to associate with molecules containing a DK-group, we programmed cpCAR T cells, either cultured with or without IL-2, with biotin-DK (Figure 21 B). We observed specific programming of $CD4^+$ and $CD8^+$ cpCAR T cells, regardless of culture conditions. However, in line with their higher EGFRt expression, activated cpCAR T cells were able to bind greater amounts of biotin-DK than resting cpCAR T cells. When EGFRt expression and biotin-DK programming were presented in one diagram, the correlation between the two parameters was also evident (Figure 21 C).

Together these data show that primary $CD4^+$ and $CD8^+$ cpCAR T cells can be specifically programmed with biotin-DK. The expression of the receptor, and thus the amount of compound that can be bound, depends on the activation state of the cpCAR T cell. Therefore, we performed functional tests with primary cpCAR T cells on days following the regular addition of fresh medium with IL-2.

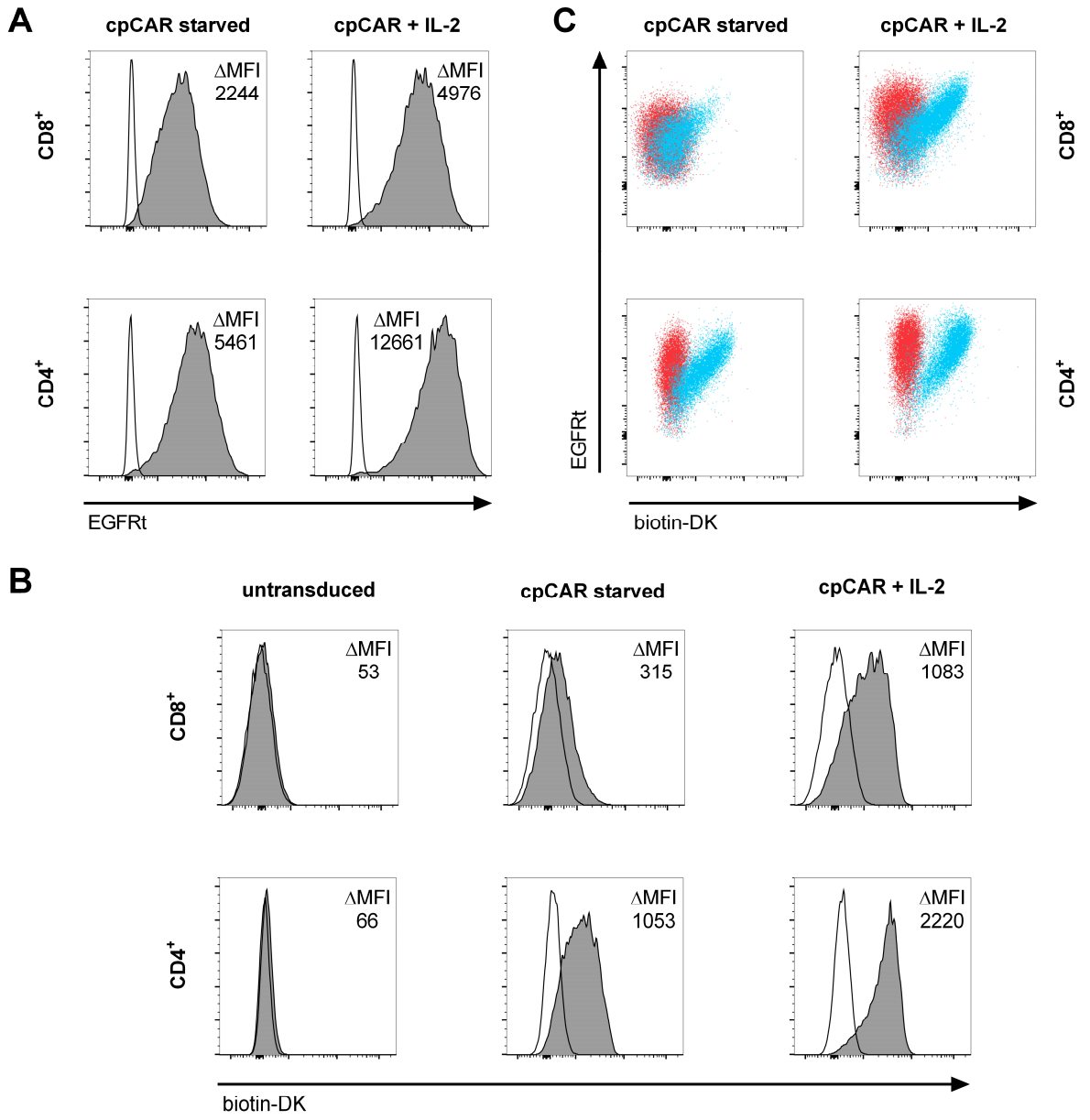

Figure 21: Activation of cpCAR T cells influences programming with biotin-DK compounds.

(A) Flow cytometric analysis of EGFRt expression on CD8⁺ and CD4⁺ T cells transduced to express cpCAR to assess CAR expression after expansion. The ΔMFI depicts the difference in geometric mean fluorescent intensity between CAR-transduced (dark grey) and untransduced (clear) T cells. **(B)** cpCAR T cells, either incubated in medium with 50 U/ml IL-2 or medium alone (starved), or untransduced T cells incubated for 1 h at 37 °C with 1000 nM biotin-DK and stained with SA-PE. The ΔMFI depicts the difference in geometric mean fluorescent intensity between biotin-DK programmed (dark grey) and unprogrammed (clear) T cells. **(C)** cpCAR T cells, either incubated in medium with 50 U/ml IL-2 or medium alone (starved), incubated for 1 h at 37°C with 1000 nM biotin-DK (blue) or unprogrammed (red) and stained with SA-PE and an anti-EGFRt mAB.

4.2.4 Activation of the T cell signalling cascade in cRGD-DK programmed cpCAR-reporter cells

The next step was to investigate whether cpCARs can be programmed to specifically recognise tumour antigens and whether this would induce activation of the T cell signalling cascade. We chose to program the cpCAR reporter cells to target integrin $\alpha_v\beta_3$. This antigen was used frequently in earlier studies to evaluate the anti-tumour effect of cpAB h38C2 (Figure 22 A). Melanoma cell line A-375 expresses high levels of this integrin on the cell membrane, so it was used as a target. The reporter cells have been modified to express fluorescent proteins under the control of NFAT and NF-κB response elements. Therefore, the activation of NFAT and NF-κB can be monitored by flow cytometry. The hapten-compound DH-12 was used to program the cpCAR reporter cells for the detection of integrin $\alpha_v\beta_3$ (Figure 22 B). DH-12 comprises a cRGD group for specific binding to the integrin and a DK group for reversible covalent docking to the cpCAR. The cRGD and DK group were spaced by a polyethylene glycol (PEG) linker. The compound was directly added to the samples at the beginning of the assay at concentrations of 1 nM to 1000 nM. At DH-12 concentrations above 10 nM for the NFAT-controlled reporter and at concentrations above 50 nM for the NF-κB-controlled reporter gene, significant expression of the fluorescent reporter proteins were detectable by flow cytometry (Figure 22 C). The response was highly specific, as no activation of untransduced reporter cells was detectable in the presence of DH-12 and target cells. The activation of NFAT and NF-κB was dose dependent with a peak reactivity between 1000 nM and 100 nM of DH-12.

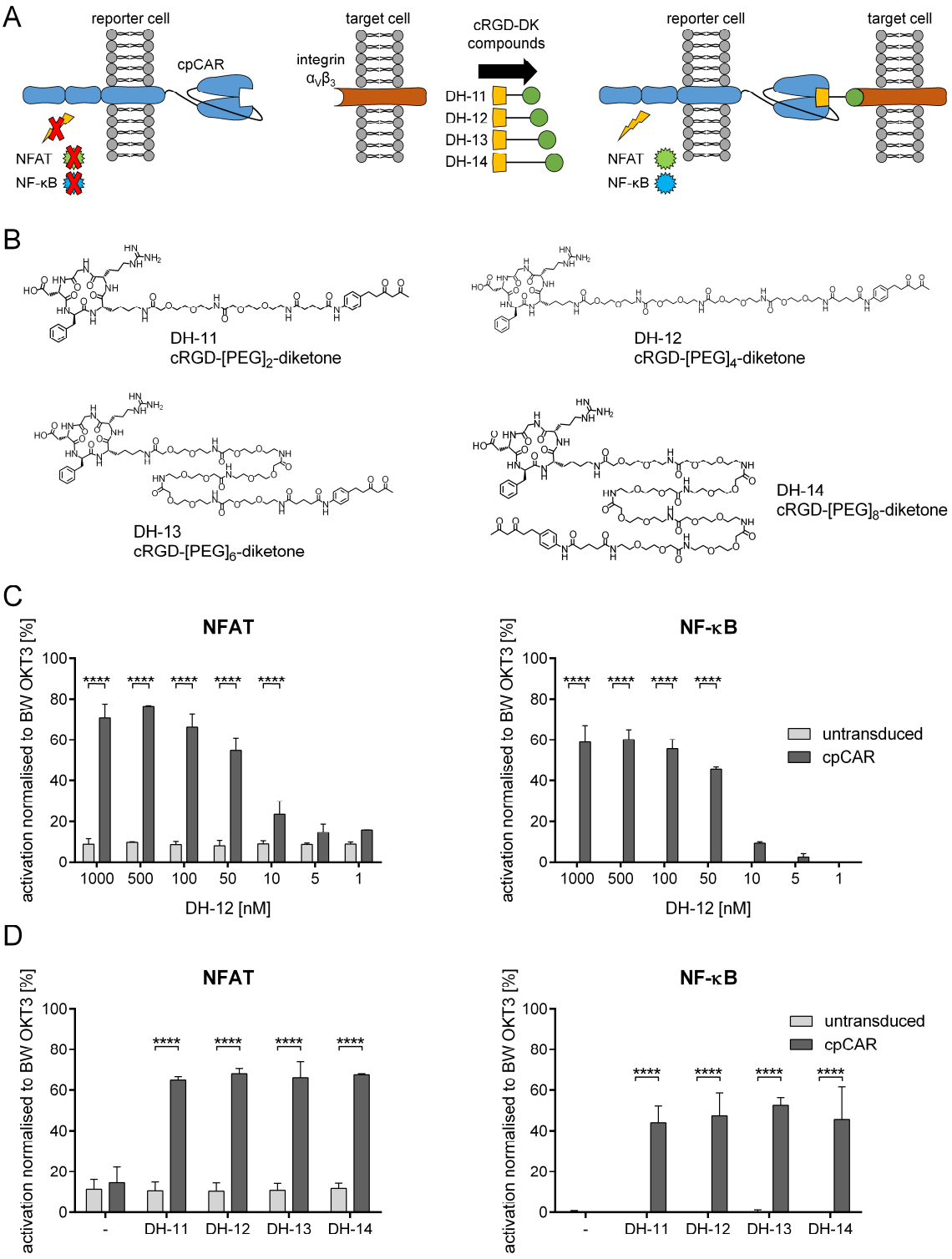

Figure 22: cpCAR T cells programmed to target tumour antigens trigger T cell signalling cascade.

(A) Schematic representation of cpCAR programming with cRGD-DK compounds to equip the cpCAR with specificity for integrin $\alpha_v\beta_3$. **(B)** Structural formula of DH-11, DH-12, DH-13 and DH-14. **(C)** Activation of NFAT and NF-κB of untransduced or cpCAR reporter cells cultured with A-375 cells and 1 nM - to 1000 nM DH-12. Presented is the mean of n = 3 experiments, error bars depict SD; **** p<0.0001. **(D)** Activation of NFAT and NF-κB of untransduced or cpCAR reporter cells cultured with A-375 cells and 100 nM DH-11, DH-12, DH-13 or DH-14. Presented is the mean of n = 3 experiments, error bars depict SD; **** p<0.0001.

Next, we analysed a panel encompassing the three additional cRGD-DK compounds DH-11, DH-13 and DH-14, each incorporating an increasing number of PEG units (Figure 22 B). We observed earlier in this study that the size of the extracellular spacer domain of hLM609-CAR constructs greatly affects the anti-tumour efficacy of $\alpha_v\beta_3$-CAR T cells. Consequently, we determined whether the size of the PEG spacer that connects DK and cRGD similarly influences T cell activation. All compounds enabled specific signal induction by programming cpCAR reporter cells to detect integrin $\alpha_v\beta_3$ on A-375 cells (Figure 22 D). No difference in signal intensity was observed regardless of the length of the PEG spacer. Importantly, there was no unspecific activation of NFAT or NF-κB by reporter cells modified to express the cpCAR.

In summary, these results show that an h38C2-based cpCAR can be programmed using DK compounds in such a way that the compounds enable the detection of specific antigens on target cells, leading to activation of the T cell signalling cascade mediated by the cpCAR.

4.2.5 *In vitro* anti-tumour function of cRGD-DK programmed cpCAR modified primary human T cells

Next, we investigated the ability of primary cpCAR T cells programmed with cRGD-DK compounds to detect integrin $\alpha_v\beta_3$ and to confer their effector functions regarding antigen-specific cytokine production, proliferation and lysis of tumour cells (Figure 23 A).

The anti-tumour efficacy of programmed, $\alpha_v\beta_3$-specific cpCAR T cells was compared to T cells expressing an hLM609v7 short CAR, which binds the same antigen with its scFv without the need of prior programming. All constructs were expressed by $CD4^+$ and $CD8^+$ cells after lentiviral transduction (Figure 23 B). T cells only expressing the transduction marker EGFRt served as control. First, the lytic capability of $CD8^+$ cpCAR T cells programmed with cRGD-DK compounds was investigated (Figure 23 C). After 4 hours, specific lysis of the $\alpha_v\beta_3^+$ cell lines K562_β_3 and A-375 was observed with cpCAR T cells in the presence of cRGD-DK compounds. All compounds were equally potent with regard to lysis of tumour cells induced by programmed cpCAR T cells. However, T cells equipped with the hLM609-CAR achieved a much higher lysis of tumour cells within the same amount of time. K562_β_3

cells seemed more susceptible to lysis by cpCAR T cells than the A-375 cells. No tumour cell lysis was observed by unprogrammed cpCAR T cells.

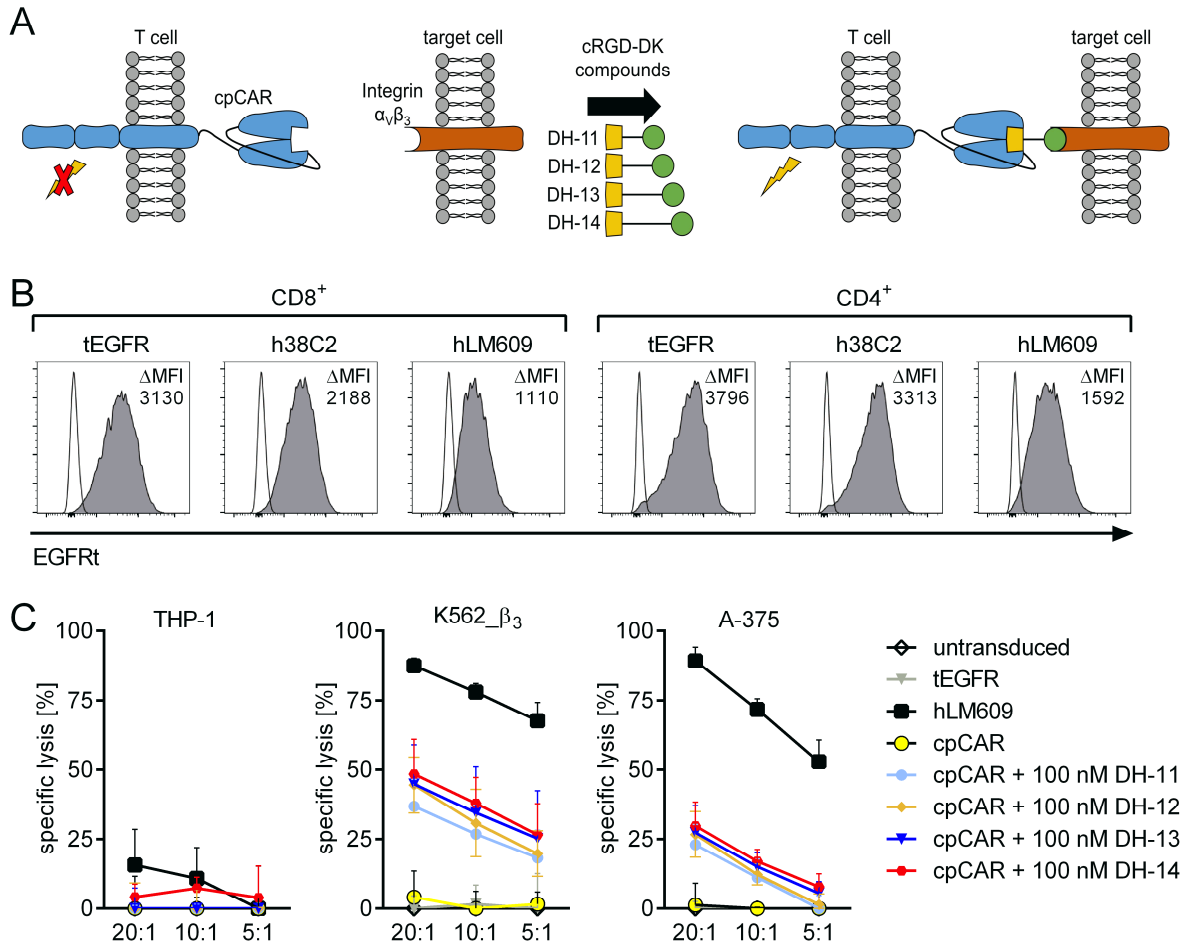

Figure 23: cpCAR T cells can be programmed to lyse tumour cells.
(A) Schematic representation of cpCAR programming with cRGD-DK compounds for specific binding to integrin $\alpha_v\beta_3$. **(B)** Flow cytometric analysis of EGFRt expression on $CD8^+$ and $CD4^+$ T cells transduced to express cpCAR, hLM609v7 or only the EGFRt marker to assess CAR expression after expansion. The ΔMFI depicts the difference in geometric mean fluorescent intensity between CAR-transduced (dark grey) and untransduced (clear) samples. **(C)** Specific lysis of ffluc_GFP^+ tumour cell lines by $\alpha_v\beta_3$-CAR or $\alpha_v\beta_3$-programmed cpCAR-modified $CD8^+$ T cells after 4 h. Presented is the mean of n = 3 experiments, error bars depict SD.

Next, the extent of T cell activation mediated by the cpCAR was addressed by quantification of cytokine production. We detected IFN-ɣ and IL-2 in the supernatant of $CD4^+$ cpCAR T cells in the presence of $\alpha_v\beta_3^+$ target cells and cRGD-DK compounds (Figure 24 A). The length of the spacer region in the compound did not significantly affect the cytokine expression induced by the cpCAR. The hLM609 CAR T cells produced higher amounts of IFN-ɣ and IL-2 compared to programmed cpCAR T cells upon co-culture with target cell lines.

Subsequently, we investigated the ability of primary cpCAR T cells to proliferate *in vitro* after co-culture with tumour cells. We detected significant proliferation of $CD4^+$ cpCAR T cells programmed with cRGD-DK compounds after stimulation with $\alpha_v\beta_3$-positive tumour cell lines, compared to unprogrammed cpCAR or untransduced T cells (Figure 24 B+C). $CD4^+$ T cells equipped with the conventional hLM609v7-CAR surpassed the proliferation capabilities of the cpCAR T cells. Only $CD8^+$ T cells expressing the hLM609v7-CAR and stimulated with A-375 cells showed significant proliferation. $CD8^+$ cells expressing the cpCAR did not proliferate. $CD4^+$ cpCAR T cells triggered a slight increase of $CD8^+$ cpCAR T cell proliferation if they were co-cultured in the assay (Figure 24 D). Again, LM609v7-CAR T cells showed significantly higher proliferation compared to programmed cpCARs in this setup.

In summary, we show that cpCAR T cells exerted their effector functions in the presence of cRGD-DK compounds and $\alpha_v\beta_3^+$ tumour cells but were surpassed in their potency by hLM609v7-CAR T cells with an scFv that directly binds to the antigen.

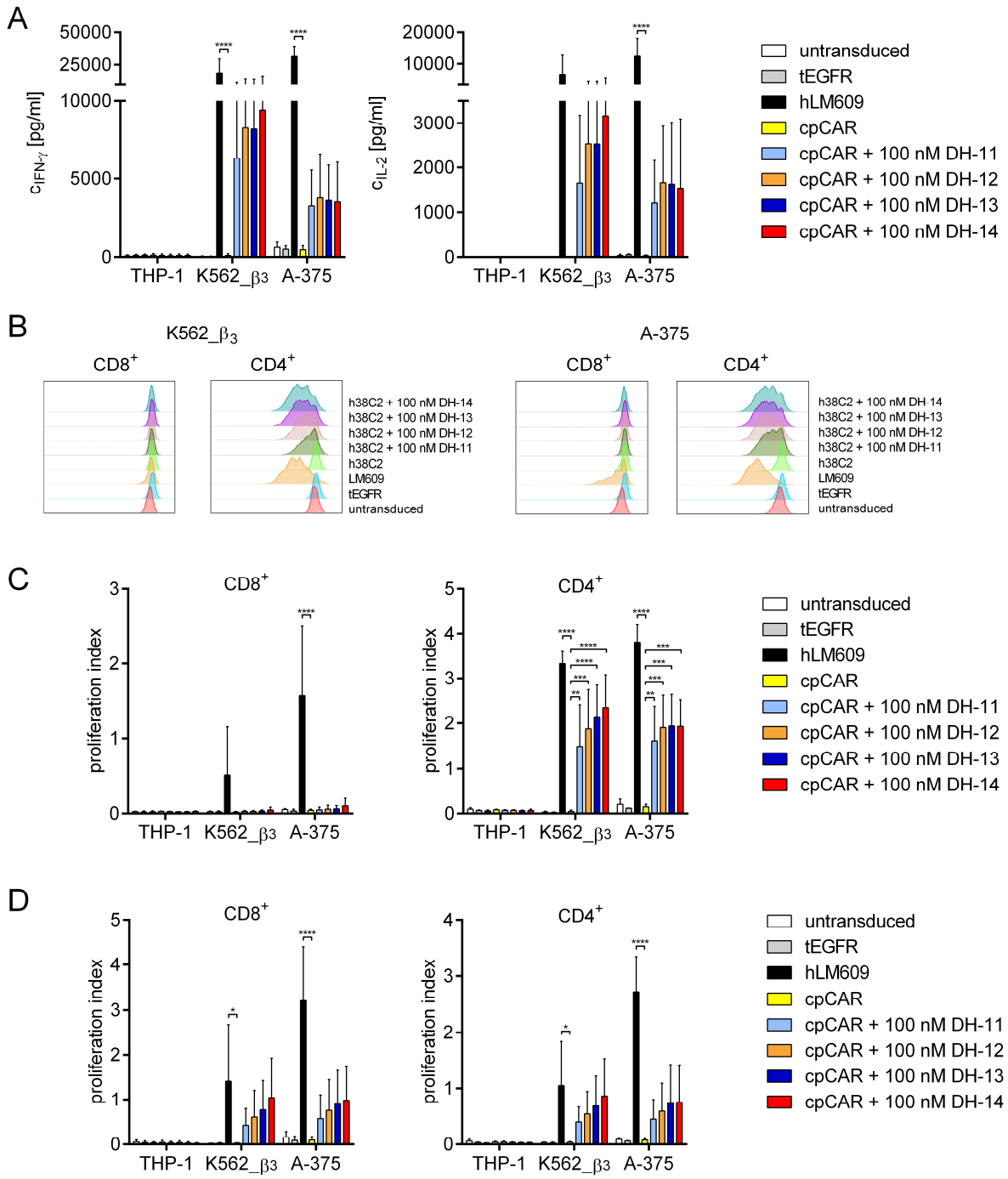

Figure 24: $\alpha_v\beta_3$-programmed cpCAR T cells produce cytokines and proliferate *in vitro*. **(A)** Concentration of IFN-ɣ and IL-2 in cell culture supernatants after 22 h co-culture of CAR-modified or untransduced CD4+ T cells with tumour cells. Presented is the mean of n = 3 experiments, error bars depict SD; **** p<0.0001 **(B)** Proliferation of CFSE-labelled CD8+ and CD4+ T cells after 72 h co-culture with irradiated tumour cells. The histograms show representative data from one out of n = 3 experiments. **(C)** Proliferation index of CD8+ and CD4+ T cells cultured separately or **(D)** together. Presented is the mean of n = 3 experiments, error bars depict SD; * p<0.05, ** p<0.01, *** p<0.001, **** p<0.0001.

4.2.6 Anti-tumour function of cpCAR T cells programmed *in vivo* with cRGD-DK in a murine xenograft model

Encouraged by their *in vitro* activity, we next sought to determine whether cpCAR T cells can control the growth of established A-375 melanoma in a xenograft mouse model.

In a first experiment, we investigated whether cpCAR T cells could be programmed to target A-375 cells after injection of compound DH-12. NSG mice were injected with $1x10^6$ A-375/ffluc_GFP$^+$ tumour cells i.v. and i.p., respectively. Seven days after tumour inoculation, the mice received i.v. injections of $5x10^6$ hLM609v7-CAR- or cpCAR-modified or untransduced T cells. Subgroups of mice that had received untransduced or cpCAR T cells were injected with DH-12 i.v. and an additional subgroup of mice that had received cpCAR T cells was i.p. injected. This study design allowed us to distinguish whether one route of DH-12 administration (i.p. or i.v.) was superior, and whether the cRGD-DK compound itself would influence tumour growth. 20.5 µg of DH-12 in PBS was administered 3 times a week for a period of 2 weeks. We confirmed the uniform engraftment of the different T cell lines by flow cytometric analysis of blood samples taken 7 days after T cell injection (Figure 25 A). The course of tumour growth was quantified by assessing the bioluminescence signal from the luciferase positive tumour cells after the administration of luciferin (Figure 25 B). We observed reduction of the tumour burden after CAR T cell administration in mice of the hLM609 group. However, mice receiving DH-12 injections showed no change in bioluminescence signal compared to mice treated with untransduced or unprogrammed T cells (Figure 25 B+C).

Most of the bioluminescence signal originated from the abdomen, suggesting that the majority of tumour cells was located in that region (Figure 25 C). Subsequently, we injected T cells and DH-12 compound i.p. because we wanted to investigate whether an additional injection of T cells and DH-12 compound close to the tumour site would enhance the anti-tumour response. We randomly reassigned mice that were previously unresponsive to T cell treatment (groups untransduced + DH-12 i.p., cpCAR, cpCAR + DH-12 i.p., cpCAR + DH-12 i.v.) to new treatments groups of n = 2 mice. Twenty-two days after tumour inoculation mice were injected i.p. with $5x10^6$ T cells, either untransduced or modified to express the hLM609v7-CAR or cpCAR. All 6 groups of mice treated with the cpCAR received i.p. injections of DH-12 compound (c = 0.062 µg - to 20.5 µg) on day 22 and day 24. When we analysed the percentage

of hCD45$^+$ T cells in the blood on day 28, we measured similar values in mice treated with untransduced or cpCAR T cells, while the proportion of human T cells in the hLM609v7 group was elevated (Figure 26 A). This observation suggests expansion of hLM609v7-CAR T cells *in vivo* whereas cpCAR T cells did not expand. Consequently, the tumour burden, assessed by bioluminescence imaging, was reduced solely by treatment with hLM609v7-CAR T cells (Figure 26 B+C).

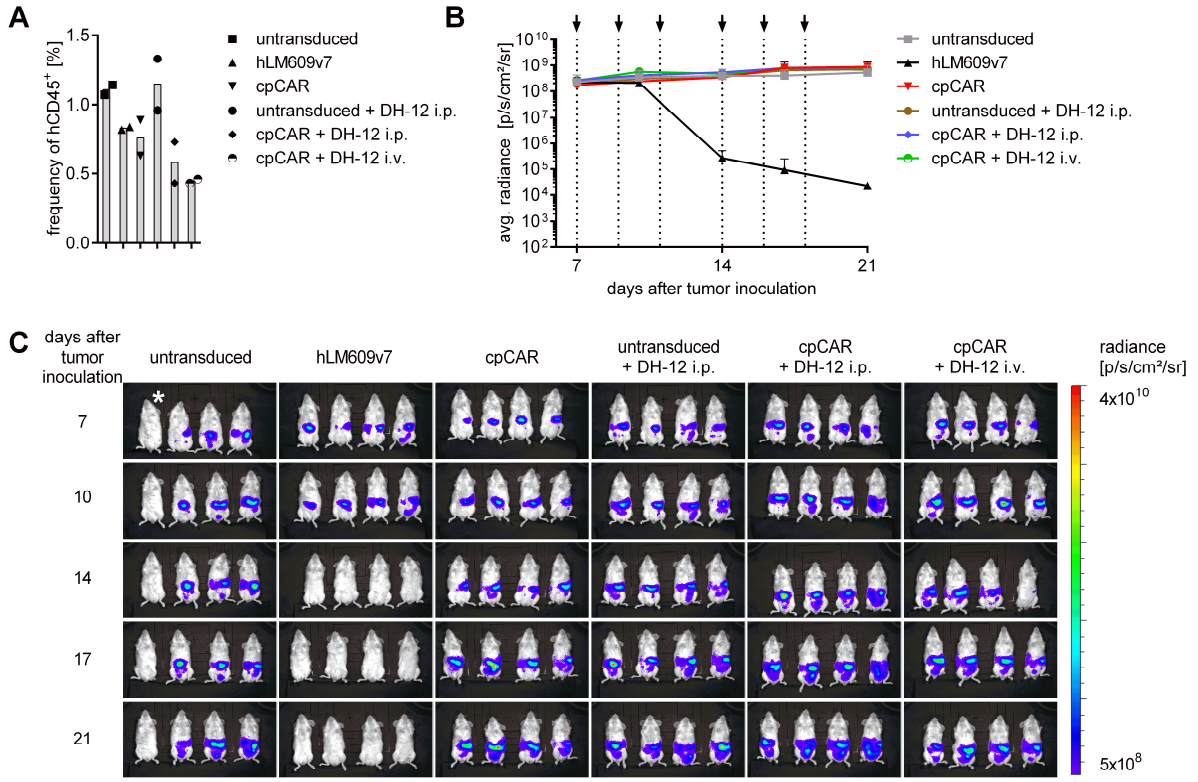

Figure 25: Effect of *in vivo* programmed cpCAR T cells on the growth of metastatic melanoma in a murine xenograft model.
Mice were injected with 1x10^6 A-375/ffluc_GFP$^+$ tumour cells i.v. as well as 1x10^6 A-375/ffluc_GFP$^+$ tumour cells i.p. and treated with a single dose of 5x10^6 T cells i.v. 7 days later. Groups of n = 4 mice either received untransduced, hLM609v7 CAR or cpCAR T cells. One group of animals treated with untransduced T cells and two groups treated with cpCAR T cells received three weekly injections of 20.5 µg DH-12 either i.v. or i.p. over a period of two weeks. **(A)** Percentage of hCD45$^+$ (gated on live 7-AAD$^-$ cells) in peripheral blood of mice on day 7 after T cell transfer. **(B)** Progression or regression of bioluminescence obtained from regions of interest encompassing the entire body of each mouse. The mean of n = 4 mice is presented, error bars depict SD. Arrows mark the injections of DH-12. **(C)** Bioluminescence images depicting signal intensity and localisation generated by A-375/ffluc_GFP$^+$ tumour cells in groups of mice that were treated with untransduced, hLM609v7 or cpCAR T cells and programming compound DH-12. * Tumour engraftment in this mouse was confirmed using a more sensitive bioluminescence scale.

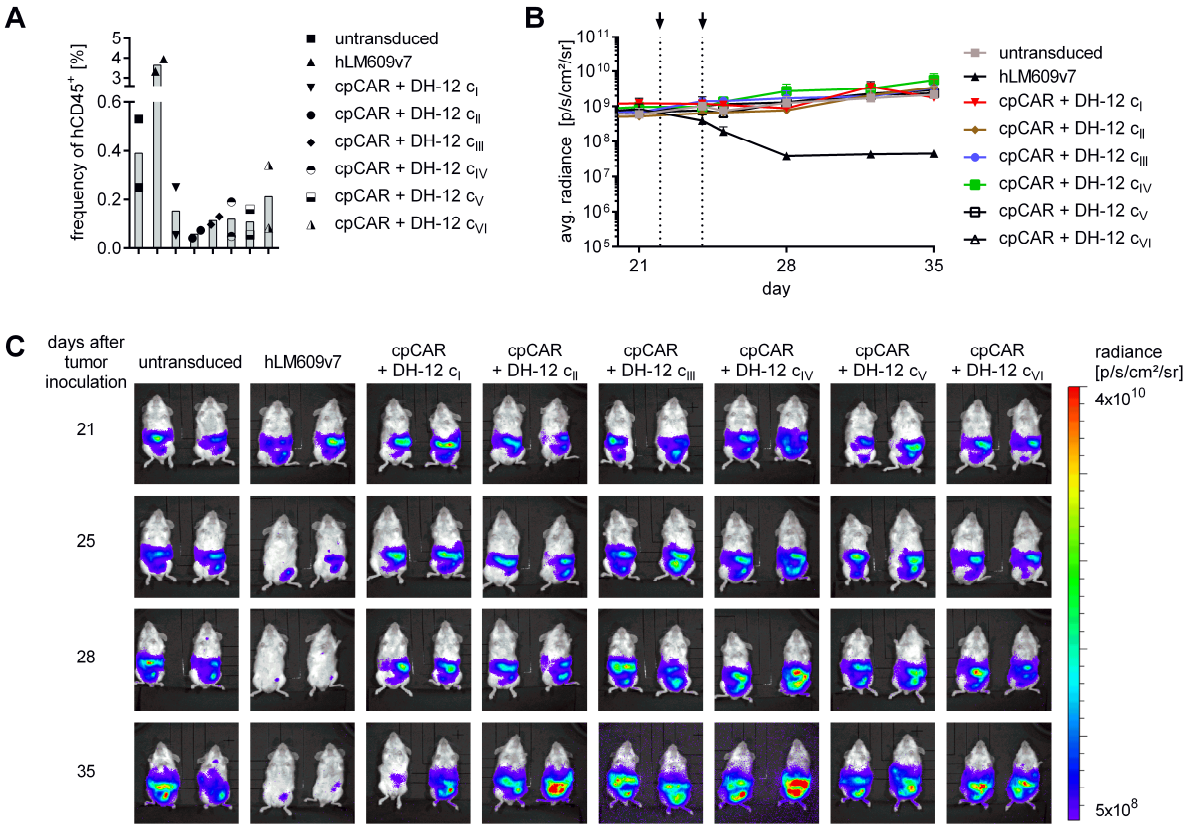

Figure 26: Effect of *in vivo* programmed cpCAR T cells on the growth of metastatic melanoma in a murine xenograft model with both components injected intraperitoneally.

Mice from the experiment shown in Figure 25 that did not respond to T cell treatment (groups untransduced + DH-12 i.p., cpCAR, cpCAR + DH-12 i.p., cpCAR + DH-12 i.v.) were randomly reassigned to new groups of n = 2 mice. Twenty-two days after initial tumour inoculation, mice were treated with a single dose of $5x10^6$ T cells i.p., either untransduced, or modified to express hLM609v7/short CAR or cpCAR. Mice of the cpCAR groups received injections of DH-12 (c_I = 205 µg/ml, c_{II} = 62.5 µg/ml, c_{III} = 20.5 µg/ml, c_{IV} = 6.25 µg/ml, c_V = 2.05 µg/ml, c_{VI} = 0.625 µg/ml) i.p. on day 22 and day 24. **(A)** Percentage of $hCD45^+$ (gated on live $7\text{-}AAD^-$ cells) in peripheral blood of mice on day 28. **(B)** Progression or regression of bioluminescence signal obtained from regions of interest encompassing the entire body of each mouse. Arrows mark the injection of DH-12. **(C)** Bioluminescence images depicting signal intensity and localisation generated by A-375/ffluc_GFP^+ tumour cells in groups of mice that remained untreated or were treated with untransduced, hLM609v7/short or hLM609v11/short $\alpha_v\beta_3$-CAR T cells.

Next, we investigated the anti-tumour effect of cpCAR T cells in a mouse xenograft model with continuous release of the hapten-compound by an osmotic pump. We hypothesised that a continuous release of cRGD-DK compound could prolong the therapeutic window in which cpCAR T cells are programmed towards integrin $\alpha_v\beta_3^+$ tumour cells. In this experiment, $1x10^6$ A-375 cells were injected i.v. into NSG mice. After 7 days, T cells, either unmodified or modified to express hLM609v7-CARs or cpCARs, were administered i.v. and osmotic pumps were implanted into the neck area of mice receiving the cpCAR. The osmotic pumps were loaded with four different concentrations of DH-14 compound (c_I = 2.5 mg/ml, c_{II} = 0.25 mg/ml, c_{III} = 0.025 mg/ml and c_{IV} = 0.0025 mg/ml), which was released over a period of 7 days. Three of the 8 animals (one of group c_{II} and two of group c_{IV}) implanted with osmotic pumps had to be excluded from the experiment during the first week of T cell treatment. We monitored the course of bioluminescence generated by A-375/ffluc$^+$ cells and observed a strong decrease in the signal in 3 of 3 mice treated with hLM609v7-CAR T cells. In 2 of 3 mice in this group, the bioluminescence decreased to background intensity, suggesting complete tumour eradication (Figure 27 A). No specific anti-tumour effect was observed for cpCAR T cells programmed with DH-14 (Figure 27 B).

Collectively, we did not observe an anti-tumour effect of cpCAR T cells in various murine xenograft models where the hapten-compound was injected i.v. or i.p. or released by an osmotic pump.

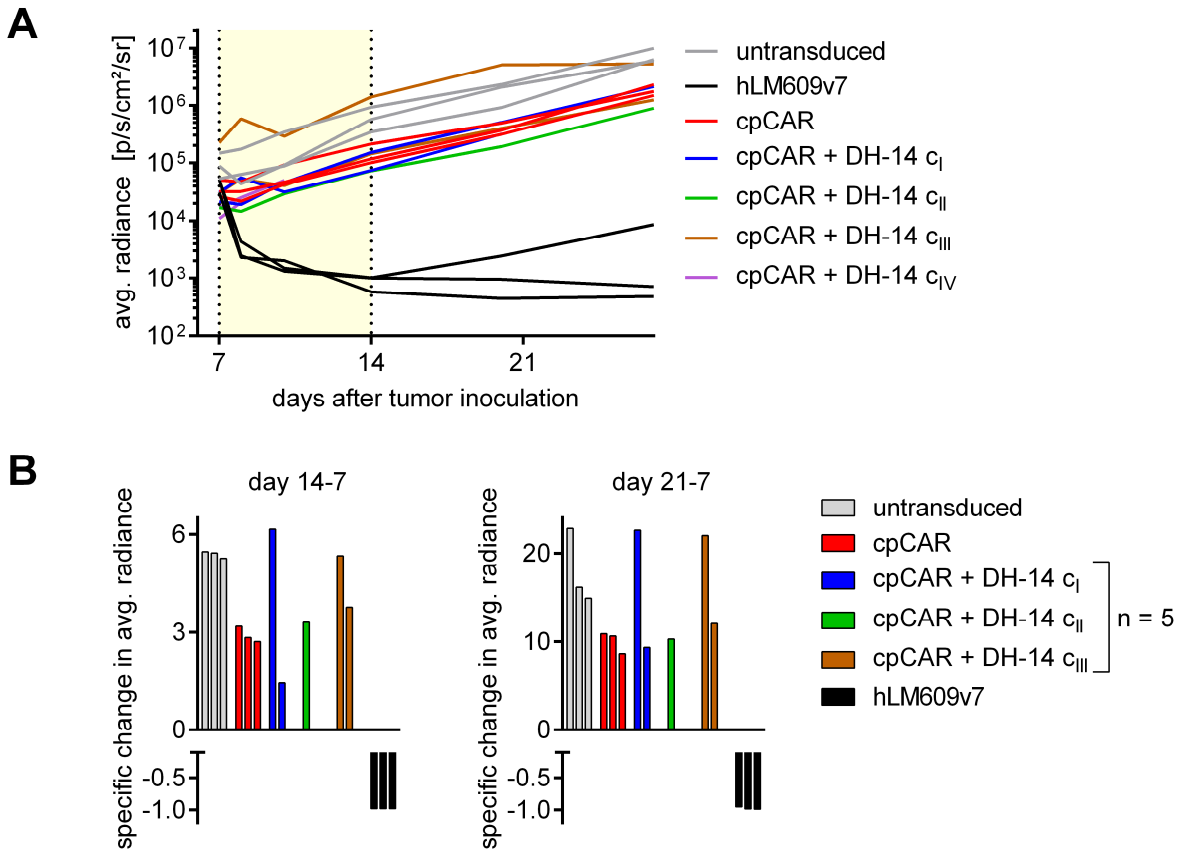

Figure 27: Growth of A-375 melanoma in a mouse xenograft model with cpCAR T cells and continuous release of the cRGD-DK compound DH-14 from an osmotic pump.
Mice were injected with 1x10^6 A-375/ffluc_GFP$^+$ tumour cells i.v. and treated with a single dose of 5x10^6 T cells i.v. 7 days later. Groups of n = 3 mice either received untransduced, hLM609v7 short or cpCAR T cells. Additionally, 4 groups of n = 2 mice received cpCAR T cells and were implanted with an osmotic pump continuously releasing DH-14 over a period of 7 days. **(A)** Progression or regression of bioluminescence obtained from regions of interest encompassing the entire body of each mouse. The shaded area indicates the period during which DH-14 was released. **(B)** Waterfall plots depicting the specific change in bioluminescence of single mice between day 7 and 14 on the left and between day 7 and 21 on the right.

4.2.7 Anti-tumour effect of cpCAR T cells pre-programmed *in vitro* with cRGD-DK in a murine xenograft model

Next, we evaluated the *in vivo* anti-tumour effect of cpCAR T cells that were pre-programmed with the cRGD-DK compound DH-14 *in vitro*. We assumed that pre-programming the cpCAR with DH-14 *in vitro* could increase the reactivity of cpCAR T cells in the mice because pre-programmed cpCAR T cells should be active directly after injection, without the need to first bind DH-14 *in vivo*. As we observed earlier in this study that the programming of cpCAR with biotin-DK is reversible, we choose to inject mice multiple times with pre-programmed cpCAR T cells.

NSG mice that were injected with $1x10^6$ A-375/ffluc_GFP$^+$ tumour cells i.v. on day 0, received a total of 3 dosages of T cells, applied on day 7, 9 and 11 after tumour inoculation. We injected n = 5 mice per group with either untransduced, hLM609v7-CAR, cpCAR or pre-programmed cpCAR T cells. The pre-programming was conducted with 1000 nM DH-14 compound at 37 °C for 1 h in medium *in vitro* shortly before the T cells were injected. We analysed blood samples obtained 7 days after the first T cell injection for the frequency of hCD45$^+$ cells (Figure 28 A). Human T cells were detectable in all treatment groups. We assessed the progression and regression of the tumour burden by bioluminescence imaging (Figure 28 B). Bioluminescence initially decreased for all mice treated with hLM609v7-CAR T cells and we did not detect any residual tumour in 2 out of the 5 animals on day 35. We calculated the specific change in average radiance of each individual mouse in order to analyse the increase and decrease of bioluminescence in greater detail (Figure 28 C). A statistically significant effect between the groups that received CAR T cells and the group that received untransduced T cells was only observed for the hLM609v7-CAR treated mice. We assessed how many mice of each group had a specific change in average radiance of >2, in the first week of treatment between day 7 and day 14. We observed a trend suggesting an anti-tumour effect of pre-programmed cpCAR T cells, because 5 out of 5 mice in the untransduced group and 4 out of 5 mice in the unprogrammed cpCAR group but only 2 out of 5 mice presented a specific change in average radiance of >2. However, this trend was only observed in the first week of T cell treatment, probably because the programming of cpCAR with DK-compounds is reversible.

In summary, the data suggest a slight *in vivo* anti-tumour effect of cpCAR T cells that have been pre-programmed with cRGD-DK *in vitro*. However, in line with

stronger anti-tumour reactivity *in vitro*, we only observed tumour eradication by hLM609-CAR T cells in this murine xenograft model.

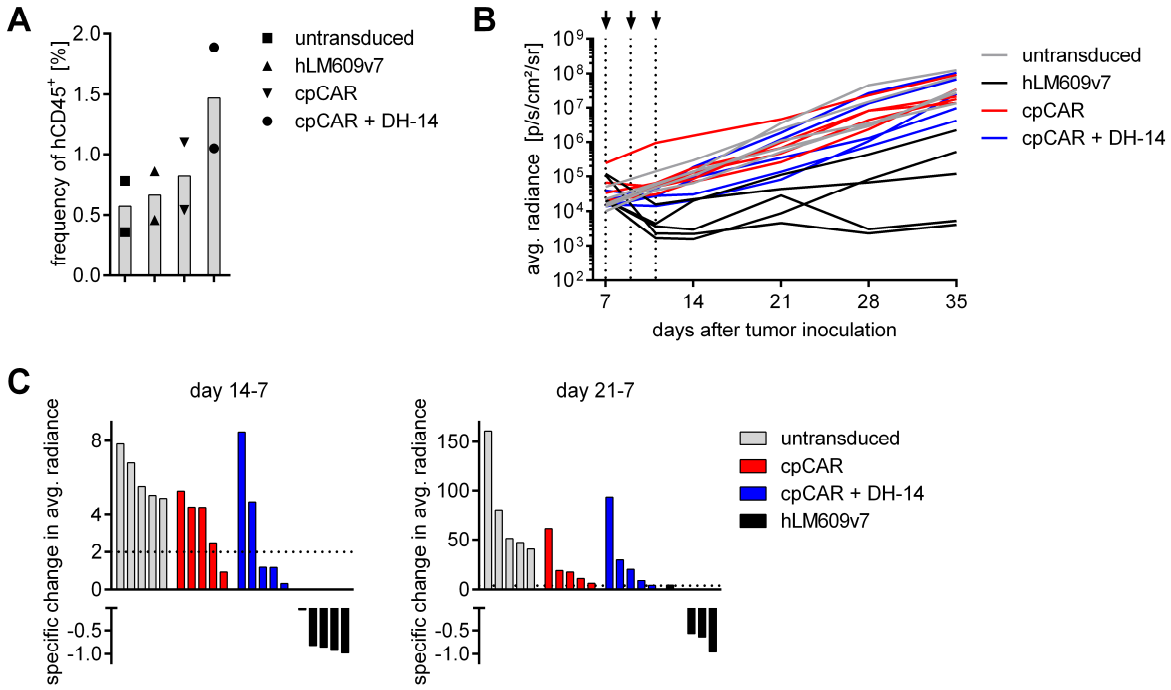

Figure 28: Effect of *in vitro* pre-programmed cpCAR T cells on the growth of metastatic melanoma in a murine xenograft model.

Mice were injected with 1x10^6 A-375/ffluc_GFP$^+$ tumour cells i.v. and treated three times (after 7 days, 9 days and 11 days) with 5x10^6 T cells i.v.. Groups of n = 5 mice either received untransduced, hLM609v7/short CAR or cpCAR T cells pre-programmed *in vitro* with DH-14. **(A)** Percentage of hCD45$^+$ (gated on live 7-AAD$^-$ cells) in peripheral blood of n =2 mice per treatment group on day 7 after T cell transfer. **(B)** Progression or regression of bioluminescence signal obtained from regions of interests encompassing the entire body of each mouse. Arrows mark the injections of DH-14. **(C)** Waterfall plots depicting the specific change in bioluminescence of single mice between day 7 and 14 (left diagram) and between day 7 and 21 (right diagram).

4.2.8 Interim conclusion

The data support our hypothesis that the chemically programmable mAB h38C2 can be integrated into a CAR design that retains the chemical reactivity towards molecules containing a DK-group. We used cRGD-DK hapten-compounds to program cpCAR T cells against the integrin $\alpha_v\beta_3$. cpCAR T cells programmed with cRGD-DK specifically lysed $\alpha_v\beta_3^+$ target cells, produced cytokines and proliferated after stimulation with $\alpha_v\beta_3^+$ target cells. We observed a trend, that cRGD-DK hapten-compounds containing longer PEG-linkers induced stronger cytokine production and proliferation of cpCAR T cells. hLM609-CAR T cells, which directly bind integrin $\alpha_v\beta_3$ via their scFv, induced stronger *in vitro* anti-tumour responses compared to cpCAR T cells programmed with cRGD-DK. This was also observed during *in vivo* testing, where only hLM609-CAR T cells were able to induce tumour eradication in an A-375 melanoma xenograft.

4.3 Targeting of integrin $\alpha_4\beta_1$ and folate receptor 1 with a chemically programmable CAR

4.3.1 Activation of the T cell signalling cascade in cpCAR reporter cells programmed against integrin $\alpha_4\beta_1$

We sought to prove the concept of universal applicability of cpCAR T cells by targeting multiple antigens on tumour cells and selected the integrin $\alpha_4\beta_1$ as a target for cpCAR T cells. We programmed cpCAR reporter cells with LLP2A-biotin-diketone (LLP2A-DK) compound CN-31 to interact with integrin $\alpha_4\beta_1$ (Figure 29 A+B). LLP2A is a peptidomimetic that binds with high affinity and specificity to the open conformation of integrin $\alpha_4\beta_1$. Acute monocytic leukaemia cell line THP-1 expresses both integrin subunits α_4 and β_1 (Figure 29 C). The CN-31 compound has a biotin unit, so we were able to use SA-PE to confirm the binding of the compound to the integrin complex on THP-1 cells by flow cytometry (Figure 29 D). Interestingly, when we used CN-31 in a reporter assay to program cpCAR reporter cells, we detected activation of NFAT and NF-κB regardless of whether or not $\alpha_4\beta_1$ positive THP-1 cells were present (Figure 29 D). We examined the reporter cells and detected high levels of both integrin subunits by flow cytometry (Figure 29 E). We also demonstrated the binding of the programming compound CN-31 to the reporter cells (Figure 29 F). This suggests that by programming cpCAR reporter cells with CN-31, the cpCAR can interact with integrin $\alpha_4\beta_1$ expressed on other reporter cells and subsequently induces the activation of the T cell signalling cascade.

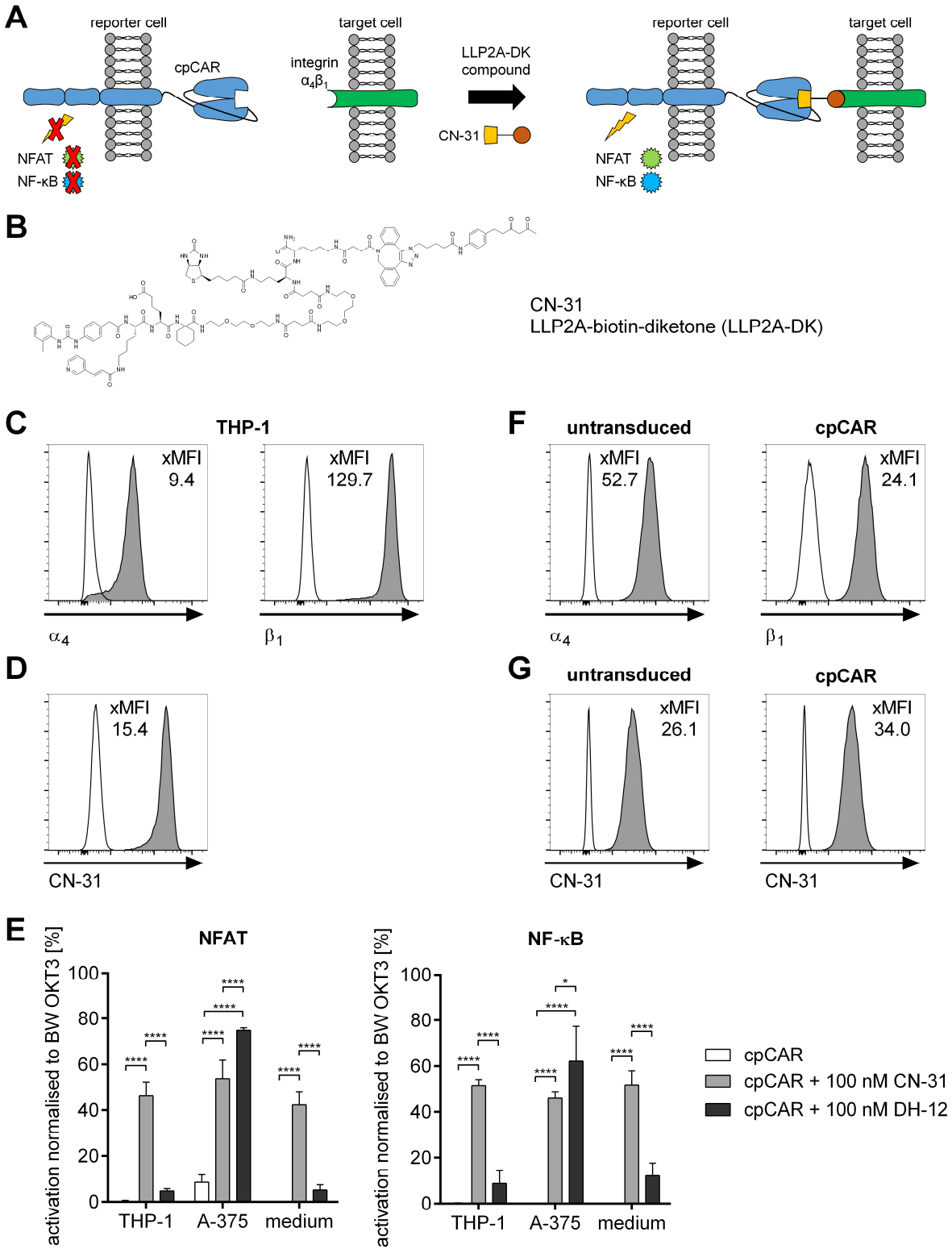

Figure 29: cpCAR reporter cells programmed to target integrin $\alpha_4\beta_1$ trigger T cell signalling cascade.

(A) Schematic representation of cpCAR programming with LLP2A-DK compound CN-31 to equip the cpCAR with a specificity against integrin $\alpha_4\beta_1$. **(B)** Structural formula of CN-31. **(C)** Flow cytometric analysis of α_4 and β_1 integrin-subunit expression on tumour cell lines. The ratio between the geometric mean fluorescent intensity of anti-α_v or anti-β_3 mABs (dark grey) and

their corresponding isotype controls (clear) is provided as fold MFI (xMFI). **(D)** THP-1 cells incubated with 100 nM CN-31. The ratio between the geometric mean fluorescent intensity of programmed (dark grey) and unprogrammed cells (clear) is provided as xMFI **(E)** Activation of NFAT and NF-κB of untransduced or cpCAR reporter cells cultured with THP-1, A-375 cells or alone and 100 nM CN-31 or DH-12. Presented is the mean of n = 3 experiments, error bars depict SD; **** $p<0.0001$. **(F)** Flow cytometric analysis of α_4 and β_1 integrin-subunit expression on reporter Jurkat cells. The ratio between the geometric mean fluorescent intensity of anti-α_v or anti-β_3 mABs (dark grey) and their corresponding isotype controls (clear) is provided as fold MFI (xMFI). **(G)** Untransduced or cpCAR reporter cells incubated with 100 nM CN-31. The ratio between the geometric mean fluorescent intensity of programmed (dark grey) and unprogrammed cells (clear) is provided as xMFI.

4.3.2 *In vitro* anti-tumour function of cpCAR T cells programmed against FOLR1

We next sought to program cpCAR T cells against the FOLR1 with folate-biotin-diketone compound (folate-DK), which has been described in a previous study with h38C2 in a diabody format (Walseng *et al.*, 2016) (Figure 30 A). Because the folate-DK compound, termed DH-02, possesses a biotin unit we used flow cytometry to validate its binding to THP-1 cells, which are reported to highly express FOLR1 (Figure 30 B).

DH-02 did not bind to THP-1 cells cultured under standard conditions in RPMI medium with 10 % FCS (Figure 30 C). However, after 20 days of folate-free culture, 4 % of THP-1 cells bound the folate compound (Figure 30 D). The percentage of DH-02 positive THP-1 cells increased rapidly over the following two weeks of folate-free culture and reached 96 % after 36 days. In addition, the specific programming of cpCAR T cells, after incubation with the DH-02 compound, was confirmed by flow cytometry (Figure 31 A+B).

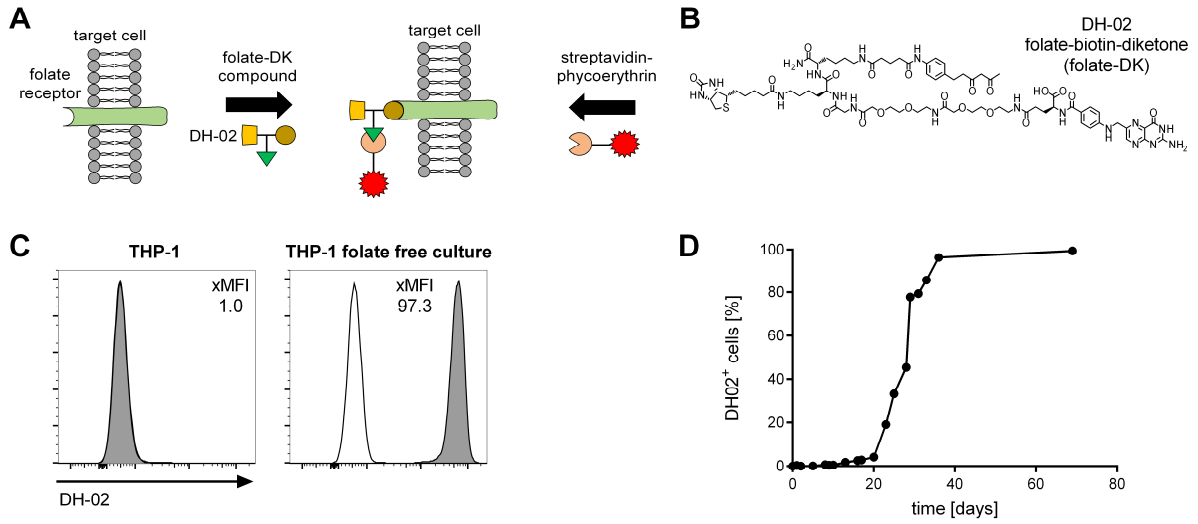

Figure 30: Binding of folate-biotin-diketone to THP-1.
(A) Schematic representation of folate-DK compound DH-02 binding to the folate receptor. **(B)** Structural formula of folate-biotin-diketone. **(C)** Flow cytometric analysis of DH-02 binding to THP-1 cells cultured with or without folate. The ratio between the geometric mean fluorescent intensity of cells incubated with DH-02 (dark grey) and cells without (clear) is provided as fold MFI (xMFI). **(D)** Time course of DH-02 binding to THP-1 cells after folate is removed from the culture medium. The percentage of DH-02$^+$ cells was determined by flow cytometry.

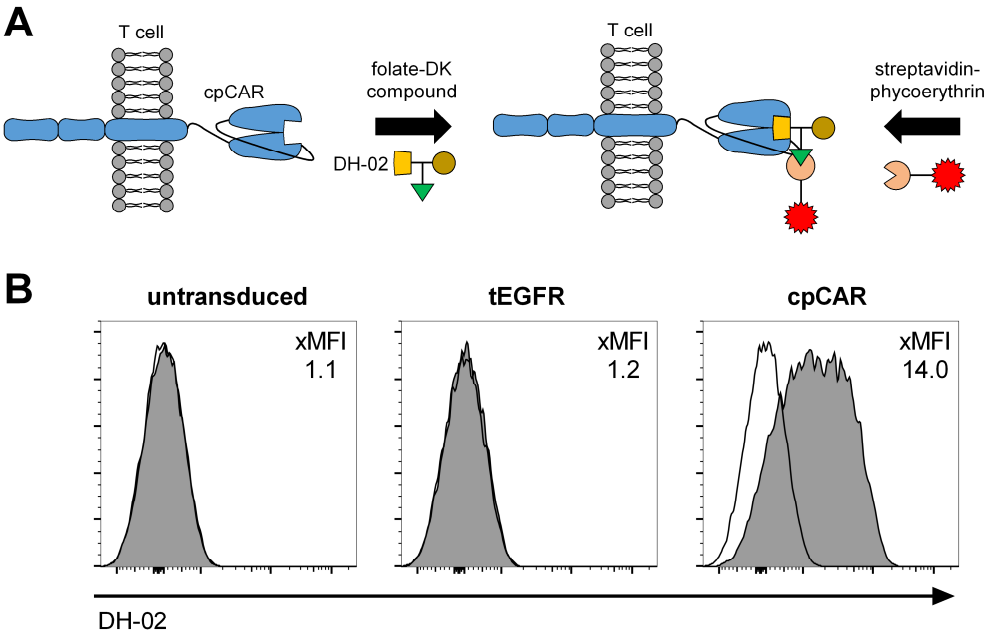

Figure 31: Binding of folate-biotin-diketone to cpCAR T cells.
(A) Schematic representation of cpCAR programming with folate-DK compound DH-02. **(B)** Flow cytometric analysis of untransduced, mock or cpCAR T cells incubated with 100 nM DH-02. The ratio between the geometric mean fluorescent intensity of programmed (dark grey) and unprogrammed cells (clear) is provided as xMFI.

We investigated if $CD8^+$ cpCAR T cells programmed with folate-DK compound could confer lysis of THP-1 cells that were cultured either with or without folate in the cell culture medium (Figure 32 A). We observed significant specific lysis of THP-1 cells cultured without folate by cpCAR T cells in the presence of c = 0.1 nM - to 100 nM DH-02 compared to unprogrammed cpCAR T cells (Figure 32 B). Interestingly, there was a trend that DH-02 concentrations between 1 nM - to 10 nM triggered the strongest anti-tumour effect. We did not observe reduced vitality of normally cultured THP-1 cells by DH-02-programmed cpCAR T cells, which further confirms the specificity of cpCAR-induced effects.

To characterise the extent of T cell activation by cpCARs programmed with folate-DK in more detail, we analysed the proliferation of $CD4^+$ cpCAR T cells in a CFSE-dye dilution assay. We detected marginal division of cpCAR T cells in the presence of 1 nM – to 10 nM DH-02 and THP-1 cells cultured without folate (Figure 32 B). We further analysed if the fraction of dividing cells can be increased by adding irradiated THP-1 cells and folate-DK compound again after 24 h and 48 h. Indeed, the repeated stimulation with folate free cultured THP-1 cells led to a clearly detectable proliferation of cpCAR T cells programmed with 1 nM – to 10 nM DH-02 (Figure 32 C). In accordance with the observations regarding the lysis of tumour cells, the highest tested concentration of 100 nM DH-02 did not mediate the strongest proliferation of cpCAR T cells. Normally cultured THP-1 cells did not induce proliferation of any of the T cell lines tested and THP-1 cells cultured without folate did not cause untransduced, EGFRt or unprogrammed cpCAR T cells to divide.

In summary, the data show the ability of the folate-DK compound DH-02 to bind to both the cpCAR and the folate receptor. When cpCAR T cells and folate-free cultured tumour cells were incubated together, DH-02 induced tumour cell lysis and cpCAR T cell proliferation.

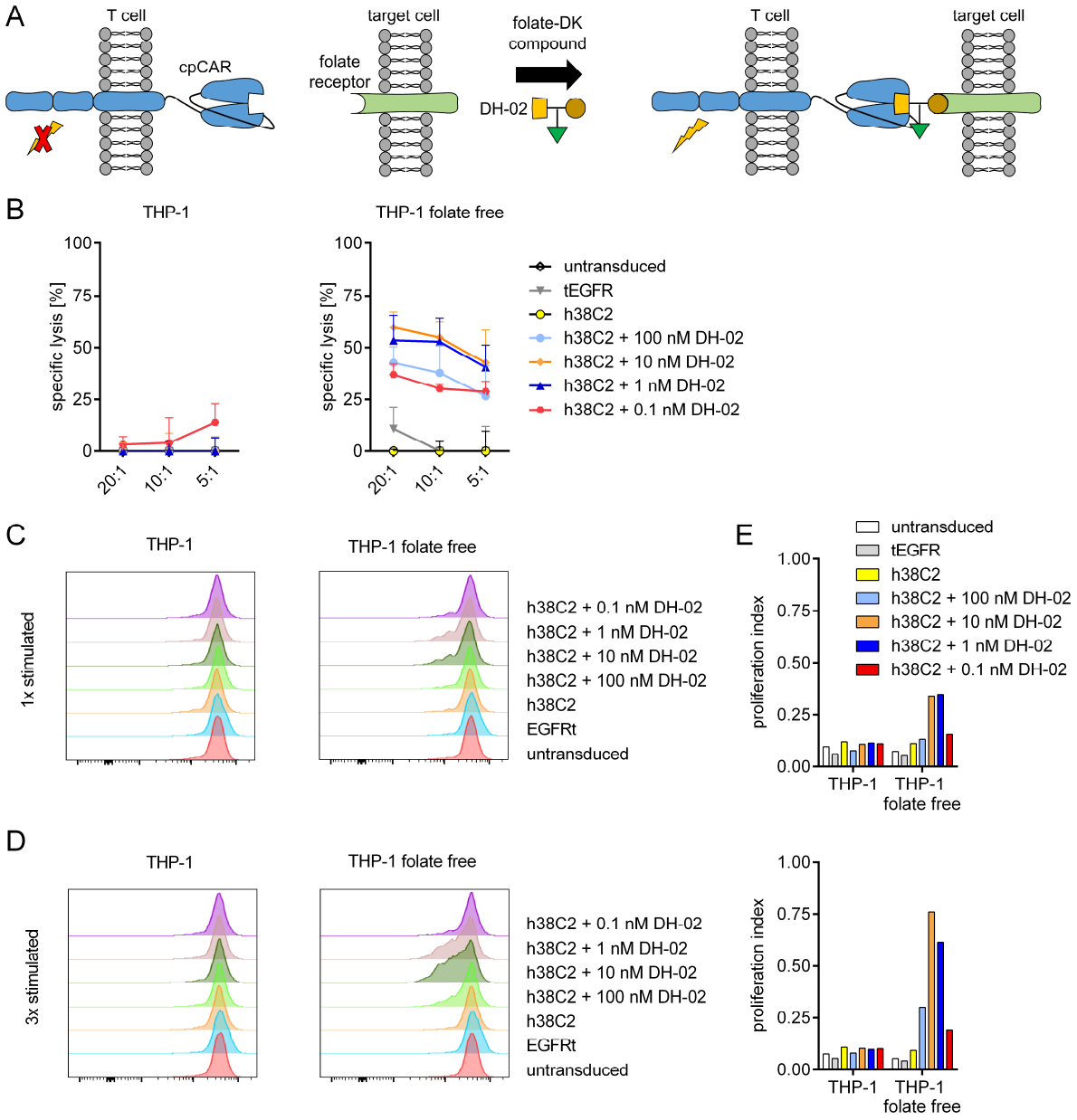

Figure 32: cpCAR T cells programmed to target the folate receptor lyse tumour cells. **(A)** Schematic representation of cpCAR programming with folate-DK compound DH-02 to equip the cpCAR with a specificity against integrin $\alpha_4\beta_1$. **(B)** Specific lysis of ffluc_GFP$^+$ tumour cell lines by folate-programmed cpCAR modified CD8$^+$ T cells after 4 h. Presented is the mean of n = 3 experiments, error bars depict SD. **(C)** Proliferation of CFSE-labelled CD4$^+$ cpCAR-expressing T cells after 72 h co-culture with irradiated tumour cells and different amounts of DH-02. The histograms show data from one experiment. **(D)** Proliferation of CFSE-labelled CD4$^+$ cpCAR-expressing T cells after 72 h co-culture with irradiated tumour cells added at 0 h, 24 h and 48 h and addition of different amounts of DH-02. The histograms show data from one experiment **(E)** Proliferation index of CD4$^+$ T cells. Presented is data from one experiment.

5 Discussion

CAR T cell therapy is an immunological treatment for cancer. The high rate of complete remission in the treatment of B cell malignancies with CD19-CAR T cells illustrates the clinical relevance of this novel therapy. However, antigen-negative relapses after CD19-CAR T cell therapy have been reported and provide a strong rationale to develop new strategies to counteract tumour escape, e.g. by simultaneously or sequentially targeting additional tumour-associated antigens such as CD22 (Fry *et al.*, 2018). Additionally, the translation of CAR T cell therapy from hematologic to prevalent solid malignancies might also require targeting of multiple tumour-associated antigens, because these antigens are often heterogeneously expressed within the tumour (Fesnak, June and Levine, 2016). Here, we introduced a novel cpCAR that can be chemically programmed with molecules containing a DK-group. Therefore, cpCAR T cells can be equipped with specificity against multiple antigens using hapten-compounds containing a DK-group. We demonstrated T cell activation mediated by programmed cpCARs against the integrins $\alpha_v\beta_3$ and $\alpha_4\beta_1$, and FOLR1. However, in the first part of this study, we generated conventional CAR T cells against $\alpha_v\beta_3$ to establish $\alpha_v\beta_3$ as a suitable target for CAR T cells and to generate a conventional CAR as a reference for evaluating the function of cpCARs.

5.1 A conventional CAR targeting integrin $\alpha_v\beta_3$

In this study, we introduced integrin $\alpha_v\beta_3$-CAR T cells based on humanised affinity variants of mAB LM609 (Rader, Cheresh and Barbas, 1998). The receptor design was optimised for maximal anti-tumour function *in vitro* and *in vivo* with regard to the length of the extracellular spacer and the affinity of the scFv towards its antigen. T cells modified to express $\alpha_v\beta_3$-CARs with the optimised receptor design exhibited specific tumour lysis, cytokine production and proliferation against $\alpha_v\beta_3^+$ cancer cells *in vitro* and completely eradicated established A-375 melanoma in in a murine xenograft model.

Based on our data, $\alpha_v\beta_3$-CAR T cells with a short spacer confer superior anti-tumour function to $\alpha_v\beta_3$-CAR T cells with a long spacer as shown by higher cytokine production and stronger proliferation. This is consistent with our previous observations that the extracellular spacer design has a major impact on CAR T cell activation and function (Hudecek *et al.*, 2013, 2015). The paradigm that emerged from these studies

is that a long spacer domain is optimal for targeting epitopes that are proximal to the tumour cell membrane, while a short spacer domain is optimal for epitopes that are distal. The mAB LM609 recognises a membrane-distal epitope of integrin $\alpha_v\beta_3$, when the integrin is in its extended conformation (Borst *et al.*, 2017). The extended conformation is presumed to be prevalent on tumour cells expressing $\alpha_v\beta_3$ (Desgrosellier and Cheresh, 2010; Demircioglu and Hodivala-Dilke, 2016). Therefore, our data, showing superior anti-tumour functions of T cells expressing either of the two $\alpha_v\beta_3$-CARs with short spacer domain, are in support of the paradigm that short spacers support stronger anti-tumour functions of CAR T cells targeting epitopes distal to the tumour cell membrane.

We show that $\alpha_v\beta_3$-CAR T cells with short spacer domains eradicated metastatic A-375 cells in a mouse xenograft model. Interestingly, T cells with the low affinity hLM609v11-CAR caused increased IFN-ɣ and GM-CSF serum concentrations compared to the high-affinity hLM609v7-CAR, suggesting a better therapeutic effect, which is in contrast to our observations *in vitro*. Others have reported similar findings, e.g. for CAR T cells targeting ErbB2 (Liu *et al.*, 2015). One possible explanation is that, as the low-affinity variant hLM609v11 has a three times faster off-rate than the high-affinity variant hLM609v7 ($16x10^{-4}$ s^{-1} versus $5.4x10^{-4}$ s^{-1} measured for the corresponding monovalent Fab), hLM609v11-CAR T cells can elicit their anti-tumour effector functions with a higher frequency than hLM609v7-CAR T cells. This could accelerate the sequential killing of tumour cells and intensify the activation of CAR T cells. Additional experiments with more affinity variants are required to clearly define the sweet spot of $\alpha_v\beta_3$-CARs affinity.

Immunogenicity of the CAR can cause rejection of CAR T cells, particularly when CAR T cells are administered multiple times (Lamers *et al.*, 2011; Turtle *et al.*, 2016).To minimise the immunogenicity of the $\alpha_v\beta_3$-CAR constructs, we used scFvs based on humanised LM609 variants. This should favour long-term persistence of CAR-modified T cells, which is a key factor for the clinical outcome. Notably, we used superhumanised variants of LM609 that only retained the third CDR of heavy and light chain variable domains of the parental mouse mAB LM609. All other CDRs and framework regions were replaced by respective human amino acid sequences (Rader, Cheresh and Barbas, 1998).

Compared to other recently published experimental treatments of A-375 melanoma in murine xenograft models, $\alpha_v\beta_3$-CAR T cells conferred superior efficacy.

Recent studies investigating a combination treatment with an oncolytic adenovirus and dacarbazine chemotherapy, and a study investigating the anti-tumour effect of itraconazole both reported tumour reduction but not tumour clearance (Yang *et al.*, 2016; Liang *et al.*, 2017)

Prior attempts of targeting integrin $\alpha_v\beta_3$ with CAR T cells have been reported that used a modified echistatin peptide, a disintegrin, which binds to both human and mouse $\alpha_v\beta_3$, as a targeting moiety, in contrast to our approach to facilitate antigen binding with an scFv (Fu *et al.*, 2013). These CAR T cells were tested in a syngeneic mouse model against B16 melanoma and reduced tumour growth compared to unmodified T cells but did not achieve tumour clearance. The echistatin-based CARs damaged the tumour vasculature, which was evident from haematomas in the tumour tissue, but spared other organs and caused no further toxicities. These results are encouraging with regards to the safety profile and to potential synergistic effects of targeting integrin $\alpha_v\beta_3$ with hLM609-based CAR T cells. Synergistic effects could result from simultaneous targeting of tumour cells and the tumour vasculature.

In addition, previous clinical studies with the humanised LM609 mAB vitaxin reported no severe side effects (Gutheil *et al.*, 2000; McNeel *et al.*, 2005; Delbaldo *et al.*, 2008; Hersey *et al.*, 2010). Integrin $\alpha_v\beta_3$ is expressed by some healthy tissues including angiogenic endothelial cells, osteoclasts, vascular smooth muscle cells, platelets, macrophages and hematopoietic stem cells (Clover, Dodds and Gowen, 1992; Felding-Habermann and Cheresh, 1993; Brooks, Clark and Cheresh, 1994; Umemoto *et al.*, 2012). However, none of these tissues were damaged by humanised LM609 mAB. While these results are not directly transferable to CAR T cells, owing to the enhanced reactivity of CAR T cells compared to mABs, which might increase the likelihood for off-tumour on-target toxicities, they still provide a strong rationale for further pursuing integrin $\alpha_v\beta_3$-CAR T cell therapy. $\alpha_v\beta_3$-CAR T cells with the low-affinity scFv hLM609v11 could provide a preferable safety profile, as it has been shown that CARs with high-affinity scFvs have reduced selectivity and are more likely to attack low antigen-expressing cells compared to CARs with low-affinity scFvs (Chmielewski *et al.*, 2004; Caruso *et al.*, 2015; Liu *et al.*, 2015). Because mAB LM609 was generated in mice and has no cross-reactivity to mouse integrin $\alpha_v\beta_3$, the safety profile has to be assessed in non-murine models. In addition to human, LM609 is known to recognize chicken, rabbit, dog, pig, cow, and monkey integrin $\alpha_v\beta_3$.

We predict that treatment with $\alpha_v\beta_3$-CAR T cells can surpass the limited therapeutic effect that was achieved with humanised LM609 mAB in clinical trials. These studies focused on the blocking effect of mAB LM609, by sterically hindering the interaction of proteins containing an RGD motif with the integrin, to limit tumour vascularisation (Borst *et al.*, 2017). As we demonstrate here, $\alpha_v\beta_3$-CAR T cells efficiently target cancer cells expressing integrin $\alpha_v\beta_3$. Additionally, we expect $\alpha_v\beta_3$-CAR T cells to also attack the tumour microenvironment and limit tumour angiogenesis by destruction of $\alpha_v\beta_3^+$ CAFs and tumour-associated blood vessels. Thus, we anticipate that our approach to target integrin $\alpha_v\beta_3$ has a stronger therapeutic effect against solid malignancies than previous attempts of targeting antigens that are solely expressed on cancer cells. Additionally, we hypothesise that $\alpha_v\beta_3$-CAR T cells will preferentially home to tumour sites due to integrin $\alpha_v\beta_3$ expression on tumour vasculature. Others have observed T cell enrichment in cancer sites *in vivo* using T cells equipped with a membrane bound fusion-molecule that targets integrin $\alpha_v\beta_3$ through the disintegrin kistrin (Legler *et al.*, 2004). Another interesting observation is the strong resistance of cancer cells expressing integrin $\alpha_v\beta_3$ to treatment with cisplatin and doxorubicin, the standard-of-care chemotherapy agents for treatment of several solid tumour malignancies (Brozovic *et al.*, 2008). This observation suggests that adoptive immunotherapy with $\alpha_v\beta_3$-CAR T cells may be used either concomitantly or sequentially do delete chemotherapy-resistant tumour cells.

In summary, we introduced novel $\alpha_v\beta_3$-CAR T cells based on mAB hLM609. In line with previous observations, the CAR's affinity to its antigen and the size of the extracellular spacer domain greatly influenced the anti-tumour efficacy of $\alpha_v\beta_3$-CAR T cells. Optimised $\alpha_v\beta_3$-CAR T cells were able to completely eliminate tumour lesions in a murine xenograft model. The broad expression of integrin $\alpha_v\beta_3$ on prevalent solid cancers and tumour-associated tissues illustrates the therapeutic potential of $\alpha_v\beta_3$-CAR T cells. Demonstrating that integrin $\alpha_v\beta_3$ is a possible target for CAR T cell therapy laid the foundation for our further studies with cpCAR T cells programmed against this antigen.

5.2 Targeting integrin $\alpha_v\beta_3$ with a novel cpCAR

Here we introduce cpCAR T cells based on the cpAB h38C2. We demonstrate that the cpCAR can be specifically programmed with hapten-compounds containing a DK-group. Additionally, the data show that cpCAR T cells programmed with cRGD-DK compounds conferred lysis of tumour cells expressing integrin $\alpha_v\beta_3$ *in vitro* and showed proliferation and production of cytokines as response to the antigen encounter.

We demonstrate that cpCARs can be specifically programmed with molecules containing a DK-group. This suggests that the scFv derived from h38C2 retains the tertiary structure observed for the mAB h38C2, which contains a hydrophobic pocket with a reactive lysine residue at its bottom (Rader, Turner, *et al.*, 2003). The cpAB forms a covalent reversible bond between this reactive lysine and the DK-group (Rader, 2014). We have also observed that the amount of DK-programmed cpCARs on the cell surface decreased over time, suggesting that the cpCAR forms a reversible bond with DK-molecules. However, apart from chemical characteristics of the bond, protein turnover on the cell membrane could also influence the quantity of detectable programmed cpCARs. The specific and reversible interaction between the cpCAR and molecules containing a DK-group supports our hypothesis that the principle mode of action of cpABs could be transferred to CAR T cell technology. Furthermore, these data are encouraging regarding the applicability of the cpCAR approach, as it has been shown that cpAB 38C2 can be programmed *in vivo* with DK-compounds, an essential feature for the generation of CARs that can be equipped with multiple specificities (Rader, Sinha, *et al.*, 2003; Popkov *et al.*, 2006).

We used cRGD-DK compounds to equip cpCARs with a specificity against integrin $\alpha_v\beta_3$. In the presence of $\alpha_v\beta_3$-positive tumour cell lines, cpCAR T cells programmed towards $\alpha_v\beta_3$ mediated lysis of tumour cells, produced pro-inflammatory cytokines and proliferated *in vitro*. This confirms that the covalent connection between cpCARs and DK-molecules is sufficient to enable T cell activation. However, the anti-tumour effects of T cells equipped with a conventional hLM609-based $\alpha_v\beta_3$-CAR exceeded the effects mediated by cpCAR T cells. A potential explanation for the difference in efficacy could be that the affinity of the cRGD to integrin $\alpha_v\beta_3$ is lower than that of the hLM609v7 scFv, as described for a similar cRGD-DK compound and the mAB LM609 (Popkov *et al.*, 2009). Additionally, the cpCAR has to bind to the DK-group of the hapten-molecule and the reversibility of this reaction may further reduce the avidity of the programmed cpCAR T cell. Further investigations how the affinity of the

hapten-molecule towards the target antigen affects cpCAR T cell function are pending. Because structurally diverse RGD compounds with different affinities to $\alpha_v\beta_3$ have been described, targeting $\alpha_v\beta_3$ with RGD-DK compounds is a suitable model for further studies on this topic (Popkov *et al.*, 2009).

cpCAR T cells did not confer complete tumour eradication in murine xenograft melanoma models, while hLM609v7-CAR T cells did. This observation correlates with our *in vitro* data showing a higher anti-tumour efficacy of hLM609-CAR T cells than of cpCAR T cells. It suggests that the design of cpCAR T cells and the pharmacokinetics of the hapten-compound need to be improved to achieve tumour reduction *in vivo*. One aspect could be to replace the promoter that regulates the expression of the cpCAR from EF1 to a promoter with higher or more stable transgene expression. We and others have observed that transgene expression under control of the EF1 promoter depends on the activation state of the T cell and increases upon T cell stimulation (Eyquem *et al.*, 2017). Possibly, the amount of cpCAR on the T cell membrane was too low to bind sufficient amounts of the cRGD-DK in order to induce complete T cell activation and subsequently control tumour growth *in vivo*. We will investigate in the future if a promoter with higher or more stable expression of the cpCAR than EF1 can enhance the anti-tumour activity mediated by cpCAR T cells. In addition, the costimulatory domain of the cpCAR could also be exchanged. It has been demonstrated that CAR T cells with a costimulatory domain derived from 4-1BB mediate a stronger anti-tumour effect and persist longer in murine xenograft models compared to CAR T cells with CD28 costimulation (Guedan *et al.*, 2018) This could be attributed to the preferential differentiation of CAR T cells with 4-1BB costimulation into persistent central memory T cells whereas CD28 costimulation favours differentiation into effector memory T cells (Kawalekar *et al.*, 2016). However, the optimal costimulatory domain needs to be identified for every CAR construct. The faster induction of anti-tumour effects observed for effector memory T cells compared to central memory T cells could also be beneficial to induce an anti-tumour response with cpCAR T cells *in vivo*. Besides the design of the cpCAR, dosage and serum half-life of hapten-compounds are probably also crucial aspects that influence the anti-tumour effect of cpCAR T cells *in vivo*. For optimal cpCAR T cell function, the sweet spot for the concentration of the cRGD-DK compound needs to be identified. The dosage should not be too high to avoid saturation of both cpCAR and $\alpha_v\beta_3$ integrin, because a saturation would inhibit their interaction. Nonetheless, the concentration has to be

sufficiently high to allow programming of the cpCAR or binding to the integrin. In order to define an adequate dosing and treatment regimen for cRGD-DK to facilitate cpCAR T cell function *in vivo*, the serum half-life of the compound is also important. A longer half-life might prolong the anti-tumour response mediated by cpCAR T cells, whereas a compound with a shorter half-life might need to be administered more frequently to maintain its concentration at the sweet spot.

We have demonstrated in this and other studies that the size of the extracellular spacer greatly affects CAR T cell function due to the spatial interaction between the CAR and its respective antigen (Hudecek *et al.*, 2015). To replicate these findings for cpCARs, we analysed a panel of cRGD-DK compounds with an increasing number of PEG units. The compounds had either 2, 4, 6 or 8 mini-PEG units. Because each of these units has a length of approximately 10 Å, they covered a range between 20 Å and 80 Å. For comparison, the length of an Ig domain is about 40 Å. The spacer of the cRGD-DK compound with 8 mini-PEG units should therefore have approximately the same length as a C_H2-C_H3 extracellular spacer. This corresponds to the difference between the short (IgG4 hinge) and long (IgG4 hinge-C_H2-C_H3) extracellular spacers we used for examination of the hLM609-CARs (correspondence with C. Rader). We observed a trend that multiple repeats of PEG-molecules in cRGD-DK compounds were favourable for cpCAR T cell function regarding cytokine production and proliferation *in vitro*. However, these results are in contrast to hLM609 based $\alpha_v\beta_3$-CARs, where a short extracellular spacer induced stronger T cell activity than a long spacer. Intriguingly, the epitope of LM609 and the binding site of the RGD ligand of $\alpha_v\beta_3$ integrin are in close proximity. Since the optimal spacer length of directly binding hLM609-CARs and cpCARs is different, there seem to be further mechanisms for the cpCAR to benefit from the longer hapten-molecules with several mini-PEG units. The greater distance between the cRGD targeting unit and the cpCAR binding DK-unit could provide greater flexibility and thus better accessibility of the ligand binding site on $\alpha_v\beta_3$ when the hapten-molecule is bound to the cpCAR. Vice versa, when the hapten-molecule is connected to $\alpha_v\beta_3$, the DK-unit could be better reached by the cpCAR, if the hapten-molecule is equipped with a longer spacer. In addition, compounds with multiple mini-PEG units bestow a larger hydrodynamic radius conveying longer half-life. However, this effect is confined to *in vivo* models.

We used cRGD-DK compounds to program cpCAR T cells against integrin $\alpha_v\beta_3$. We did not observe an anti-tumour effect of the cRGD-DK compound alone.

However, RGD compounds with an intrinsic anti-tumour reactivity have been described (Duro-Castano *et al.*, 2017). For example, the small molecule cilengitide, an integrin α_v antagonist, can trigger anoikis, which is a form of programmed cell death, in angiogenic blood vessels and brain tumour cells by preventing interactions with matrix ligands such as fibronectin or vitronectin (Yamada *et al.*, 2006). Cilengitide reduced tumour growth in murine xenograft models and proceeded to phase III clinical trials, where it was considered safe, but its therapeutic effect was limited (Weller *et al.*, 2016). However, it is encouraging that such compounds have already been tested in clinical trials without causing critical adverse events. The failure of cilengitide has been partially attributed to suboptimal binding properties of RGD-peptidomimetics to integrin $\alpha_v\beta_3$ since the therapeutic success did not correlate with integrin expression. RGD-mimetics can only bind to integrin $\alpha_v\beta_3$ with high affinity if it is in its extended conformation with an open head and has no ligand bound (Demircioglu and Hodivala-Dilke, 2016). This shows that the binding properties of RGD-based hapten-compounds need to be carefully investigated before clinical translation.

The scFv encompassing the reactive centre of the cpCAR is derived from the humanised mAB h38C2. For construction of h38C2, the catalytic centre of the mouse mAB 38C2, which comprises a deep hydrophobic pocket with a reactive lysine residue at the bottom, was introduced into a human antibody framework (Rader, Turner, *et al.*, 2003). A clinical study with CAR T cells targeting carbonic anhydrase IX (CAIX) reported on immune responses against the CAR in a majority of the patients (Lamers *et al.*, 2011). The CAIX-CAR was based on a murine scFv and immunogenic epitopes were identified in the V_H and V_L regions of the scFv. We assume that the humanised scFv is less immunogenic and should allow for better engraftment than CARs with murine scFv. However, clinical trials with CovX-Bodies reported on occurrence of anti-cpAB antibodies in a fraction of patients (Rader, 2014). *In silico* T cell epitope analysis predicted that the h38C2 V_L domain has a higher risk of immunogenicity than the V_H domain (Nanna *et al.*, 2017). Further research is necessary to determine, whether the scFv used in the CAR format would induce an immune reaction.

5.3 Targeting of integrin $\alpha_4\beta_1$ and folate-receptor with cpCAR

Our data demonstrate specific cpCAR T cell activation and toxicity against tumour cell lines that either express $\alpha_v\beta_3$, $\alpha_4\beta_1$ or folate receptor. This supports our hypothesis that cpCAR T cells can be programmed to target different antigens on malignant cells and are a major advantage over monospecific CAR T cells. The necessity to target multiple antigens is evident from the clinical experience with CAR T cell therapy. On the one hand, antigens on tumour cells can be downregulated or mutated as reported in clinical studies targeting CD19 or CD22 (Sotillo *et al.*, 2015; Fry *et al.*, 2018). On the other hand, malignant cells, especially from solid cancers, can have heterogeneous expression of tumour-associated antigens. Thus, monospecific CAR T cell therapy may select for tumour cells with dim or absent target expression as observed in a clinical trial with glioblastoma patients treated with EGFRvIII-CAR T cells (O'Rourke *et al.*, 2017).

Integrin $\alpha_4\beta_1$, also termed very late antigen-4 (VLA-4), is expressed on hematopoietic cells, e.g. thymocytes, monocytes and activated T and B lymphocytes (Schlesinger and Bendas, 2015). Through interaction with its ligands, fibronectin 1 and vascular cell adhesion molecule 1 (VCAM-1), VLA-4 controls homing and trafficking of lymphocytes (Masumoto and Hemler, 1993; Cui *et al.*, 2012). The expression of integrin $\alpha_4\beta_1$ is documented on B-ALL, AML, mantle cell lymphoma and other hematologic malignancies, but also on solid cancers, e.g. melanoma and ovarian cancer (Blenc *et al.*, 2003; Matsunaga *et al.*, 2003; Kurtova *et al.*, 2009; Scalici *et al.*, 2014). The expression of integrin $\alpha_4\beta_1$ contributes to the metastasis of tumour cells and can enhance their resistance to chemotherapeutics, which makes it an interesting target for cancer therapy. However, the expression on healthy hematopoietic cells suggests a risk for on-target off-tumour effects. Interestingly, LLP2A, which we use as targeting moiety for cpCAR T cells, binds preferentially to malignant cells and only in the presence of Mn^{2+} to PBMCs, suggesting that it can only bind to the activated form of integrin $\alpha_4\beta_1$ (Peng *et al.*, 2006). Further inquiries into the binding of LLP2A to healthy and malignant tissues are necessary to decide if targeting $\alpha_4\beta_1$ on cancer cells with cpCAR T cells can be translated into the clinic.

Folate, or vitamin B9, is critical for the one-carbon metabolism and DNA synthesis. Thus, the uptake of folate is especially important for proliferating cells. High expression of FOLR1 on tumour cells allows them to compete with other cells for folate. High and uniform expression of folate receptors has been shown for nasopharyngeal,

cervical and ovarian carcinoma (Antony, 1996). Conventional CAR T cells, targeting folate receptor α or folate receptor β by directly binding via their scFv, have shown tumour eradication both *in vitro* and *in vivo* in preclinical studies (Lynn *et al.*, 2015, 2016; Song *et al.*, 2015). Programming cpCAR T cells with folate-DK resulted in the specific destruction of FOLR1-positive tumour cells and mediated T cell proliferation. However, higher cell division rates of cpCAR T cells programmed against $\alpha_v\beta_3$ were observed than for cpCAR T cells programmed against FOLR1. This could be attributed to the low levels of folate in the medium, that can reduce the proliferation of T cells (Courtemanche *et al.*, 2004). Our data also suggest that in the presence of 1 nM – 10 nM of the folate-DK compound, the anti-tumour effect of cpCAR T cells is stronger compared to both higher and lower concentrations of folate-DK. This observation is in line with our theory that there is a sweet spot of hapten-molecule concentration, where the concentration is high enough to occupy all cpCARs on the T cell surface, but not too high that all cpCAR receptors on the T cell membrane and integrin $\alpha_v\beta_3$ on the tumour cell are occupied, preventing cross-linking of cpCAR and antigen.

The peptidomimetics cRGD and LLP2A as well as the vitamin folate were used as targeting units for the hapten-compounds in this study. All three compounds equipped cpCAR T cells with a specificity for the respective antigens on tumour cells. LLP2A was selected from a one-bead-one-compound combinatorial peptidomimetic library that was screened against Jurkat cells (Peng *et al.*, 2006). Accordingly, we observed specific activation of the T cell signalling cascade induced by LLP2A-DK-programmed cpCAR Jurkat-reporter cells. Many tumour homing peptides have already been discovered by screening combinatorial peptide libraries against various targets, including established CAR targets like PSMA or EGFRvIII (Gade *et al.*, 2005; Johnson *et al.*, 2015; Junghans *et al.*, 2016; Liu *et al.*, 2017). Peptides specific for Her2 have also been described (Shadidi and Sioud, 2003). Conventional CAR T cells with an scFv specific for Her2 were toxic in one clinical trial (Morgan *et al.*, 2010). The simple control of cpCAR activity by the presence and absence of hapten-compounds could allow targeting antigens that are minimally expressed on healthy tissue. We assume that analogous to small molecule haptens, larger molecules, e.g. RNA or DNA aptamers, could also be used to program cpCAR T cells for targeting tumour-associated antigens. Interestingly, LLP2A and RGD are orally available (Peng *et al.*, 2006). The possibility of administering hapten-compounds orally should be further investigated as this would

contribute to the feasibility of the cpCAR method and simplify its testing in animal models.

5.4 Safety of cpCAR T cell therapy

Besides the intended anti-tumour effect, CAR T cell therapy can induce potentially harmful side effects. We suspect that cpCAR T cells have an enhanced safety profile compared to conventional CARs because they are only activated in the presence of a hapten-compound. Additionally, the interaction between cpCAR and DK-molecule is reversible. We also observed decreased activation of the T cell signalling cascade at low concentrations of programming compound. Because small molecules have a short circulatory half-life, usually in a range from minutes to hours (Rader, 2014), we hypothesise that activation of cpCAR T cells could be well regulated through the dosage of hapten-compound. Additionally, high doses of DK-compounds, which have no specificity for human tissues, could be applied to block the interaction between cpCAR receptor and hapten-compound, effectively acting as OFF-switch.

Other CAR designs have been described, where the presence of a drug controlled the activation of CAR T cells. The ON-switch CAR has a split design that can only mediate T cell activation in the presence of rapalog (Wu *et al.*, 2015). In this approach, the extracellular part and the intracellular costimulatory domain of the CAR are expressed together and the CD3ζ domain is expressed separately. Both transgenes comprise one of the heterodimerising domains of the rapalog module. The ON-switch CAR construct assembles after the addition of rapalog and T cells can be activated. In contrast, Mamonkin *et al.* introduced an approach, where expression of a CD5-CAR was regulated by a Tet-OFF system (Mamonkin *et al.*, 2018). The presence of doxocycline inhibited transgene expression.

Other safety strategies are focused on ablation of CAR T cells. CAR T cells can be equipped with a depletion marker or suicide gene to provide a safety switch in case of toxicity (Casucci *et al.*, 2015). The CAR T cells presented in our study are equipped with an EGFRt marker that can be used to deplete CAR T cells by administering the anti-EGFR mAB cetuximab (Wang *et al.*, 2011). The inducible caspase-9 suicide gene system can also be implemented into the design of CAR T cells (Straathof *et al.*, 2005; Gargett and Brown, 2014). In contrast to approaches in which CAR T cells are removed in case of complications, cpCARs and other drug-controlled methods offer the

possibility of reactivating CAR T cells after the toxicity has subsided, e.g. in the case of cytokine release syndrome (CRS).

5.5 Alternative strategies to generate CAR T cells with multiple specificities

In contrast to our approach, CAR T cells with multiple specificities can also be generated by expressing multiple conventional CARs with distinct specificities, as has been shown for CD19 and CD123 (Ruella *et al.*, 2016). Expression of both CARs improved the anti-tumour response of CAR T cells compared to the mono-specific CAR T cell products in a murine xenograft model simulating CD19 loss. Bispecific CARs or tandem CARs with an antigen-binding domain that comprises two different scFvs have also been introduced. Bispecific CAR T cells against Her2 and IL13Rα2 or CD19 and CD20 prevented antigen escape of malignant cells in preclinical models (Hegde *et al.*, 2016; Zah *et al.*, 2016). These concepts demonstrate the feasibility of targeting multiple antigens with CAR T cells. However, the specificity of bispecific CAR T cells is limited to the specificity of the scFvs that constitute the antigen-binding domain, whereas cpCAR T cells could be conceptually programmed against any antigen.

Several alternative approaches to generate CAR T cells that can be equipped with different specificities have been reported. In contrast to our cpCARs, two of these designs do not use an scFv as antigen-binding domain, but an avidin molecule (Urbanska *et al.*, 2012) or a subunit of a heterodimeric transcription factor (Cho, Collins and Wong, 2018). Biotinylated mABs or scFvs fused to the respective subunits of the transcription factors are used to provide the CARs with the desired specificity. The other approaches utilise scFvs to bind targeting-molecules, e.g. CD16-CARs that detect the Fc domain of human Igs (Kudo *et al.*, 2014). Also, CAR T cells with an scFv against a 14 aa sequence of the yeast transcription factor GCN4 (Rodgers *et al.*, 2016) and a 10 aa 5B9-tag (Cartellieri *et al.*, 2016) have been reported. The 5B9-tag was used to label scFvs and nanobodies to target CD33, CD123, GD2, PSMA and other antigens (Albert *et al.*, 2017; Feldmann *et al.*, 2017; Mitwasi *et al.*, 2017). Another method utilised CARs equipped with an scFv specific for FITC. The adapter molecules were typically mABs (Tamada *et al.*, 2012), Fabs (Ma *et al.*, 2016) or small molecules such as folate (Kim *et al.*, 2015) conjugated to FITC. It is worth mentioning that successful *in vivo* anti-tumour effects have only been demonstrated, when conjugated mABs or their derivatives were used to facilitate binding of CAR T cells to the respective antigens. Because these molecules have a longer circulatory half-life than

small-peptides, this would suggest that prolonging the presence of the hapten-compounds could enhance the efficacy of cpCAR T cells. This could be further investigated by adding a DK-unit to a mAB, Fab or scFv in order to generate a hapten-compound with enhanced half-life.

5.6 Conclusion and perspective

In this study, we introduce a novel chemically programmable CAR with an scFv derived from mAB h38C2. Our data show that the cpCAR specifically binds to molecules containing a DK-group. We demonstrate that hapten-molecules can equip a cpCAR T cell with specificity for distinct target antigens. We programmed cpCAR T cells against the integrins $\alpha_v\beta_3$ and $\alpha_4\beta_1$ and the folate receptor and observed potent anti-tumour reactivity of cpCAR T cells against tumour cell lines *in vitro*. Thereby, our data support our initial hypothesis that cpCAR T cells can be directed against multiple antigens and challenges the paradigm that one T cell has only one specificity.

In addition, we introduce novel $\alpha_v\beta_3$-CARs based on mAB hLM609. Our data support the concept that the affinity of the antigen binding domain and spacer length can be calibrated to increase the anti-tumour effect of CARs. CAR T cells with specificity for integrin $\alpha_v\beta_3$ have substantial therapeutic potential in the treatment of solid tumours because integrin $\alpha_v\beta_3$ is expressed on metastatic and chemotherapy-resistant cancer cells, endothelial cells of tumour vasculature and tumour stromal cells.

Conventional $\alpha_v\beta_3$-CAR T cells were able to completely eradicate $\alpha_v\beta_3$-positive tumour lesions in a mouse xenograft model. In order to translate hLM609-CAR T cells to the clinic, the safety of CAR T cell therapy directed against $\alpha_v\beta_3$ should be investigated. This safety evaluation requires detailed expression analyses of healthy tissue. Furthermore, relevant animal models should be established. However, assessing the safety of $\alpha_v\beta_3$-CAR T cells in animal models requires the cross-recognition of $\alpha_v\beta_3$ from different species by the CAR. Since cross-recognition is readily in place for the hapten-molecule we used for programming cpCARs against integrin $\alpha_v\beta_3$, further advancement of cpCAR technology could help to drive the translation of conventional $\alpha_v\beta_3$-CAR T cells to the patient.

The ability to attack multiple antigens positions cpCARs as an attractive technology in a clinical setting. However, to gain clinical relevance, the efficacy of cpCAR T cells needs to be improved. On the one hand, the design of the receptor could be optimised, e.g. by switching to a promoter that enhances expression of the

cpCAR. On the other hand, the pharmacokinetics of hapten-molecules must be investigated in order to define administration route and dose regimen that allows cpCAR T cells to be effective *in vivo*.

Eventually, the treatment regimen with cpCAR T cells we envision for cancer patients would be as follows: While the patient's T cells are modified to express the cpCAR and expanded *in vitro*, tumour biopsies could be analysed for expression of tumour-associated antigens. Based on the expression pattern, an individual panel of hapten-compounds would be composed. After infusion of cpCAR T cells to the patient, the hapten-compounds would be applied separately. The sequential use of the hapten-compounds would allow to assure the safety of the individual compounds. If undesired side effects should occur, e.g. on-target off-tumour toxicity or CRS, these may be controlled by an immediate discontinuation of compound administration without the need to ablate the cpCAR T cells. After the symptoms have subsided, therapy could be continued with an appropriately modified composition of hapten-compounds. In the absence of adverse effects, a simultaneous administration of several hapten-molecules could be considered in order to increase the efficacy of the treatment.

References

Albelda, S. M. *et al.* (1990) 'Integrin distribution in malignant melanoma: association of the beta 3 subunit with tumor progression.', *Cancer research*. American Association for Cancer Research, 50(20), pp. 6757–64.

Albert, S. *et al.* (2017) 'A novel nanobody-based target module for retargeting of T lymphocytes to EGFR-expressing cancer cells via the modular UniCAR platform.', *Oncoimmunology*, 6(4), p. e1287246. doi: 10.1080/2162402X.2017.1287246.

Algarra, I., Cabrera, T. and Garrido, F. (2000) 'The HLA crossroad in tumor immunology.', *Human immunology*, 61(1), pp. 65–73.

Antony, A. C. (1996) 'Folate receptors.', *Annual review of nutrition*, 16(1), pp. 501–21. doi: 10.1146/annurev.nu.16.070196.002441.

Attieh, Y. *et al.* (2017) 'Cancer-associated fibroblasts lead tumor invasion through integrin-β3–dependent fibronectin assembly', *The Journal of Cell Biology*, 216(11), pp. 3509–3520. doi: 10.1083/jcb.201702033.

Barbas, C. F. *et al.* (1997) 'Immune versus natural selection: antibody aldolases with enzymic rates but broader scope.', *Science (New York, N.Y.)*. American Association for the Advancement of Science, 278(5346), pp. 2085–92. doi: 10.1126/science.278.5346.2085.

Blenc, A. M. *et al.* (2003) 'VLA-4 affinity correlates with peripheral blood white cell count and DNA content in patients with precursor B-ALL.', *Leukemia*. Nature Publishing Group, 17(3), pp. 641–3. doi: 10.1038/sj.leu.2402827.

Borst, A. J. *et al.* (2017) 'The Therapeutic Antibody LM609 Selectively Inhibits Ligand Binding to Human αVβ3 Integrin via Steric Hindrance', *Structure*, 25(11), p. 1732–1739.e5. doi: 10.1016/j.str.2017.09.007.

Brentjens, R. J. *et al.* (2013) 'CD19-targeted T cells rapidly induce molecular remissions in adults with chemotherapy-refractory acute lymphoblastic leukemia.', *Science translational medicine*. NIH Public Access, 5(177), p. 177ra38. doi: 10.1126/scitranslmed.3005930.

Brooks, P. C. *et al.* (1994) 'Integrin alpha v beta 3 antagonists promote tumor regression by inducing apoptosis of angiogenic blood vessels.', *Cell*, 79(7), pp. 1157–64.

Brooks, P. C. *et al.* (1995) 'Antiintegrin alpha v beta 3 blocks human breast cancer growth and angiogenesis in human skin.', *The Journal of clinical investigation*, 96(4), pp. 1815–22. doi: 10.1172/JCI118227.

Brooks, P. C., Clark, R. A. and Cheresh, D. A. (1994) 'Requirement of vascular integrin alpha v beta 3 for angiogenesis.', *Science (New York, N.Y.)*, 264(5158), pp. 569–71.

Brown, C. E. *et al.* (2005) 'Biophotonic cytotoxicity assay for high-throughput screening of cytolytic killing', *Journal of Immunological Methods*, 297(1–2), pp. 39–52. doi: 10.1016/j.jim.2004.11.021.

Brozovic, A. *et al.* (2008) 'alpha(v)beta(3) Integrin-mediated drug resistance in human laryngeal carcinoma cells is caused by glutathione-dependent elimination of drug-induced reactive oxidative species.', *Molecular pharmacology*. American Society for Pharmacology and Experimental Therapeutics, 74(1), pp. 298–306. doi: 10.1124/mol.107.043836.

Buss, N. A. P. S. *et al.* (2012) 'Monoclonal antibody therapeutics: history and future.', *Current opinion in pharmacology*. Elsevier, 12(5), pp. 615–22. doi: 10.1016/j.coph.2012.08.001.

Campbell, I. D. and Humphries, M. J. (2011) 'Integrin structure, activation, and interactions.', *Cold Spring Harbor perspectives in biology*, 3(3), pp. a004994–a004994. doi: 10.1101/cshperspect.a004994.

Cartellieri, M. *et al.* (2016) 'Switching CAR T cells on and off: a novel modular platform for retargeting of T cells to AML blasts.', *Blood cancer journal*. Nature Publishing Group, 6(8), p. e458. doi: 10.1038/bcj.2016.61.

Caruso, H. G. *et al.* (2015) 'Tuning sensitivity of CAR to EGFR density limits recognition of normal tissue while maintaining potent antitumor activity', *Cancer Research*, 75(17), pp. 3505–3518. doi: 10.1158/0008-5472.CAN-15-0139.

Casucci, M. *et al.* (2015) 'Overcoming the toxicity hurdles of genetically targeted T cells.', *Cancer immunology, immunotherapy : CII*, 64(1), pp. 123–30. doi: 10.1007/s00262-014-1641-9.

Chmielewski, M. *et al.* (2004) 'T Cell Activation by Antibody-Like Immunoreceptors: Increase in Affinity of the Single-Chain Fragment Domain above Threshold Does Not Increase T Cell Activation against Antigen-Positive Target Cells but Decreases Selectivity', *The Journal of Immunology*. American Association of Immunologists, 173(12), pp. 7647–7653. doi: 10.4049/jimmunol.173.12.7647.

Cho, J. H., Collins, J. J. and Wong, W. W. (2018) 'Universal Chimeric Antigen Receptors for Multiplexed and Logical Control of T Cell Responses.', *Cell*, 173(6), p. 1426–1438.e11. doi: 10.1016/j.cell.2018.03.038.

Clover, J., Dodds, R. A. and Gowen, M. (1992) 'Integrin subunit expression by human osteoblasts and osteoclasts in situ and in culture.', *Journal of cell science*, 103(1), pp. 267–271. doi: 10.1016/S8756-3282(96)00281-5.

Courtemanche, C. *et al.* (2004) 'Folate deficiency inhibits the proliferation of primary human CD8+ T lymphocytes in vitro.', *Journal of immunology (Baltimore, Md. : 1950)*. American Association of Immunologists, 173(5), pp. 3186–92. doi: 10.4049/jimmunol.173.5.3186.

Cui, H. *et al.* (2012) 'Chemically programmed bispecific antibodies that recruit and activate T cells.', *The Journal of biological chemistry*. American Society for Biochemistry and Molecular Biology, 287(34), pp. 28206–14. doi: 10.1074/jbc.M112.384594.

Delbaldo, C. *et al.* (2008) 'Phase I and pharmacokinetic study of etaracizumab (Abegrin™), a humanized monoclonal antibody against αvβ3 integrin receptor, in patients with advanced solid tumors', *Investigational New Drugs*, 26(1), pp. 35–43. doi: 10.1007/s10637-007-9077-0.

Demircioglu, F. and Hodivala-Dilke, K. (2016) 'αvβ3 Integrin and tumour blood vessels-learning from the past to shape the future.', *Current opinion in cell biology*. Elsevier Current Trends, 42, pp. 121–127. doi: 10.1016/j.ceb.2016.07.008.

Desgrosellier, J. S. *et al.* (2009) ‘An integrin alpha(v)beta(3)-c-Src oncogenic unit promotes anchorage-independence and tumor progression.’, *Nature medicine*. Nature Publishing Group, 15(10), pp. 1163–9. doi: 10.1038/nm.2009.

Desgrosellier, J. S. and Cheresh, D. A. (2010) ‘Integrins in cancer: biological implications and therapeutic opportunities.’, *Nature reviews. Cancer*, 10(1), pp. 9–22. doi: 10.1038/nrc2748.

Doppalapudi, V. R. *et al.* (2007) ‘Chemically programmed antibodies: endothelin receptor targeting CovX-Bodies.’, *Bioorganic & medicinal chemistry letters*. Pergamon, 17(2), pp. 501–6. doi: 10.1016/j.bmcl.2006.10.009.

Doppalapudi, V. R. *et al.* (2010) ‘Chemical generation of bispecific antibodies.’, *Proceedings of the National Academy of Sciences of the United States of America*. National Academy of Sciences, 107(52), pp. 22611–6. doi: 10.1073/pnas.1016478108.

Duro-Castano, A. *et al.* (2017) ‘Modulating angiogenesis with integrin-targeted nanomedicines’, *Advanced Drug Delivery Reviews*. Elsevier, 119, pp. 101–119. doi: 10.1016/j.addr.2017.05.008.

Eshhar, Z. *et al.* (1993) ‘Specific activation and targeting of cytotoxic lymphocytes through chimeric single chains consisting of antibody-binding domains and the gamma or zeta subunits of the immunoglobulin and T-cell receptors.’, *Proceedings of the National Academy of Sciences of the United States of America*. National Academy of Sciences, 90(2), pp. 720–4. doi: 10.1073/PNAS.90.2.720.

Eyquem, J. *et al.* (2017) ‘Targeting a CAR to the TRAC locus with CRISPR/Cas9 enhances tumour rejection.’, *Nature*, 543(7643), pp. 113–117. doi: 10.1038/nature21405.

Felding-Habermann, B. *et al.* (2001) ‘Integrin activation controls metastasis in human breast cancer.’, *Proceedings of the National Academy of Sciences of the United States of America*, 98(4), pp. 1853–8. doi: 10.1073/pnas.98.4.1853.

Felding-Habermann, B. and Cheresh, D. A. (1993) ‘Vitronectin and its receptors.’, *Current opinion in cell biology*. Elsevier Current Trends, 5(5), pp. 864–8. doi: 10.1016/0955-0674(93)90036-P.

Feldmann, A. *et al.* (2017) ‘Retargeting of T lymphocytes to PSCA- or PSMA positive prostate cancer cells using the novel modular chimeric antigen receptor platform technology “UniCAR”.’, *Oncotarget*. Impact Journals, 8(19), pp. 31368–31385. doi: 10.18632/oncotarget.15572.

Fesnak, A. D., June, C. H. and Levine, B. L. (2016) ‘Engineered T cells: the promise and challenges of cancer immunotherapy.’, *Nature reviews. Cancer*. Nature Publishing Group, 16(9), pp. 566–81. doi: 10.1038/nrc.2016.97.

Finney, H. M. *et al.* (1998) ‘Chimeric receptors providing both primary and costimulatory signaling in T cells from a single gene product.’, *Journal of immunology (Baltimore, Md. : 1950)*, 161(6), pp. 2791–7.

Finney, H. M., Akbar, A. N. and Lawson, A. D. G. (2004) ‘Activation of resting human primary T cells with chimeric receptors: costimulation from CD28, inducible costimulator, CD134, and CD137 in series with signals from the TCR zeta chain.’, *Journal of immunology (Baltimore, Md. : 1950)*, 172(1), pp. 104–13.

Frigault, M. J. *et al.* (2015) 'Identification of chimeric antigen receptors that mediate constitutive or inducible proliferation of T cells.', *Cancer immunology research*. American Association for Cancer Research, 3(4), pp. 356–67. doi: 10.1158/2326-6066.CIR-14-0186.

Fry, T. J. *et al.* (2018) 'CD22-targeted CAR T cells induce remission in B-ALL that is naive or resistant to CD19-targeted CAR immunotherapy.', *Nature medicine*. Nature Publishing Group, 24(1), pp. 20–28. doi: 10.1038/nm.4441.

Fu, X. *et al.* (2013) 'Genetically modified T cells targeting neovasculature efficiently destroy tumor blood vessels, shrink established solid tumors and increase nanoparticle delivery.', *International journal of cancer*, 133(10), pp. 2483–92. doi: 10.1002/ijc.28269.

Furnari, F. B. *et al.* (2015) 'Heterogeneity of epidermal growth factor receptor signalling networks in glioblastoma.', *Nature reviews. Cancer*. Nature Publishing Group, 15(5), pp. 302–10. doi: 10.1038/nrc3918.

Gade, T. P. F. *et al.* (2005) 'Targeted elimination of prostate cancer by genetically directed human T lymphocytes.', *Cancer research*, 65(19), pp. 9080–8. doi: 10.1158/0008-5472.CAN-05-0436.

Galliher, A. J. and Schiemann, W. P. (2006) 'Beta3 integrin and Src facilitate transforming growth factor-beta mediated induction of epithelial-mesenchymal transition in mammary epithelial cells.', *Breast cancer research : BCR*, 8(4), p. R42. doi: 10.1186/bcr1524.

Gargett, T. and Brown, M. P. (2014) 'The inducible caspase-9 suicide gene system as a "safety switch" to limit on-target, off-tumor toxicities of chimeric antigen receptor T cells.', *Frontiers in pharmacology*. Frontiers, 5(OCT), p. 235. doi: 10.3389/fphar.2014.00235.

Gattinoni, L. *et al.* (2005) 'Removal of homeostatic cytokine sinks by lymphodepletion enhances the efficacy of adoptively transferred tumor-specific CD8+ T cells.', *The Journal of experimental medicine*. Rockefeller University Press, 202(7), pp. 907–12. doi: 10.1084/jem.20050732.

Gavrilyuk, J. I. *et al.* (2009) 'An efficient chemical approach to bispecific antibodies and antibodies of high valency.', *Bioorganic & medicinal chemistry letters*, 19(14), pp. 3716–20. doi: 10.1016/j.bmcl.2009.05.047.

Gay, L. J. and Felding-Habermann, B. (2011) 'Contribution of platelets to tumour metastasis.', *Nature reviews. Cancer*. Nature Publishing Group, 11(2), pp. 123–34. doi: 10.1038/nrc3004.

Gomes-Silva, D. *et al.* (2017) 'Tonic 4-1BB Costimulation in Chimeric Antigen Receptors Impedes T Cell Survival and Is Vector-Dependent.', *Cell reports*. Cell Press, 21(1), pp. 17–26. doi: 10.1016/j.celrep.2017.09.015.

Goswami, R. K. *et al.* (2011) 'Chemically programmed antibodies targeting multiple alpha(v) integrins and their effects on tumor-related functions in vitro.', *Bioconjugate chemistry*, 22(8), pp. 1535–44. doi: 10.1021/bc2000879.

Grada, Z. *et al.* (2013) 'TanCAR: A Novel Bispecific Chimeric Antigen Receptor for Cancer Immunotherapy.', *Molecular therapy. Nucleic acids*. American Society of Gene & Cell Therapy, 2(7), p. e105. doi: 10.1038/mtna.2013.32.

Guedan, S. *et al.* (2018) 'Enhancing CAR T cell persistence through ICOS and 4-1BB costimulation.', *JCI insight*. American Society for Clinical Investigation, 3(1). doi: 10.1172/jci.insight.96976.

Guest, R. D. *et al.* (2005) 'The role of extracellular spacer regions in the optimal design of chimeric immune receptors: evaluation of four different scFvs and antigens.', *Journal of immunotherapy (Hagerstown, Md.: 1997)*, 28(3), pp. 203–11. doi: 10.1097/01.cji.0000161397.96582.59.

Guo, F. *et al.* (2006) 'Breaking the one antibody-one target axiom.', *Proceedings of the National Academy of Sciences of the United States of America*. National Academy of Sciences, 103(29), pp. 11009–14. doi: 10.1073/pnas.0603822103.

Gutheil, J. C. *et al.* (2000) 'Targeted antiangiogenic therapy for cancer using Vitaxin: a humanized monoclonal antibody to the integrin alphavbeta3', *Clinical cancer research : an official journal of the American Association for Cancer Research*, 6(8), pp. 3056–3061.

Hegde, M. *et al.* (2016) 'Tandem CAR T cells targeting HER2 and IL13Rα2 mitigate tumor antigen escape.', *The Journal of clinical investigation*. American Society for Clinical Investigation, 126(8), pp. 3036–52. doi: 10.1172/JCI83416.

Hersey, P. *et al.* (2010) 'A randomized phase 2 study of etaracizumab, a monoclonal antibody against integrin αvβ3, ± dacarbazine in patients with stage IV metastatic melanoma', *Cancer*, 116(6), pp. 1526–1534. doi: 10.1002/cncr.24821.

Hosotani, R. *et al.* (2002) 'Expression of integrin alphaVbeta3 in pancreatic carcinoma: relation to MMP-2 activation and lymph node metastasis.', *Pancreas*, 25(2), pp. e30-5. doi: 00006676-200208000-00021 [pii].

Hsu, M. Y. *et al.* (1998) 'Adenoviral gene transfer of beta3 integrin subunit induces conversion from radial to vertical growth phase in primary human melanoma.', *The American journal of pathology*. Elsevier, 153(5), pp. 1435–42. doi: 10.1016/S0002-9440(10)65730-6.

Hudecek, M. *et al.* (2013) 'Receptor affinity and extracellular domain modifications affect tumor recognition by ROR1-specific chimeric antigen receptor T cells.', *Clinical cancer research : an official journal of the American Association for Cancer Research*. American Association for Cancer Research, 19(12), pp. 3153–64. doi: 10.1158/1078-0432.CCR-13-0330.

Hudecek, M. *et al.* (2015) 'The nonsignaling extracellular spacer domain of chimeric antigen receptors is decisive for in vivo antitumor activity.', *Cancer immunology research*. American Association for Cancer Research, 3(2), pp. 125–35. doi: 10.1158/2326-6066.CIR-14-0127.

Hynes, R. O. (2002) 'Integrins: bidirectional, allosteric signaling machines.', *Cell*. Cell Press, 110(6), pp. 673–87. doi: 10.1016/S0092-8674(02)00971-6.

Irving, B. A. and Weiss, A. (1991) 'The cytoplasmic domain of the T cell receptor zeta chain is sufficient to couple to receptor-associated signal transduction pathways.', *Cell*, 64(5), pp. 891–901. doi: 10.1016/0092-8674(91)90314-O.

Johnson, L. A. *et al.* (2015) 'Rational development and characterization of humanized anti-EGFR variant III chimeric antigen receptor T cells for glioblastoma.', *Science translational medicine*. American Association for the Advancement of Science, 7(275), p. 275ra22. doi: 10.1126/scitranslmed.aaa4963.

Junghans, R. P. *et al.* (2016) ‘Phase I Trial of Anti-PSMA Designer CAR-T Cells in Prostate Cancer: Possible Role for Interacting Interleukin 2-T Cell Pharmacodynamics as a Determinant of Clinical Response.’, *The Prostate*. Wiley-Blackwell, 76(14), pp. 1257–70. doi: 10.1002/pros.23214.

Jutz, S. *et al.* (2016) ‘Assessment of costimulation and coinhibition in a triple parameter T cell reporter line: Simultaneous measurement of NF-κB, NFAT and AP-1.’, *Journal of immunological methods*, 430, pp. 10–20. doi: 10.1016/j.jim.2016.01.007.

Jutz, S. *et al.* (2017) ‘A cellular platform for the evaluation of immune checkpoint molecules.’, *Oncotarget*, 8(39), pp. 64892–64906. doi: 10.18632/oncotarget.17615.

Karlstrom, A. *et al.* (2000) ‘Using antibody catalysis to study the outcome of multiple evolutionary trials of a chemical task.’, *Proceedings of the National Academy of Sciences of the United States of America*. National Academy of Sciences, 97(8), pp. 3878–83. doi: 10.1073/PNAS.97.8.3878.

Kawalekar, O. U. *et al.* (2016) ‘Distinct Signaling of Coreceptors Regulates Specific Metabolism Pathways and Impacts Memory Development in CAR T Cells.’, *Immunity*, 44(2), pp. 380–90. doi: 10.1016/j.immuni.2016.01.021.

Kim, M. S. *et al.* (2015) ‘Redirection of genetically engineered CAR-T cells using bifunctional small molecules.’, *Journal of the American Chemical Society*. American Chemical Society, 137(8), pp. 2832–5. doi: 10.1021/jacs.5b00106.

Kochenderfer, J. N. *et al.* (2015) ‘Chemotherapy-refractory diffuse large B-cell lymphoma and indolent B-cell malignancies can be effectively treated with autologous T cells expressing an anti-CD19 chimeric antigen receptor.’, *Journal of clinical oncology : official journal of the American Society of Clinical Oncology*. American Society of Clinical Oncology, 33(6), pp. 540–9. doi: 10.1200/JCO.2014.56.2025.

Kolb, H. J. *et al.* (1995) ‘Graft-versus-leukemia effect of donor lymphocyte transfusions in marrow grafted patients.’, *Blood*, 86(5), pp. 2041–50.

Kowolik, C. M. *et al.* (2006) ‘CD28 costimulation provided through a CD19-specific chimeric antigen receptor enhances in vivo persistence and antitumor efficacy of adoptively transferred T cells’, *Cancer Research*. American Association for Cancer Research, 66(22), pp. 10995–11004. doi: 10.1158/0008-5472.CAN-06-0160.

Kudo, K. *et al.* (2014) ‘T lymphocytes expressing a CD16 signaling receptor exert antibody-dependent cancer cell killing.’, *Cancer research*. American Association for Cancer Research, 74(1), pp. 93–103. doi: 10.1158/0008-5472.CAN-13-1365.

Kurtova, A. V. *et al.* (2009) ‘Mantle cell lymphoma cells express high levels of CXCR4, CXCR5, and VLA-4 (CD49d): importance for interactions with the stromal microenvironment and specific targeting.’, *Blood*, 113(19), pp. 4604–13. doi: 10.1182/blood-2008-10-185827.

Lamers, C. H. J. *et al.* (2011) ‘Immune responses to transgene and retroviral vector in patients treated with ex vivo-engineered T cells.’, *Blood*. American Society of Hematology, 117(1), pp. 72–82. doi: 10.1182/blood-2010-07-294520.

Legler, D. F. *et al.* (2004) ‘The αvβ3 integrin as a tumor homing ligand for lymphocytes’, *European Journal of Immunology*. WILEY-VCH Verlag, 34(6), pp. 1608–1616. doi: 10.1002/eji.200424938.

Liang, G. *et al.* (2017) ‘Itraconazole exerts its anti-melanoma effect by suppressing Hedgehog, Wnt, and PI3K/mTOR signaling pathways.’, *Oncotarget*. Impact Journals, 8(17), pp. 28510–28525. doi: 10.18632/oncotarget.15324.

Liapis, H., Flath, A. and Kitazawa, S. (1996) 'Integrin αvβ3 Expression by Bone-residing Breast Cancer Metastases', *Diagnostic Molecular Pathology*, 5(2), pp. 127–135. doi: 10.1097/00019606-199606000-00008.

Liu, R. *et al.* (2017) 'Tumor-targeting peptides from combinatorial libraries.', *Advanced drug delivery reviews*. NIH Public Access, 110–111, pp. 13–37. doi: 10.1016/j.addr.2016.05.009.

Liu, X. *et al.* (2015) 'Affinity-tuned ErbB2 or EGFR chimeric antigen receptor T cells exhibit an increased therapeutic index against tumors in mice', *Cancer Research*. American Association for Cancer Research, 75(17), pp. 3596–3607. doi: 10.1158/0008-5472.CAN-15-0159.

Ludbrook, S. B. *et al.* (2003) 'The integrin alphavbeta3 is a receptor for the latency-associated peptides of transforming growth factors beta1 and beta3', *Biochemical Journal*, 369(Pt 2), pp. 311–318. doi: 10.1042/BJ20020809.

Lynn, R. C. *et al.* (2015) 'Targeting of folate receptor β on acute myeloid leukemia blasts with chimeric antigen receptor-expressing T cells.', *Blood*. American Society of Hematology, 125(22), pp. 3466–76. doi: 10.1182/blood-2014-11-612721.

Lynn, R. C. *et al.* (2016) 'High-affinity FRβ-specific CAR T cells eradicate AML and normal myeloid lineage without HSC toxicity.', *Leukemia*. Nature Publishing Group, 30(6), pp. 1355–64. doi: 10.1038/leu.2016.35.

Ma, J. S. Y. *et al.* (2016) 'Versatile strategy for controlling the specificity and activity of engineered T cells.', *Proceedings of the National Academy of Sciences of the United States of America*. National Academy of Sciences, 113(4), pp. E450-8. doi: 10.1073/pnas.1524193113.

Mackensen, A. *et al.* (2006) 'Phase I study of adoptive T-cell therapy using antigen-specific CD8+ T cells for the treatment of patients with metastatic melanoma.', *Journal of clinical oncology : official journal of the American Society of Clinical Oncology*. American Society of Clinical Oncology, 24(31), pp. 5060–9. doi: 10.1200/JCO.2006.07.1100.

Mamonkin, M. *et al.* (2018) 'Reversible Transgene Expression Reduces Fratricide and Permits 4-1BB Costimulation of CAR T Cells Directed to T-cell Malignancies.', *Cancer immunology research*. American Association for Cancer Research, 6(1), pp. 47–58. doi: 10.1158/2326-6066.CIR-17-0126.

Masumoto, A. and Hemler, M. E. (1993) 'Multiple activation states of VLA-4. Mechanistic differences between adhesion to CS1/fibronectin and to vascular cell adhesion molecule-1.', *The Journal of biological chemistry*, 268(1), pp. 228–34.

Matsunaga, T. *et al.* (2003) 'Interaction between leukemic-cell VLA-4 and stromal fibronectin is a decisive factor for minimal residual disease of acute myelogenous leukemia.', *Nature medicine*. Nature Publishing Group, 9(9), pp. 1158–65. doi: 10.1038/nm909.

Maude, S. L. *et al.* (2014) 'Chimeric antigen receptor T cells for sustained remissions in leukemia.', *The New England journal of medicine*, 371(16), pp. 1507–17. doi: 10.1056/NEJMoa1407222.

Maude, S. L. *et al.* (2018) 'Tisagenlecleucel in Children and Young Adults with B-Cell Lymphoblastic Leukemia.', *The New England journal of medicine*. Massachusetts Medical Society, 378(5), pp. 439–448. doi: 10.1056/NEJMoa1709866.

McCabe, N. P. *et al.* (2007) 'Prostate cancer specific integrin αvβ3 modulates bone metastatic growth and tissue remodeling', *Oncogene*. Nature Publishing Group, 26(42), pp. 6238–6243. doi: 10.1038/sj.onc.1210429.

McNeel, D. G. *et al.* (2005) 'Phase I Trial of a Monoclonal Antibody Specific for αvβ3 Integrin (MEDI-522) in Patients with Advanced Malignancies, Including an Assessment of Effect on Tumor Perfusion', *Clinical Cancer Research*, 11(21), p. 7851 LP-7860. doi: 10.1158/1078-0432.CCR-05-0262.

Mitwasi, N. *et al.* (2017) 'Development of novel target modules for retargeting of UniCAR T cells to GD2 positive tumor cells.', *Oncotarget*. Impact Journals, 8(65), pp. 108584–108603. doi: 10.18632/oncotarget.21017.

Morgan, R. A. *et al.* (2010) 'Case report of a serious adverse event following the administration of T cells transduced with a chimeric antigen receptor recognizing ERBB2.', *Molecular therapy : the journal of the American Society of Gene Therapy*. Cell Press, 18(4), pp. 843–51. doi: 10.1038/mt.2010.24.

Moritz, D. *et al.* (1994) 'Cytotoxic T lymphocytes with a grafted recognition specificity for ERBB2-expressing tumor cells.', *Proceedings of the National Academy of Sciences of the United States of America*. National Academy of Sciences, 91(10), pp. 4318–22. doi: 10.1073/pnas.91.10.4318.

Nanna, A. R. *et al.* (2017) 'Harnessing a catalytic lysine residue for the one-step preparation of homogeneous antibody-drug conjugates', *Nature Communications*. Nature Publishing Group, 8(1), p. 1112. doi: 10.1038/s41467-017-01257-1.

O'Rourke, D. M. *et al.* (2017) 'A single dose of peripherally infused EGFRvIII-directed CAR T cells mediates antigen loss and induces adaptive resistance in patients with recurrent glioblastoma.', *Science translational medicine*. American Association for the Advancement of Science, 9(399), p. eaaa0984. doi: 10.1126/scitranslmed.aaa0984.

Peng, L. *et al.* (2006) 'Combinatorial chemistry identifies high-affinity peptidomimetics against alpha4beta1 integrin for in vivo tumor imaging.', *Nature chemical biology*. Nature Publishing Group, 2(7), pp. 381–9. doi: 10.1038/nchembio798.

Perica, K. *et al.* (2015) 'Adoptive T cell immunotherapy for cancer.', *Rambam Maimonides medical journal*. Rambam Health Care Campus, 6(1), p. e0004. doi: 10.5041/RMMJ.10179.

Petitclerc, E. *et al.* (1999) 'Integrin alpha(v)beta3 promotes M21 melanoma growth in human skin by regulating tumor cell survival.', *Cancer research*, 59(11), pp. 2724–30.

Popkov, M. *et al.* (2006) 'Small molecule drug activity in melanoma models may be dramatically enhanced with an antibody effector.', *International journal of cancer*. Wiley Subscription Services, Inc., A Wiley Company, 119(5), pp. 1194–207. doi: 10.1002/ijc.21924.

Popkov, M. *et al.* (2009) 'Instant immunity through chemically programmable vaccination and covalent self-assembly.', *Proceedings of the National Academy of Sciences of the United States of America*, 106(11), pp. 4378–83. doi: 10.1073/pnas.0900147106.

Raab-Westphal, S., Marshall, J. F. and Goodman, S. L. (2017) 'Integrins as therapeutic targets: Successes and cancers', *Cancers*, 9(9), pp. 1–28. doi: 10.3390/cancers9090110.

Rader, C., Turner, J. M., *et al.* (2003) 'A humanized aldolase antibody for selective chemotherapy and adaptor immunotherapy.', *Journal of molecular biology*. Academic Press, 332(4), pp. 889–99. doi: 10.1016/S0022-2836(03)00992-6.

Rader, C., Sinha, S. C., *et al.* (2003) 'Chemically programmed monoclonal antibodies for cancer therapy: adaptor immunotherapy based on a covalent antibody catalyst.', *Proceedings of the National Academy of Sciences of the United States of America*. National Academy of Sciences, 100(9), pp. 5396–400. doi: 10.1073/pnas.0931308100.

Rader, C. (2014) 'Chemically programmed antibodies.', *Trends in biotechnology*. Elsevier Current Trends, 32(4), pp. 186–97. doi: 10.1016/j.tibtech.2014.02.003.

Rader, C., Cheresh, D. A. and Barbas, C. F. 3rd (1998) 'A phage display approach for rapid antibody humanization: designed combinatorial V gene libraries.', *Proceedings of the National Academy of Sciences of the United States of America*, 95(15), pp. 8910–8915. doi: 10.1073/pnas.95.15.8910.

Riddell, S. R. and Greenberg, P. D. (1990) 'The use of anti-CD3 and anti-CD28 monoclonal antibodies to clone and expand human antigen-specific T cells.', *Journal of immunological methods*, 128(2), pp. 189–201.

Roberts, L. R. *et al.* (2012) 'Kappa agonist CovX-Bodies.', *Bioorganic & medicinal chemistry letters*. Pergamon, 22(12), pp. 4173–8. doi: 10.1016/j.bmcl.2012.04.040.

Rodgers, D. T. *et al.* (2016) 'Switch-mediated activation and retargeting of CAR-T cells for B-cell malignancies.', *Proceedings of the National Academy of Sciences of the United States of America*. National Academy of Sciences, 113(4), pp. E459-68. doi: 10.1073/pnas.1524155113.

Rosenberg, S. A. *et al.* (1988) 'Use of tumor-infiltrating lymphocytes and interleukin-2 in the immunotherapy of patients with metastatic melanoma. A preliminary report.', *The New England journal of medicine*, 319(25), pp. 1676–80. doi: 10.1056/NEJM198812223192527.

Ruella, M. *et al.* (2016) 'Dual CD19 and CD123 targeting prevents antigen-loss relapses after CD19-directed immunotherapies.', *The Journal of clinical investigation*. American Society for Clinical Investigation, 126(10), pp. 3814–3826. doi: 10.1172/JCI87366.

Sadelain, M. (2015) 'CAR therapy: the CD19 paradigm.', *The Journal of clinical investigation*. American Society for Clinical Investigation, 125(9), pp. 3392–400. doi: 10.1172/JCI80010.

Sadelain, M., Rivière, I. and Riddell, S. (2017) 'Therapeutic T cell engineering.', *Nature*. Nature Publishing Group, 545(7655), pp. 423–431. doi: 10.1038/nature22395.

Scalici, J. M. *et al.* (2014) 'Inhibition of α4β1 integrin increases ovarian cancer response to carboplatin.', *Gynecologic oncology*. Elsevier Inc., 132(2), pp. 455–61. doi: 10.1016/j.ygyno.2013.12.031.

Scheuermann, R. H. and Racila, E. (1995) 'CD19 antigen in leukemia and lymphoma diagnosis and immunotherapy.', *Leukemia & lymphoma*, 18(5–6), pp. 385–97. doi: 10.3109/10428199509059636.

Schlesinger, M. and Bendas, G. (2015) 'Contribution of very late antigen-4 (VLA-4) integrin to cancer progression and metastasis.', *Cancer metastasis reviews*, 34(4), pp. 575–91. doi: 10.1007/s10555-014-9545-x.

Schnell, O. *et al.* (2008) 'Expression of integrin αvβ3 in gliomas correlates with tumor grade and is not restricted to tumor vasculature', *Brain Pathology*. Blackwell Publishing Ltd, 18(3), pp. 378–386. doi: 10.1111/j.1750-3639.2008.00137.x.

Schuster, S. J. *et al.* (2017) 'Chimeric Antigen Receptor T Cells in Refractory B-Cell Lymphomas.', *The New England journal of medicine*. NIH Public Access, 377(26), pp. 2545–2554. doi: 10.1056/NEJMoa1708566.

Shadidi, M. and Sioud, M. (2003) 'Identification of novel carrier peptides for the specific delivery of therapeutics into cancer cells.', *FASEB journal : official publication of the Federation of American Societies for Experimental Biology*, 17(2), pp. 256–8. doi: 10.1096/fj.02-0280fje.

Sloan, E. K. *et al.* (2006) 'Tumor-specific expression of alphavbeta3 integrin promotes spontaneous metastasis of breast cancer to bone.', *Breast cancer research : BCR*, 8(2), p. R20. doi: 10.1186/bcr1398.

Song, D.-G. *et al.* (2015) 'A fully human chimeric antigen receptor with potent activity against cancer cells but reduced risk for off-tumor toxicity', *Oncotarget*. Impact Journals, 6(25), pp. 21533–21546. doi: 10.18632/oncotarget.4071.

Sotillo, E. *et al.* (2015) 'Convergence of Acquired Mutations and Alternative Splicing of CD19 Enables Resistance to CART-19 Immunotherapy.', *Cancer discovery*. American Association for Cancer Research, 5(12), pp. 1282–95. doi: 10.1158/2159-8290.CD-15-1020.

Straathof, K. C. *et al.* (2005) 'An inducible caspase 9 safety switch for T-cell therapy.', *Blood*. American Society of Hematology, 105(11), pp. 4247–54. doi: 10.1182/blood-2004-11-4564.

Tamada, K. *et al.* (2012) 'Redirecting gene-modified T cells toward various cancer types using tagged antibodies.', *Clinical cancer research : an official journal of the American Association for Cancer Research*, 18(23), pp. 6436–45. doi: 10.1158/1078-0432.CCR-12-1449.

Till, B. G. *et al.* (2012) 'CD20-specific adoptive immunotherapy for lymphoma using a chimeric antigen receptor with both CD28 and 4-1BB domains: pilot clinical trial results.', *Blood*. American Society of Hematology, 119(17), pp. 3940–50. doi: 10.1182/blood-2011-10-387969.

Torre, L. A. *et al.* (2015) 'Global cancer statistics, 2012.', *CA: a cancer journal for clinicians*, 65(2), pp. 87–108. doi: 10.3322/caac.21262.

Turtle, C. J. *et al.* (2016) 'CD19 CAR-T cells of defined CD4+:CD8+ composition in adult B cell ALL patients.', *The Journal of clinical investigation*. American Society for Clinical Investigation, 126(6), pp. 2123–38. doi: 10.1172/JCI85309.

Umemoto, T. *et al.* (2012) 'Integrin-αvβ3 regulates thrombopoietin-mediated maintenance of hematopoietic stem cells', *Blood*. American Society of Hematology, 119(1), pp. 83–94. doi: 10.1182/blood-2011-02-335430.

Urbanska, K. *et al.* (2012) ‘A universal strategy for adoptive immunotherapy of cancer through use of a novel T-cell antigen receptor.’, *Cancer research*, 72(7), pp. 1844–52. doi: 10.1158/0008-5472.CAN-11-3890.

Wagner, J., Lerner, R. A. and Barbas, C. F. (1995) ‘Efficient aldolase catalytic antibodies that use the enamine mechanism of natural enzymes.’, *Science (New York, N.Y.)*, 270(5243), pp. 1797–800.

Walseng, E. *et al.* (2016) ‘Chemically Programmed Bispecific Antibodies in Diabody Format.’, *The Journal of biological chemistry*. American Society for Biochemistry and Molecular Biology, 291(37), pp. 19661–73. doi: 10.1074/jbc.M116.745588.

Wang, X. *et al.* (2011) ‘A transgene-encoded cell surface polypeptide for selection, in vivo tracking, and ablation of engineered cells.’, *Blood*. American Society of Hematology, 118(5), pp. 1255–63. doi: 10.1182/blood-2011-02-337360.

Weller, M. *et al.* (2016) ‘Cilengitide in newly diagnosed glioblastoma: biomarker expression and outcome.’, *Oncotarget*. Impact Journals, LLC, 7(12), pp. 15018–32. doi: 10.18632/oncotarget.7588.

Welniak, L. A., Blazar, B. R. and Murphy, W. J. (2007) ‘Immunobiology of allogeneic hematopoietic stem cell transplantation.’, *Annual review of immunology*, 25(1), pp. 139–70. doi: 10.1146/annurev.immunol.25.022106.141606.

Wohlfarth, P., Worel, N. and Hopfinger, G. (2018) ‘Chimeric antigen receptor T‐cell therapy-a hematological success story.’, *Memo*. Springer, 11(2), pp. 116–121. doi: 10.1007/s12254-018-0409-x.

Wu, C.-Y. *et al.* (2015) ‘Remote control of therapeutic T cells through a small molecule-gated chimeric receptor.’, *Science (New York, N.Y.)*. American Association for the Advancement of Science, 350(6258), p. aab4077. doi: 10.1126/science.aab4077.

Xiao, J. *et al.* (2009) ‘Targeting a homogeneously glycosylated antibody Fc to bind cancer cells using a synthetic receptor ligand.’, *Journal of the American Chemical Society*. American Chemical Society, 131(38), pp. 13616–8. doi: 10.1021/ja9045179.

Yamada, S. *et al.* (2006) ‘Effect of the angiogenesis inhibitor Cilengitide (EMD 121974) on glioblastoma growth in nude mice.’, *Neurosurgery*. Oxford University Press, 59(6), p. 1304–12; discussion 1312. doi: 10.1227/01.NEU.0000245622.70344.BE.

Yang, C. *et al.* (2016) ‘Oncolytic adenovirus expressing interleukin-18 improves antitumor activity of dacarbazine for malignant melanoma.’, *Drug design, development and therapy*. Dove Press, 10, pp. 3755–3761. doi: 10.2147/DDDT.S115121.

Yang, W. *et al.* (2005) ‘Diminished expression of CD19 in B-cell lymphomas.’, *Cytometry. Part B, Clinical cytometry*. Wiley-Blackwell, 63(1), pp. 28–35. doi: 10.1002/cyto.b.20030.

Yang, Y. (2015) ‘Cancer immunotherapy: harnessing the immune system to battle cancer.’, *The Journal of clinical investigation*. American Society for Clinical Investigation, 125(9), pp. 3335–7. doi: 10.1172/JCI83871.

Yee, C. *et al.* (2002) ‘Adoptive T cell therapy using antigen-specific CD8+ T cell clones for the treatment of patients with metastatic melanoma: in vivo persistence, migration, and antitumor effect of transferred T cells.’, *Proceedings of the National Academy of Sciences of the United States of America*. National Academy of Sciences, 99(25), pp. 16168–73. doi: 10.1073/pnas.242600099.

Zah, E. *et al.* (2016) ‘T Cells Expressing CD19/CD20 Bispecific Chimeric Antigen Receptors Prevent Antigen Escape by Malignant B Cells.’, *Cancer immunology research*. American Association for Cancer Research, 4(6), pp. 498–508. doi: 10.1158/2326-6066.CIR-15-0231.

Zhou, W. *et al.* (2015) ‘Periostin secreted by glioblastoma stem cells recruits M2 tumour-associated macrophages and promotes malignant growth.’, *Nature cell biology*. Nature Publishing Group, 17(2), pp. 170–82. doi: 10.1038/ncb3090.

Abbreviations

aa	amino acid(s)
ALL	acute lymphoblastic leukaemia
ATCT	adoptive T cell transfer
B-ALL	B cell acute lymphoblastic leukaemia
biotin-DK	1,3-diketone-biotin
CAIX	carbonic anhydrase IX
CAF	cancer-associated fibroblast
CD	cluster of differentiation
CDR	complementarity-determining regions
CFSE	carboxyfluorescein succinimidyl ester
C_H	constant heavy chain
CML	chronic myelogenous leukaemia
cRGD	cyclic arginyl-glycyl-aspartic acid
CRS	cytokine release syndrome
DK	1,3-diketone
E. coli	*Escherichia coli*
EGFRvIII	epidermal growth factor receptor variant III
f.c.	final concentration
FC	fragment crystallisable
folate-DK	Mono-Folate-Diketone
FOLR1	folate receptor 1
FR	framework region
Fv	variable fragment
GLP-1	glucagon-like peptide-1
HLA	human leukocyte antigen
HSC	hematopoietic stem cell
HSCT	hematopoietic stem cell transplantation
i.p.	intraperitoneal
i.v.	intravenous
IgG	immunoglobulin G
LHRH	luteinizing hormone releasing hormone
mAB	monoclonal antibody

MCL	mantle cell lymphoma
MHC	major histocompatibility complex
MOI	multiplicity of infection
NF-κB	nuclear factor-κB
NFAT	nuclear factor of activated T cells
NSG	NOD.Cg-*Prkdc*^{scid} *Il2rg*^{tm1Wjl}/SzJ
PEG	polyethylene glycol
RGD	arginyl-glycyl-aspartic acid
s.c.	subcutaneous
SA-PE	streptavidin-phycoerythrin
TCR	T cell receptor
TIL	tumour infiltrating lymphocytes
TU	transforming units
VCAM-1	vascular cell adhesion molecule 1
VEGF	vascular endothelial growth factor
VLA-4	very late antigen-4

List of figures

List of tables

Curriculum vitae

Publications

Original article

Wallstabe L, Mades A, Frenz S, Einsele H, Rader C, Hudecek M. CAR T cells targeting $\alpha_v\beta_3$ integrin are effective against advanced cancer in preclinical models. Adv Cell Gene Ther. 2018;e11. https://doi.org/10.1002/acg2.11

Contributions to symposia and conferences

10.-12.06.2015	4th International Conference "Strategies in Tissue Engineering“ - “WITE” Contribution: Talk “Engineered T cells modified to express a ROR1-specific CAR confer potent anti-tumor reactivity in pre-clinical tumor models”
16.-17.03.2017	9th International Symposium on the Clinical Use of Cellular Products “Cellular Therapy 2017” Contribution: Poster “Tumor invasion and destruction by ROR1-specific CAR T cells in novel 3D models of breast and lung cancer””
04.-05.05.2017	Else-Kröner-Forschungskolleg Würzburg “Translational Immunology – From Target to Therapy IV” Contribution: Poster “Tumor invasion and destruction by ROR1-specific CAR T cells in novel 3D models of breast and lung cancer”
08.11.2017	Fachtagung Humane 3D-Gewebemodelle Contribution: Talk “Novel 3D tumor models to interrogate the efficacy of chimeric antigen receptor (CAR) T cells”
18.-21.03.2018	44th Annual Meeting of the European Society for Blood and Marrow Transplantation “EBMT” Contribution: Poster “CAR-T cells targeting $\alpha_v\beta_3$-integrin confer complete remission of epithelial cancers in pre-clinical models *in vivo*” **Award:** Springer Nature Poster Award for Best Scientific Poster

Affidavit and statement on copyright and self-plagiarism

Affidavit

I hereby confirm that my thesis entitled ‘Development and preclinical evaluation of tumour-reactive T cells expressing a chemically programmable chimeric antigen receptor’ is the result of my own work. I did not receive any help or support from commercial consultants. All sources and / or materials applied are listed and specified in the thesis.

Furthermore, I confirm that this thesis has not yet been submitted as part of another examination process neither in identical nor in similar form.

Eidesstattliche Erklärung

Hiermit erkläre ich an Eides statt, die Dissertation ‘Entwicklung und präklinische Evaluierung tumorreaktiver T Zellen, die einen chemisch programmierbaren chimären Antigenrezeptor exprimieren’ eigenständig, d.h. insbesondere selbständig und ohne Hilfe eines kommerziellen Promotionsberaters, angefertigt und keine anderen als die von mir angegebenen Quellen und Hilfsmittel verwendet zu haben.

Ich erkläre außerdem, dass die Dissertation weder in gleicher noch in ähnlicher Form bereits in einem anderen Prüfungsverfahren vorgelegen hat.

Würzburg, 23.10.2018

Statement on copyright and self-plagiarism

The data presented in this thesis has been in part published as an original article in Advances in Cell and Gene therapy. In accordance with the regulations of the journal, text passages and illustrations from the manuscript were used in identical or modified form in this thesis.

Acknowledgment

My sincere gratitude goes to …

… the members of my thesis committee. My first supervisor Dr. Michael Hudecek, who gave me the opportunity to do research in a highly interesting field, to write this dissertation and for his guidance in doing so. Prof. Dr. Christoph Rader, whose constructive feedback over the course of the project gave new momentum, and Prof. Dr. Thomas Herrmann and Prof. Dr. Hermann Einsele who have been involved in the process from the beginning.

… David Hymel, who synthesised most of the compounds, and Silke, without her the mouse experiments would not have been possible.

… all the current and former members of the AG Hudecek not only for all the scientific discussions but also for all the good times we had at work and afterwards. Especially Julian, Katrin and Hardik, who were sitting next to me in the office and endured my habits, and also Markus, Andreas, Sabrina, Thomas, Silvi and Vasco who were a great help in the lab, gave great feedback on my writing or were just there when I needed someone to talk with. I am happy that I found so many friends among you.

… the staff of the Graduate School of Life Sciences, who kindly answered all my questions and guided me around the bureaucratic hurdles during my doctoral studies.

… my parents and my brother, who always supported me.

… my little family, the most important part of my life. Julia and Ella - you are the best.